Cell cycle and DNA damage-dependent control of the checkpoint mediator Rad9

zur Erlangung des Doktorgrades

der Fakultät für Biologie Ludwig-Maximilians-Universität München

vorgelegt von

Giulia di Cicco, M.Sc. Biologie

München 2018

Eidesstattliche Erklärung

Hiermit erkläre ich an Eides statt, dass ich die vorliegende Dissertation selbstständig und ohne unerlaubte Hilfe angefertigt habe. Ich habe weder anderweitig versucht, eine Dissertation einzureichen oder eine Doktorprüfung durchzuführen, noch habe ich diese Dissertation oder Teile derselben einer anderen Prüfungskommission vorgelegt.

Giulia di Cicco
München, den 22.03.2018

Promotionsgesuch eingereicht: 22.03.2018
Tag der mündlichen Prüfung: 19.10.2018
Erstgutachter: Prof. Dr. Heinrich Leonhardt
Zweitgutachter: Prof. Dr. Peter Becker

Essential parts of this work have been published in the following publication:

Di Cicco G, Bantele CS, Reusswig KU and Pfander B (2017) A cell cycle-independent mode oft he Rad9-Dpb11 interaction is induced by DNA damage. Scientific Reports 7:11650.

Table of contents

SUMMARY

The DNA damage checkpoint is a complex surveillance mechanism, which allows cells to recognize and react to endogenous or exogenous DNA damage. After detection of DNA damage, the checkpoint triggers many cellular responses, including cell cycle arrest, activation of transcription of DNA repair genes, inhibition of DNA replication initiation and, in higher eukaryotes, senescence and programmed cell-death upon high DNA damage load. The DNA damage checkpoint activation relies on the formation of specific protein complexes, which are assembled on damaged chromatin both in proximity and around the site of DNA damage. However, due to their transient nature, such protein complexes have never been purified and biochemically characterized. These chromatin-bound protein complexes include the apical checkpoint kinases Mec1 and Tel1 in budding yeast (ATR and ATM in humans), which initiate the DNA damage checkpoint signal transduction pathways, leading to activation of effector kinases. The DNA damage checkpoint signaling pathways are facilitated by mediator proteins such as Rad9 (homologous to human 53BP1). Budding yeast Rad9, like its orthologs, controls two aspects of the DNA damage response: signaling of the DNA damage checkpoint and DNA end resection. In order to function as a mediator protein, Rad9 has to be recruited to chromatin. Rad9 binds damaged chromatin via modified nucleosomes independently of the cell cycle phase; it is known to bind to S129-phosphorylated histone H2A (γH2A) generated by DNA damage-activated Mec1 and Tel1 and to K79-methylated Histone H3 (H3-K79^{me}), a constitutive chromatin mark generated by the methyltransferase Dot1. Furthermore, Rad9 binds to Dpb11, which in turn binds to the 9-1-1 clamp and the apical kinase Mec1. The interaction with Dpb11 generates a second pathway for recruiting Rad9 to DNA damage sites. Interestingly, Rad9 binding to Dpb11 was previously shown to depend on specific S/TP phosphorylation sites of Rad9, which are modified by cyclin-dependent kinase (CDK) therefore allowing the interaction in cell cycle phases with active CKD. However, the exact role of the Rad9-Dpb11 interaction in the context of the DNA damage checkpoint in G1 is yet to be discovered. This work describes a second mode of the Rad9-Dpb11 interaction. Specifically, it shows that phosphorylation of Rad9 S/TP sites involved in the Dpb11 binding is induced upon DNA damage. This mode of S/TP phosphorylation is independent of the cell cycle or CDK activity, but requires prior recruitment of Rad9 to damaged chromatin, suggesting involvement of a chromatin-bound kinase. The DNA damage-dependent hyperphosphorylation of the Rad9 SCD domain by the checkpoint kinases Mec1 and Tel1 is required for Rad9 S/TP phosphorylation. Notably, the DNA damage-induced S/TP phosphorylation triggers Dpb11 binding to Rad9, but the DNA damage-induced Rad9-Dpb11 interaction is dispensable for recruitment to DNA damage sites, suggesting functions beyond Rad9 recruitment. S/TP site phosphorylation is often interpreted as CDK-dependent phosphorylation, however this study on Rad9 shows that after DNA damage, S/TP sites can be targeted by kinases other than CDK and therefore be regulated by signals other than the cell cycle.

2 INTRODUCTION

2.1 DNA damage and Double Strand Break repair

Environmental agents, but also endogenous stress pose a constant threat to the genetic information encoded in the DNA. Spontaneous DNA damage is an intrinsic and frequently occurring feauture of cellular life: it has been estimated that a single cell can encounter an average of 10^5 spontaneous lesions per day (2). Spontaneous DNA alterations can come from normal DNA metabolism: dNTP misincorporation during replication, loss of DNA bases caused by depurination, DNA base interconversion following deamination, DNA bases modification by alkylation, etc. Additionally, cellular metabolism can generate reactive oxygen species that can cause oxidation of DNA bases and DNA breaks (1, 2).

DNA damage can also come from a number of exogenous sources. UV rays coming from sunlight can generate pyrimidine dimers and (6-4) photoproducts amounting to up to 10^5 DNA lesions per cell, per day (2). Ionizing radiation (IR), generated from cosmic radiation or medical treatments such as X rays and radiotherapy, can cause single- and double-strand breaks (SSBs and DSBs) by oxidizing DNA bases. A number of chemical agents contained in chemotherapic can cause different of DNA lesions. Alkylating agents like MMS attach to alkyl groups in DNA generating bulky adducts eventually leading to DNA breaks; crosslinking agents like mitomycin C (MMC), cisplatin, psoralen and nitrogen mustard cause intra- and inter-strand crosslinks, covalent bonds between bases of the same or different DNA strands; topoisomerase inhibitors like camptothecin (CPT) and etoposide can cause covalent bonds between the topoisomerase I or II and the DNA, leading to SSBs or DSBs.

Cells have evolved various repair mechanisms specific for different types of DNA lesions in order to counteract DNA damage: mismatch repair (MMR) replaces mispaired DNA bases with correct bases, base excision repair (BER) removes chemically altered bases, nucleotide excision repair (NER) repairs complex lesions like pyrimidine dimers or intrastrand crosslinks, SSBs are repaired by single-strand break repair (SSBR), whereas DSBs are processed either by non-homologous end joining (NHEJ) or homologous recombination (HR) (3, 4).

Double-strand breaks are among the most cytotoxic form of DNA damage as they present a break in the chromosomal structure. Moreover, this lesion has the potential to promote gross chromosomal rearrangements (GCRs) eventually leading to the development of various diseases and tumorigenesis (5). Mutations in many proteins involved in the repair of such lesion have been connected to cancer but also neurodegenerative diseases, sterility, immunodeficiency disorders and developemental defects (6).

In specific contexts DSBs are programmed by the cell. Meiotic DSB are for example generated by the evolutionarily conserved Spo11 protein (7) in order to initiate homologous recombination as an essential mechanism for correct chromosome segregation at the first meiotic division (8). In vertebrates, during development of immune-cells the process of VDJ

recombination involves the induction of DSBs to ensure rearrangements at immunoglobulin genes, a critical event to achieve antigen receptor diversity (9). In yeast, the mating type switch also relies on the formation of programmed double strand breaks. Typically, molecular events at damage sites ensure programmed DSBs that are steered toward the appropriate repair outcome, yet upon misregulation, aberrant repair events may result in oncogenic translocations (10).

Cells have evolved different pathways for the repair of DSBs: HR, NHEJ, alternative-NHEJ (alt-NHEJ) single-strand annealing (SSA) and Break-induced replication (BIR). The main factor determining which repair pathways to choose is the extent of DSB processing called DNA end resection, a process in which specific endonucleases generate single-stranded DNA around a DSB. Resected DNA is a prerequisite for recombination-based repair and also constitutes a crucial signal for the DNA damage recognition. NHEJ does not require resection while HR, BIR and SSA in particular require extensive resection of DSBs, minimal processing (5-25nt) is sufficient for alt-NHEJ (also known as micro-homology-mediated end-joining or MMEJ) (11).

Non-homologous end joining and homologous recombination are the two main pathways for DSBs repair: NHEJ does not require resection and ligates the two DNA ends with little or no processing (12). In NHEJ, the DSB ends are blocked from 5' end resection and held in close proximity by the double-stranded DNA (dsDNA) end-binding protein complex, the Ku70-Ku80 heterodimer (Ku). As the DSB ends are directly ligated, NHEJ is an error-prone process that frequently results in small insertions, deletions or substitutions at the break site, if DNA was lost upon induction of the break. NHEJ can also result in translocations if DSBs from different parts of the genome are joined (13). In contrast to NHEJ, HR requires resection. The central Rad51 recombinase loads on the 3' single-stranded DNA (ssDNA) generated via resection, forming a nucleoprotein filament. This structure then invades homologous duplex DNA, which is used as a template for repair DNA synthesis. The resulting joint molecule intermediates are metabolized by different pathways leading either to crossover or noncrossover products depending on the different contexts (14). HR is often considered a largely error-free process as it copies DNA sequences from the sister chromatid or ectopic sequences in the genome. However, in ectopic recombination crossing over occurs at non-homologous loci and this can result in dramatic and deleterious chromosomal rearrangements.

NHEJ is active throughout the cell cycle and is favored in G1 cells while HR is more prevalent after DNA replication, since the identical sister chromatid is available as a template for repair.

2.2 The DNA damage checkpoint

In order to recognize DNA damage and trigger a proper response, cells have evolved complex surveilance mechanisms collectively termed the DNA damage checkpoint. The DNA damage checkpoint monitors the genome for the presence of DNA damage and elicits an appropriate response (15-17) - the major components of this response are listed in table 1.

Activation of the DNA damage checkpoint can lead to a transient cell cycle arrest, activation of transcriptional programs to boost DNA repair or, in case the damage cannot be repaired, senescence or programmed cell-death. The checkpoint response is reversible and downregulated once the DNA damage is repaired and allows cells to re-enter the cell cycle in a process known as recovery. When the DNA lesion cannot be repaired, cells may undergo a process called adaptation and re-enter the cell cycle inspite of the continued presence of DNA damage (18).

Class of proteins	***S. cerevisiae***	***S. pombe***	**Humans**
PIKKs	Mec1-Ddc2	Rad3-Rad26	ATR-ATRIP
	Tel1	Tel1	ATM
Sensors	Mre11-Rad50-Xrs2	Rad32-Rad50-Nbs1	MRE11-RAD50-NBS1
	Rad24-Rfc2-5	Rad17-Rfc2-5	RAD17-RFC2-5
	Ddc1-Rad17-Mec3	Rad9-Rad1-Hus1	RAD9-RAD1-HUS1
	(9-1-1)		
DSBs processing	Sae2	Ctp1	CtIP
	Exo1	Exo1	EXO1
	Sgs1	Rqh1	BLM
	Dna2	Dna2	DNA2
Adaptors/Mediators	Rad9	Crb2	53BP1; BRCA1; MDC1
	Mrc1	Mrc1	Claspin
	Dpb11	Cut5	TopBP1
Effectors	Rad53	Cds1	CHK2
	Chk1	Chk1	CHK1

Table 1: components of the DNA damage checkpoint in eukaryotes. DNA damage checkpoint proteins and protein complexes involved in the initial steps of the response to DNA Double strand break in *S. cerevisiae* with their orthologs in *S. pombe* and humans.

The underlying mechanism of the DNA damage checkpoint is highly conserved from yeast to humans and it controls the cell cycle progression. Like in other vertebrates, the mitotic cell cycle of *S. cerevisiae* consists of four phases (Figure 1, 19). The first phase is called gap phase 1 (G1), during this phase cells grow in size and activate transcriptional pathways useful for the subsequent DNA replication, which takes place in the subsequent S- phase

(20). When cells reach a critical size and in presence of sufficient nutrients they pass through a critical point termed START in yeast and restriction point in vertebrates. Once START is passed cells irreversibly enter the S phase and start to replicate their genome. Following S-phase cells enter the gap phase 2 (G2) during which they prepare to enter mitosis (M), the phase in which the duplicated chromosomes are segregated between mother and daughter cell. In eukaryotes all events of the cell cycle phases are regulated by Cyclin-Dependent Kinases (CDKs), a family of serine/threonine kinases that phosphorylate numerous substrates active during S- and M-phase. In *S. cerevisiae* Cdc28 (also called Cdk1) is the essential CDK regulating the entire cell cycle progression (22).

There are two major critical transition points in the cell cycle: the G1/S transition and the G2/M phase transition (21). The DNA damage checkpoint ensures that the cellular processes specific for each phase are correctly carried out before the cells enter the next phase of the cell cycle, therefore they operate during G1/S (G1 DNA damage checkpoint) and G2/M transitions (G2/M DNA damage checkpoint). Additionally, the intra S-phase DNA damage checkpoint provides control during DNA replication. Is important to note that in *S. cerevisiae* the G2/M transition is not as well defined like in *S. pombe* or other vertebrates, indeed some events traditionally considered as mitotic, actually happen during S phase (like spindle pole bodies duplication and mitotic spindle formation), therefore the G2/M DNA damage checkpoint in *S. cerevisiae* rather regulates the crucial mitotic transition from metaphase to anaphase (22, 23, 24).

The G1 checkpoint induces cell cycle arrest at the G1/S transition prior to START, before cells irreversibly commit to DNA replication (25-27). This transient arrest gives cells time to repair the DNA damage therefore delaying onset of DNA replication, bud emergence and spindle pole body duplication (25, 26, 28). Some lesions escape the G1 checkpoint, for example alkylated DNA needs to be converted to secondary lesion during DNA replication in order to be recognized as DNA damage (29). Such lesions will only activate the intra-S-phase checkpoint. The S-phase checkpoint slows the rate of DNA replication and coordinates repair mechanisms at stalled replication forks with cell cycle progression (30), allowing repair of DNA damage before the cell transits into mitosis. Finally the G2/M checkpoint stops cell cycle porgression through mitosis in presence of DNA damage.

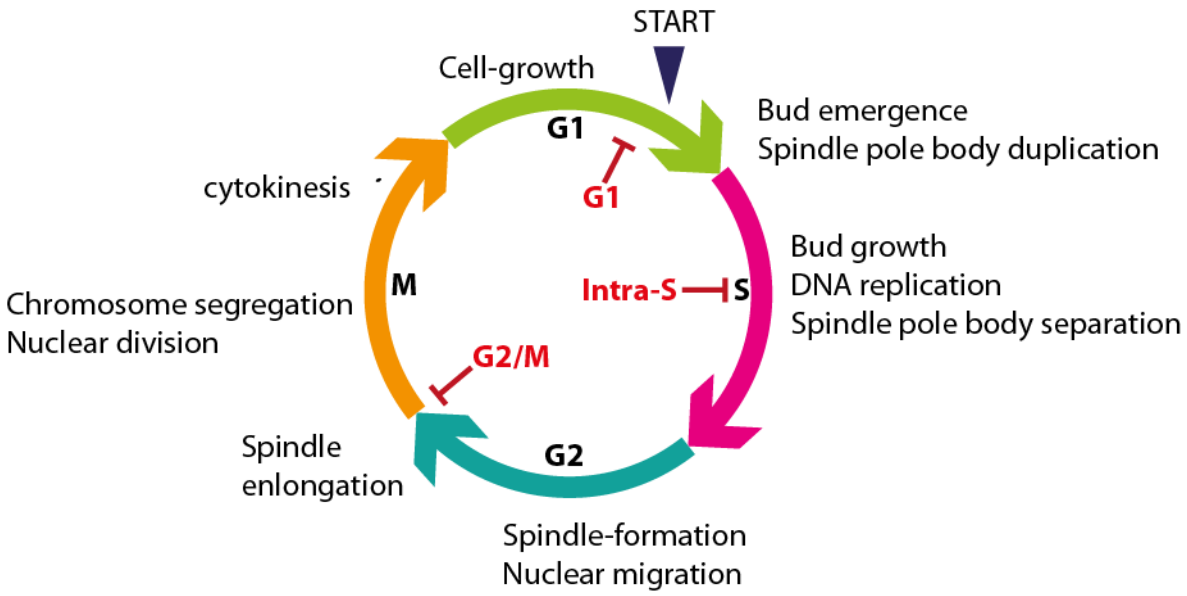

Fig. 1: cell cycle of *S. cerevisiae* and the DNA damage checkpoint. The budding yeast cell cycle is controlled by three main genome integrity checkpoints that respond to DNA damage. The G1 checkpoint arrests cells prior START, the intra-S checkpoint slows the rate of DNA replication and the G2/M checkpoint arrests cells at the metaphase/anaphase transition.

A DNA damage recognized by the cell does not induce cell cycle arrest if it can be rapidly repaired (31). When DNA damage cannot be repaired quickly, it activates the DNA damage checkpoint (32, 33). The signal transduction is initiaed by the so called apical checkpoint kinases, members of the phosphoinositide 3-kinase-related kinase family (PIKKs). In *S. cerevisiae* these kinases are called Mec1 and Tel1, (*S. Pombe* Rad3 and Tel1 and mammalian ATM (ataxia-telangiectasia mutated) ATR (ATM and Rad3-related) and DNA PKcs (DNA-dependent protein kinase catalytic subinit) in higher eukaryotes (16, 34).

Tel1 and Mec1 are homologues to vertebrate ATM and ATR respectively. Both kinases respond to different DNA structures. Mec1 is often considered the principal PIKK given the severe DNA damage sensitivity of mec1 mutants (32, 35), however both Mec1 and Tel1 have important roles in DSBs repair signaling. Tel1 (human ATM) is known to respond and be recruited to unprocessed DSBs (36) while Mec1 (human ATR) is recruited to long stretches of ssDNA coated with replication protein A (RPA) (37, 38) a structure generated by uncoupling of DNA unwinding and synthesis during DNA replication or by nucleolytic processing of DSBs, which depends on prior activation of ATM (39-41, 132, 133). Once the PIKKs are recruited to the site of DNA damage they initiate the signal transduction by phosphorylating downstream targets leading to phosphorylation and activation of the checkpoint effector kinases Rad53 and Chk1 in *S. cerevisiae* (Chk1 and Cds1 in *S. pombe* and human CHK1 and CHK2). The function of these effector kinases is to amplify the DDR signal and activate downstream components (42). The activation of downstream targets by the effector kinases results in modulation of transcriptional levels of repair genes, and regulation of cell cycle transition by influencing stability and localization of proteins involved in cell cycle progression or checkpoint maintenance (43).

The PIKK-dependent activation of effector kinases is facilitated by mediator proteins that function as scaffolds for the kinase reaction or by recruiting additional checkpoint

factors (44). One of these scaffolds and the first checkpoint protein ever identified is Rad9 (homolog to spCrb2, equivalent to human 53BP1, BRCA1, MDC1) (45). In figure 2 is presented an overview of the DNA-damage checkpoint cascade.

The DNA damage checkpoint has various targets, which differ at least in part depending on the cell cycle phase of its activation.

When DNA damage checkpoint is activated in G1, cells are arrested prior to START. The effector kinase Rad53 downregulates transcription of G1/S cyclins Cln1 and Cln2 by phosphorylating SBF transcription factor on its regulatory subunit Swi6, inactivating it (46, 47). Furhermore Rad53 delays accumulation of Cln2 by promoting activation of Gcn4 transcription factor (48). This two-fold control of G1 cyclins prevents the destruction of Sic1, a B-type cyclin inhibitor, which impedes transition into S-phase.(49, 50). Although DNA-damage-dependent phosphorylation of Chk1 in G1 arrested cells suggests an additional role for this effector kinase, the mechanisms of its contribution to the G1 DNA damage checkpoint are yet to be described (51). While budding yeast only transiently delay entry into S-phase, vertebrates posess a very robust G1 checkpoint (52). This checkpoint can be subdivided into two responses: the first involves ATM-dependent phosphorylation of CHK2, which in turn phosphorylates Cdc25A phosphatase, whose function is to remove inhibitory phosphorylation of T14/Y15 on Cdk2, targeting it for degradation (53-55). The resulting loss of Cdc25A activity prevents CDK2-CyclinE kinase complex activation, required for S-phase entry (55, 56). A second response is the ATM and CHK2 mediated phosphorylation of p53 tumor suppressor (57-60). This event stimulates activation and accumulation of p53 (61). The p53 activation results in the induction of the CDK inhibitor p21, which inhibits CDK-cyclinE activity (62, 63).

In *S. cerevisiae*, checkpoint activation in response to faulty replication during S-phase depends entirely on Mec1 and Rad53 kinase (30). The intra-S checkpoint slows down DNA replication rate via a Mec1-dependent phosphorylation of protein RPA (64-66) and inhibition of DNA polymerase α-primase activity, preventing DNA synthesis downstream of the lesion (67, 68).

The intra-S checkpoint inhibits origin firing (69). To this end, Rad53 was shown to phosphorylate the replication initiation protein Sld3, which blocks the interaction with replication proteins Dpb11 and Cdc5 (70, 71). Moreover, Rad53 targets Dbf4, the regulatory subunit of Dbf4-dependent kinase (DDK), which results in inhibition of DDK activity, by a mechanism yet to be elucidated. (70, 71). Additionally, the checkpoint leads to stabilization of replication forks. In this regard, Rad53 phosphorylates the Exo1 nuclease, which is recruited at stalled replication forks, and inhibits Exo1-dependent resection of DNA ends (72-75).

In vertebrates the primary S-phase checkpoint kinase in considered to be ATR (scMec1), with ATM playing a minor role in DSBs response (76). Again, the main function of

the intra-S-phase checkpoint is to suppress origin firing and stabilize the stalled replication forks (77-80). There are two main separate pathways operating, the first pathway is dependent on ATR-CHK1 signaling while a second pathway is dependent on ATM, NBS1, BRCA1 and SMC1. In the first pathway CHK1 is activated by ATR and it globally inhibits origin firing by phosphorylating Cdc25 phosphatases, an event that causes inhibition of replication initiator factor Cdc45 loading onto replication origins (55, 81, 82). A second, ATM-dependent pathway, mediates phosphorylation of SMC1 and SMC3 subunits of the cohesin complex (83-86) which promotes DNA damage repair and cell survival (85, 86).

The G2/M checkpoint is the most prominent checkpoint response in most eukaryotes. In *S. pombe* and vertebrates this pathway operates by stalling mitotic entry trough inhibition of CDK activity. Such inhibition is dependent on the Wee1 family of kinases (scSwe1, spWee1 and Mik1, human Wee1 and Myt1) and the Cdc25 phosphatase family (87). In *S. cerevisiae*, the G2/M arrest is not achieved by regulation of CDK activity. (88, 89) but mitotic arrest is induced by directly inhibiting the metaphase-to-anaphase transition (90). Here, the checkpoint target is Pds1 and both effector kinases Rad53 and Chk1 take part in its regulation. Chk1-dependent phosphorylation of Pds1 prevents its degradation via the APC/C^{Cdc20} complex therefore inhibiting sister chromatid separation and anaphase entry (91-93) Rad53 also contributes to Pds1 stability by inhibiting the interaction between Pds1 and Cdc20 (93). In addition to inhibiting mitotic entry, a second, parallel pathway prevents mitotic exit by Rad53-dependent inhibition of Cdc5 (91, 94). Cdc5 is a polo-like kinase, component of the mitotic exit network (MEN), following checkpoint activation Cdc5 is phopshorylated by Rad53 and is so inactivated. Rad53 additionally inhibits the MEN by preventing the release of Cdc14 from the nucleolus (95).

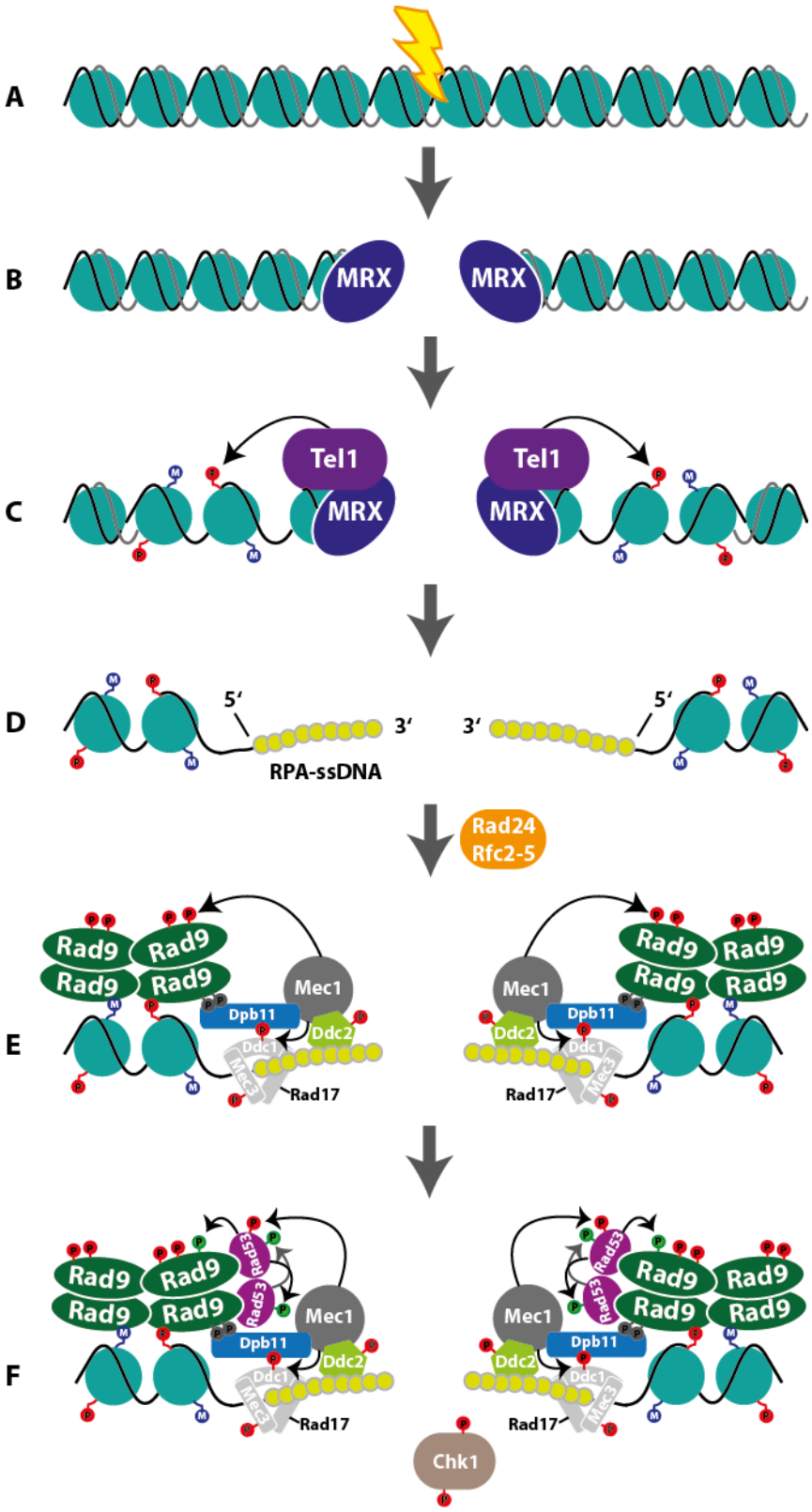

Fig. 2: activation of the DNA damage checkpoint in response to DSBs in *S. cerevisiae*. **(A)** Endogenous or exogenous sources of DNA damage cause DSB **(B)** The MRX complex binds to the blunt DSB ends. **(C)** MRX recruits Tel1 which phosphorylates histone H2A on S129 creating the γ H2A histone mark. **(D)** DNA end resection produces ssDNA which is rapidly coated with RPA. **(E)** RPA-coated ssDNA promotes independent recruitment of Mec1-Ddc2 and the 9-1-1 heterotrimeric clamp (via 5'-ssDNA/dsDNA junctions). Mec1 phosphorylates Ddc1 and Mec3 subunits of 9-1-1. Dpb11 binds to the Mec1-phosphorylated Ddc1 subunit of the 9-1-1 clamp. Hypophosphorylated Rad9 is recruited to chromatin by binding to histone marks γ H2A and H3-K79^{me} and/or via association with Dpb11. Rad9 is then phosphorylated in a Mec1-dependent manner which allows Rad9 oligomerization. Chromatin-bound Rad9 then facilitates the Mec1-dependent phosphorylation of effector kinases Rad53 and Chk1. **(F)** Activated Rad53 and Chk1 phosphorylate downstream effectors of the response to DNA damage.

- PIKK dependent phosphorylation
- Rad53 dependent phosphorylation
- Dot1 dependent methylation
- CDK/Chromatin-bound-Kinase-X dependent phosphorylation

2.3 The ATR/Mec1 and ATM/Tel1 apical checkpoint kinases

2.3.1 The PIKK protein kinase family

Damaged DNA triggers the activation of the DNA damage checkpoint signal transduction pathway, which coordinates cell cycle and DNA damage repair mechanisms (96). Key players of the checkpoint are the phosphatidylinositol 3-kinase related kinases (PIKKs). This family of kinases contains mammalian ATM (ataxia-telangiectasia-mutated) and ATR (ATM and Rad3-related), Saccharomyces cerevisiae Tel1 and Mec1, and Schizosaccharomyces pombe Tel1 and Rad3. In humans, ATM deficiency results in ataxia telangiectasia, a rare autosomal recessive disorder characterized by cerebellar ataxia, neurodegeneration, radiosensitivity, checkpoint defects, genome instability and cancer predisposition (97). Also mutations in ATR are associated with Seckel Syndrome, a disorder characterized by proportionate growth retardation and microcephaly (98).

There is a common, evolutionary conserved structure among all PIKK-like proteins: they are large enzymes (270-450 kDa) characterized by a large N-terminal HEAT repeat domain followed by a small kinase domain (99) located near the C-terminus. The kinase domain is flanked by two regions called FAT (FRAP, ATM, TRRAP) and FACT (FAT C-terminus). FAT and FACT domains are thought to interact and participate in the regulation of kinase activity (100) while regions containing HEAT repeats are predicted to adopt large superhelical conformations creating a surface that mediates protein and DNA interactions.

Both hATM/scTel1 and hATR/scMec1 are activated by DNA damage and initiate the signaling cascade of the checkpoint by phosphorylating downstream targets on the consensus motif hydrophobic-X-hydrophobic-S/T-Q. ATM/Tel1 and ATR/Mec1 respond to different DNA lesions. ATM/Tel1 is known to be activated in response to DSBs, while ATR/Mec1 responds to all those DNA lesions that induce the generation of ssDNA (96). ATM/Tel1 and ATR/Mec1 phosphorylate downstream effector kinases: Rad53 and Chk1 in *S. cerevisiae* and CHK2 and CHK1 in vertebrates (91). While Mec1 activates both Rad53 and Chk1 human ATM and ATR activate CHK2 and CHK1 respectively

2.3.2 ATM/Tel1

ATM/Tel1 is activated in response to DSBs formation. ATM/Tel1 exists as a homodimer that dissociates into active monomers in response to DSBs (101, 102). Yeast Tel1 (Telomerase maintenance 1) was originally identified in *S. cerevisiae* screening for genes involved in telomere length maintenance (103-105). Indeed, in addition to its role in DSB repair, Tel1 is required to maintain telomere length by promoting telomerase recruitment through phosphorylation events (106). Human ATM was identified as the gene mutated in the ataxia telangiectasia syndrome and, like Tel1, is involved in telomere maintenance (107-109).

Both ATM and Tel1 are recruited to DSBs via interaction with the highly conserved protein complexes Mre11-Rad50-Xrs2 (MRX) in *S. cerevisiae* and MRE11-RAD50-NBS1 (MRN) in mammals, which are among the first factors to be recruited at DSBs (110). In S. cerevsisiae MRX complex initiates DSBs resection toghether with Sae2 (111, 112). The Mre11 component

displays a 3'-5' double strand DNA exonuclease activity and ssDNA endonuclease activity. Toghether with Sae2, Mre11 generates 3'-ended ssDNA tails which are then subjected to further resection (113, 114). Furthermore, MRX/MRN mantain tethering of DSB ends, to allow their repair by NHEJ or HR (115, 116, 117)

Various studies have demonstrated that the localization of Tel1/ATM to the site of damage is mediated by direct interaction of Tel1/ATM with C-terminus of Xrs2/Nbs1 subunit (102, 118-120). Besides recruitment of Tel1/ATM and its accumulation to the damage site Tel1 kinase activity is also stimulated by MRX at DNA ends (121), Furthermore, purified MRX/MRN increases catalitic activity of Tel1/ATM in presence of DNA fragments (121). Notably, cells defective in any component of the MRN/MRX complex are also defective in ATM/Tel1 activation. Tel1 activity is also required for DNA-damage-dependent phosphorylation of Xrs2, Mre11 and Sae2, promoting their functions in DNA repair and checkpoint activation (121-124, 112). however, the exact molecular mechanisms of Tel1/ATM activation remains to be elucidated.

Functionally, Tel1 signaling can be considered to be in part redundant with Mec1. A *tel1n* mutant is indeed checkpoint proficient and does not exibit a strong sensitivity to genotoxic agents, while additional deletion of TEL1 aggravates sensitivity of *mec1Δ* (125,126). Importantly, the Tel1 signaling substrate is disrupted by DNA end resection (125). Similarly, in mammals, ATM activation is inhibited by long overhangs of 3' or 5' ssDNA (127). Given that resected DNA promotes signaling by ATR/Mec1, DNA end resection can be seen as handover mechanism from one PIKK-like kinase to the other.

2.3.3 ATR/Mec1

In contrast to ATM/Tel1, ATR/Mec1 is always found tightly associated with ATRIP/Ddc2 and there is no evidence of it acting as a monomer (128). In addition to the heterodimeric Mec1/ATR-Ddc2/ATRIP complex, also higher-order assemblies may form (129, 130). While ATM/Tel1 is activated mainly by DNA double-strand breaks (DSBs), ATR/Mec1 responds to a wide range of DNA damage, including stalled replication forks, base adducts, UV-induced nucleotide damage, and DSBs (76). However, ATR/Mec1 does not recognize the primary lesion itself, but long stretches of single-stranded DNA (ssDNA), which are generated either by the uncoupling of DNA unwinding and synthesis during DNA replication or by nucleolytic processing of DSBs (132, 133)

In both mammals and yeast, the recruitment of ATR/Mec1 to sites of DNA damage requires the interaction between RPA (which is itself a target of ATR/Mec1) and ATRIP/Ddc2. Loss of ATRIP/Ddc2 results in the same phenotypes as loss of ATR/Mec1 in both yeast and mammals, indicating that both ATRIP and Ddc2 are required for ATR/Mec1 functions (134, 135).

ATR/Mec1 activation requires not only recruitment to RPA-coated ssDNA, but also involves other factors, the so called Mec1 activators (Fig. 3). One of these is the 9-1-1 checkpoint clamp, a heterotrimer structurally related to PCNA. In budding yeast, co-

recruitment of Mec1-Ddc2 and 9-1-1 to a DNA locus is sufficient to activate the checkpoint. thanks to stimulation of Mec1 kinase activity by the Ddc1 component of 9-1-1 (136, 137), however evidence for the same 9-1-1 dependent activation of ATR/Rad3 in humans or *S. pombe* is lacking. In physiological conditions, activation of Mec1 by 9-1-1 critically depends on 9-1-1 loading via Rad24-RFC clamp loader onto the appropriate DNA structure. In particular the critical motifs for Mec1 activation are found in the Ddc1 subunit (129). Ddc1 contains a bipartite Mec1 activation domain that has one motif near the C-terminal end of the PCNA-like domain and the second motif in the unstructured C-terminal tail (Fig. 3). Each motif has a critical tryptophane residue (Trp352 and Trp544) followed by 1 or 2 hydrophobic aminoacids. A *ddc1-2W2A* mutant bearing mutations of these two aromatic residues fails to activate Mec1 in vitro and in the G1 activation in vivo (136). The artificial colocalization of Ddc1 with Mec1 via Ddc2 subunit was demonstrated to be sufficient to activate the DNA damage checkpoint even in absence of DNA damage (137). In humans instead, 9-1-1 appears to work by recruiting another activator - TopBP1 (topoisomerase-binding protein 1 (138, 139, 140). TopBP1 stimulation of ATR activity is evolutionary conserved, as the *S. cerevisiae* ortholog Dpb11 is also recruited to DNA damage sites, where it stimulates Mec1 (141, 142, 143). As with Ddc1, a bipartite domain in the unstructured C-terminal tail mediates the Mec1 activation, with each motif containing the critical aromatic aminoacids W700 and Y735 (144). Since phosphorylation of Ddc1 by Mec1 is critical for Dpb11 function in checkpoint signaling, the Mec1-Ddc2 recruited via RPA must have sufficient activity to phosphorylate Ddc1 before its interaction with Dpb11 (143).
Mec1 is activated by 9-1-1 in G1 and by both 9-1-1 and Dpb11/TopBP1 in M-phase (136). Additionally, Dna2 was identified as a third Mec1/ATR kinase activator in a biochemical screen for DNA replication mutants in *S. cerevisiae* (145, 146). Dna2 is an essential nuclease-helicase that toghether with Rad27, homolog of human Flap endonuclease 1 (FEN1), works on the maturation of Okazaky fragments during DNA replication, by cleaving long 5' -end flap structures generated by DNA polymerase δ. Furthermore, Dna2 also participates to DSBs end resection by working toghether with the Sgs1-Top3-Rmi1 complex (114, 147-149). The stimulatory effect of Dna2 on Mec1 is independent of its helicase and nuclease activities, and relies on two aromatic residues residing in its N-terminal domain, Trp128 and Tyr130. When these residues were replaced with alanines the resulting mutant Dna2-WY-AA was completely lacking Mec1/ATR stimulatory activity both *in vitro* and *in vivo*, when replication forks were stalled by Hydroxyurea (150).The stimulatory effect of Dna2 on Mec1/ATR appears specific for S-phase and Dna2 does not seem to have significant role in activation of G1 and G2/M checkpoints.

Remerkably, although the three Mec1/ATR activators are structurally unrelated and have different biological roles, they share high similarities in their Mec1/ATR activating features: all three activators contain structured domain(s) responsible for specific binding to different DNA lesions/structures, plus an unstructured activation tail that mediates the

Mec1/ATR activation, provided vicinity to RPA-coated ssDNA sufficient to recruit Mec1/ATR via Ddc2/ATRIP.

There seems to be a high level of redundancy between the three Mec1/ATR activators in S-phase. Full abrogation of the S-phase checkpoint requires inactivation of all three Mec1/ATR activators or Mec1 itself, and Tel1/ATM (150). The reason for this functional overlap is currently unclear, but highlights the importance of the S-phase checkpoint. Indeed while cells lacking G1 or G2/M checkpoint do not show a significant growth defect (like *ddc1 Δ* cells, 136) cells lacking replication checkpoint signaling are extremely sick and even in absence of DNA damage grow poorly and are unable to complete DNA replication efficiently (150, 151). Therefore an efficient checkpoint during S-phase seems to contribute to DNA replication, even in the absence of exogenous DNA damage.

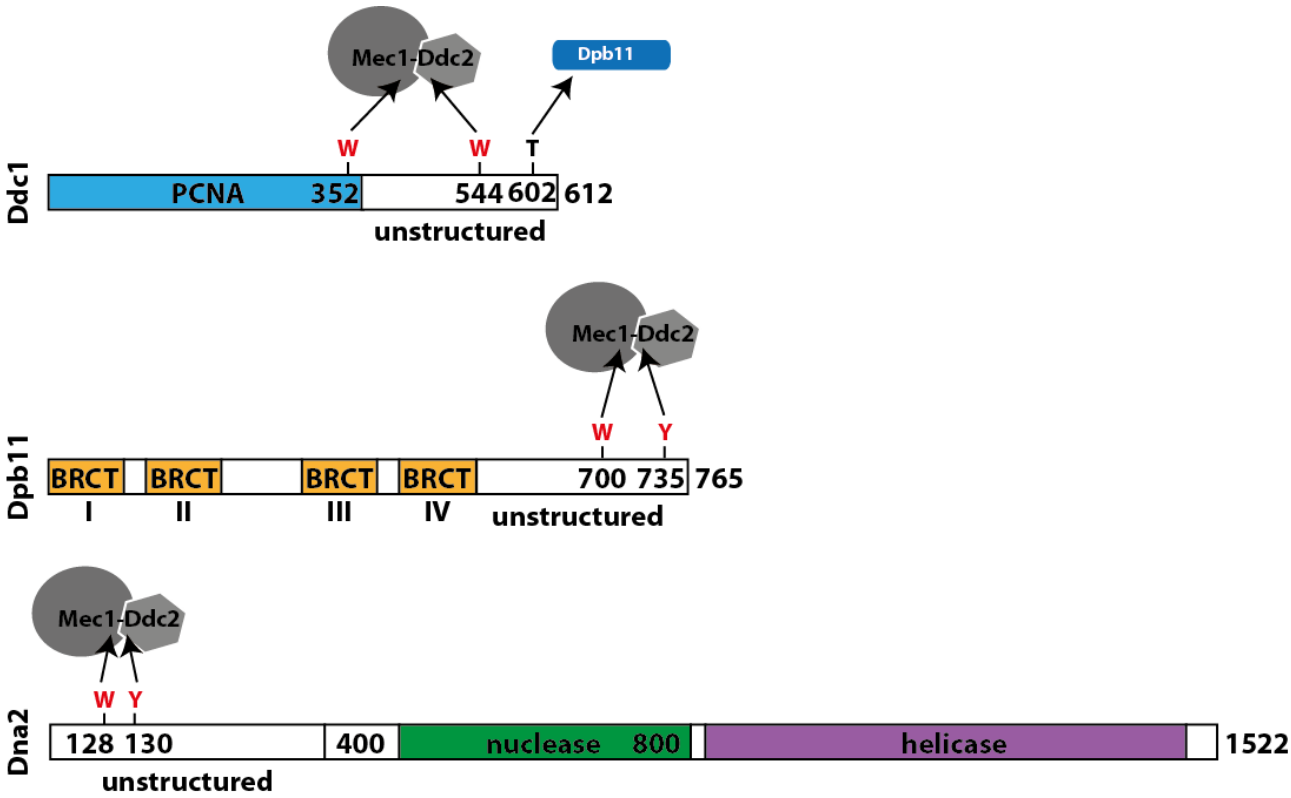

Fig. 3: activators of Mec1. Domain structures of the three Mec1 activators. Indicated in red are the central aromatic aminoacids in the motifs critical for Mec1 activation. Also indicated the T602 mediating Ddc1 binding to Dpb11.

2.3.4 Interplays between Tel1/ATM and Mec1/ATR signaling

ATM/Tel1 and ATR/Mec1 initiate the checkpoint signaling cascade by phosphorylating various targets: they are responsible for the accumulation of DNA-damage-dependent histone mark γH2A and they target and activate several proteins involved in the DNA damage checkpoint signaling cascade. Importantly ATM/Tel1 and ATR/Mec1 phosphorylate the downstream effector kinases: Rad53 and Chk1 in *S. cerevisiae* and CHK2 and CHK1 in vertebrates (91). The apical checkpoint kinases mediated signaling is activated by DSBs for both Mec1/ATR and Tel1/ATM (Fig. 2), but how are the activities of these kinases coordinated at DSBs?

In both yeast and humans Tel1/ATM and Mec1/ATR are oppositely regulated by DNA end resection and ssDNA generated at DSBs. As these ssDNA streches increase in length the Tel1/ATM-dependent signaling is reduced and simultaneously the Mec1/ATR-dependent signaling is increased (125).

In both humans and yeast Tel1/ATM activation also promotes the acumulation of ssDNA at DSB ends and thus promotes the activation of the Mec1/ATR-dependent checkpoint cascade (40, 41, 125, 127, 152). In the current model, MRX is recruited to the DSB ends in its ATP-bound state and this configuration keeps the DSBs ends toghether to allow repair by NHEJ. ATP hydrolysis by Rad50 is likely coupled to endonucleolytic nicking by MRX/Sae2 at a certain distance from the DSB. This provides an internal entry site for long-range resecting nucleases capable of 5'-3' exonucleolytic DNA degradation activity, Exo1 and Dna2, the latter of which cooperates with the Sgs1-Rmi1-Top3 complex. The initial cleavage provided by MRX and Sae2 is therefore followed by bidirectional resection by the Mre11 3'-5' exonuclease and the 5'-3' endonuclease activity of Exo1 and Dna2-Sgs1. This Tel1 mediated generation of ssDNA in turn activates Mec1/ATR and at the same time inhibits Tel1/ATM signaling.

Budding yeast are highly proficient in resection of DNA ends, thus explaining why Tel1-deficient cells do not show hypersensitivity to DNA damage and are still proficient in checkpoint activation even in the presence of a single DSB (125). Furthermore Mec1 itself regulates the generation of 3'-ssDNA, since Mec1-dependent phosphorylation of Sae2 is important for Sae2 function in DSB resection in mitosis and meiosis (124, 153). Mec1 also phosphorylates histone H2A on Serine 129, and this event is involved in regulation of resection resection rate at DSBs (154).

Finally, Rad53 activated by Mec1/ATR in turn phosphorylates and downregulates Exo1-dependent resection (73). This suggests that Mec1/ATR regulates ist own activity via a negtive feedback loop that prevents excessive resection by acting directly on the resection machinery.

2.4 Checkpoint protein scaffolds and activators

2.4.1 The 9-1-1 clamp

The heterotrimeric clamp 9-1-1 is the first activator of the checkpoint, and is loaded onto 5'- ssDNA/dsDNA (5'-junctions). These stretches of ssDNA rapidly coated with RPA protein can be generated in various ways in the cell and toghether with the 5' junctions are instrumental for the recruitment of checkpoint complexes. DSBs are processed by several nucleases and helicases in a mechanism called DNA end resection that creates single-stranded DNA regions with 3' single-stranded DNA overhangs and 5'-junctions (113, 114). The damage caused by UV irradiation and other DNA damaging agents elicits Nucleotide Excision Repair (NER) pathway, and damage processing by the NER machinery leads to the formation of single stranded DNA gaps (155, 156). ssDNA accumulates at stalled replication

forks due to the uncoupling of DNA polymerase and helicase activities. Lastly, the loss of telomere ss-DNA binding protein Cdc13 causes accumulation of ssDNA at telomeres (157).

The 9-1-1 clamp is structurally related to the replicating clamp PCNA (158, 159) , but is loaded onto DNA with an opposite polarity respect to PCNA (136). The clamp consists of RAD9-RAD1-HUS1 in humans and Rad17-Mec3-Ddc1 in *S. cerevisiae*. 9-1-1 is loaded in an ATP driven reaction at the junctions between ssDNA and dsDNA by the clamp loader RAD17-RFC2-5 (human) or Rad17-Rfc2-5 (yeast), in a manner that is independent of ATR/ATRIP or Mec1/Ddc2 (76, 129). The clamp loader Rad24-RFC has an ATP binding site in its Rad24 subunit that is essential for loading 9-1-1 *in vitro* and for checkpoint function *in vivo* (160, 161). To date there is no further function known for the Rad24-RFC other than 9-1-1 loading and the three subunits are only known to act as a heterotrimer, while the monomers are apprently devoid of function. Like PCNA the 9-1-1 clamp has the ability to slide across DNA, but was so far only observed to do so when the clamp was loaded onto naked DNA, while the presence of RPA appears to restrict movement of the clamp specifically to the 5'-ssDNA/dsDNA junctions (162). The clamp 9-1-1 has two main roles in the checkpoint activation, while it directly stimulates the Mec1 kinase activity, it also provides a binding site for an additional Mec1 activator and protein scaffold: scDpb11 (hTopBP1, spCut5, Fig. 3). The respective homologs of Ddc1, Mec3 and Rad17, in *S. pombe* and humans are Rad9, Hus1 and Rad1, hence the name 9-1-1 (163). In contrast to the PCNA-like domain, which is similar in each of the three subunits, their C-terminal tails show high evolutionary divergence. In particular the C-terminal tail of the Ddc1/Rad9 subunit is important for the 9-1-1 function in the checkpoint activation, as it contains a bipartite domain responsible for Mec1 kinase activation.

Mec1 kinase has a low basal activity that can phosphorylate its Ddc2 co-factor in G2 (128), however phosphorylation of the other known Mec1 targets requires its activation. Once loaded and in proximity, the 9-1-1 clamp stimulates kinase activity of Mec1 towards ist targets Rad53, RPA, Rad24 and Ddc1 and Mec3 subunits of 9-1-1 itself (129).

In addition to the stimulatory effect of its Ddc1 subunit, 9-1-1 helps the activation of Mec1 also by functioning as a scaffold for another Mec1 activator called Dpb11 in *S. cerevisiae* (ortholog of human TopBP1). In this context, loaded 9-1-1 becomes itself a target of Mec1 and it is phosphorylated on the Ddc1 subunit, creating a binding site for the BRCT III and IV of Dpb11 (143, 164). While activation of Mec1 by 9-1-1 in G2/M is additionally mediated by the binding of TopBP1 in humans and Dpb11 in *S. cerevisiae*, In the G1-phase of *S. cerevisiae* loading of 9-1-1 to RPA coated DNA is sufficient for the activation of Mec1, indeed while *ddc1-2W2A* mutant is completely defective for Mec1 activation in vitro and G1 checkpoint activation in vivo, a Ddc1 mutant that cannot be phosphorylated by Mec1, and therefore cannot recruit Dpb11 to sites of damage, still shows a robust G1 checkpoint (136).

2.4.2 TopBP1/Cut5/Dpb11

Vertebrate TopBP1, *S. pombe* Cut5/Rad4 and *S. cerevisiae* Dpb11 are BRCT repeat-containing (Breast-Cancer-1 C terminal domain) proteins (Fig. 3 and Fig. 4), with multiple

conserved functions in genome stability. Dpb11 is essential for DNA replication initaition and replisome assembly in S-phase (165). In *S. cerevisiae* Dpb11 interacts with initiator proteins Sld2 and Sld3 after they have been phosphorylated by the S-phase CDK-cyclin complex. Formation of a stable Sld2-Dpb11-Sld3 complex is essential for DNA replication initiation (166, 167). Dpb11 is also necessary for the loading of Pol ε onto the pre-replication complex. However once replication in initiated Dpb11 does not appear to travel along with the replication fork during enlongation but rather dissociates from DNA (168-170). Also in human cells TopBP1 is not found to localize to PCNA containing foci (171).

In a second function, TopBP1/Cut5/Dpb11 is recruited back at the forks, when these are stalled for example by hydroxyhurea treatment. Here, it becomes important for checkpoint signaling, where it interacts with the Rad9/Ddc1 subunit of the 9-1-1 clamp and checkpoint mediators such as 53BP1/Rad9 (131).

Initially, studies in Xenopous revealed that TopBP1 is able to activate the kinase activity of ATR (172). Following studies confirmed that this mechanism is higly conserved in human cells and S.cerevisiae (141, 142, 173). Xenopus TopBP1 has 8 BRCT repeats, and the ATR activation domain (AAD) is located between BRCT6 and BRCT7, but this architecture of the C-terminal half of TopBP1 is only conserved in vertebrates and is not found in either *S. pombe* or *S. cerevisiae*. However, like in Xenopus, addition of Dpb11 to Mec1 is sufficient to stimulate Mec1 activity towards all tested phosphorylation targets *in vitro*, without the need for DNA or RPA (141, 164). Mutants that lack the C-terminus of Dpb11, are also unable to to activate Mec1, suggesting that the AAD of Dpb11 resides in its C-terminal tail (143).

The mechanism of activation of Mec1 by Dpb11 or ATR by TopBP1 is similar to Mec1 activation via the the Ddc1 subunit of 9-1-1 clamp as it requires the bipartite domain in the unstructured C-terminal tail (Fig. 4, 136, 141, 142) (see above) . The *ddc1-2W2A* mutant previously described, contains mutations in these aromatic residues and while it can still bind both DNA and Dpb11 it is unable to stimulate Mec1 activity. Although no similarities can be found between the AAD of Dpb11 and TopBP1, the vertebrate AAD is also unstructured and mutation of a conserved aromatic residue (tryptophane) leads to decreased ATR activation (172). Dpb11-activated and Ddc1-activated Mec1 show very similar kinase activity towards Mec1 targets such as Rad53, RPA or the PIKK model substrate PHAS1 (phosphorylated heat- and acid-stable protein regulated by insulin 1, a common PIKK target) (129, 141).

In G2/M-phase, Dpb11 contributes to the activation of DNA damage checkpoint toghether with Ddc1. Indeed, while the Mec1 activation mutant *ddc1-2W2A* is completely defective for Mec1 activation in G1, it is still proficient for Rad53 phosphorylation during G2/M-phase in response to DNA damage. However, when an additional *ddc1-T602A* mutant is introduced in the context of the *ddc1-2W2A* mutant, the G2/M-phase checkpoint is compeletely abbrogated (136). As the *ddc1-T602A* mutant is deficient in the interaction between Dpb11 and the 9-1-1 complex, this suggests that Dpb11 acts to activate Mec1 redundantly with Ddc1. Consistently, a *ddc1-2W2A dpb11-1* double mutant in which the

activation domain of both Ddc1 and Dpb11 are defective, also lacks G2/M checkpoint response (136).

In G1-phase, the checkpoint seems not to require Dpb11, but only the 9-1-1 dependent pathway. (174). While a *ddc1-2W2A* mutant is completely defective for the G1 checkpoint, a robust G1 checkpoint response is observed in *ddc1-T602A*, which is deficient in Dpb11 recruitment (136).

The orthologs of Dpb11 and Ddc1 in S.pombe - Cut5 (scDpb11) and Rad9 (scDdc1) are also found to interact with similar mechanisms: Rad3-dependent phosphorylation of Rad9 on T412/S423 in the C-terminus of the Rad9 (scDdc1) subunit of the 9-1-1 complex allows binding to C-terminal BRCT repeats of replication factor Cut5 (scDpb11) promoting its recruitment to chromatin (140). Similary, in vertebrates, the first two BRCT repeats of TopBP1 (scDbb11 and spCut5) interact with C-terminal phsopshorylation site S387 of RAD9 (scDdc1) which is constitutively phosphorylated during the cell cycle (Fig. 4, 138, 139,). The TopBP1-Rad9 interaction promotes TopBP1-dependent ATR activation, mediated by the AAD domain of TopBP1, thus facilitating ATR-dependent phosphorylation and activation of effector kinase CHK1. Finally Dpb11 binds to Rad9, a central scaffold protein of the DNA damage checkpoint: (143, 175). The binding sites of Rad9 in Dpb11 are BRCT I and II (Fig. 4), suggesting that Dpb11 can engage in simultaneous interactions with Rad9, the 9-1-1 complex and Mec1-Ddc2. Indeed, in vitro experiments suggests that Dpb11 employs its BRCT I and II domain to interact with S/TP phosphorylated Rad9, its middle BRCT III and IV to bind Mec1-phosphorylated Ddc1 and its C-terminal unstructured domain to bind Mec1-Ddc2 (143).

Dpb11 is furthermore known to engage in additional protein complexes involved in DNA repair, such as with the scaffold proteins Slx4 and Rtt107 (176-179), the structure-selective nuclease Mus81-Mms4 (176) or the resection-promoting nucleosome remodeller Fun30 (179).

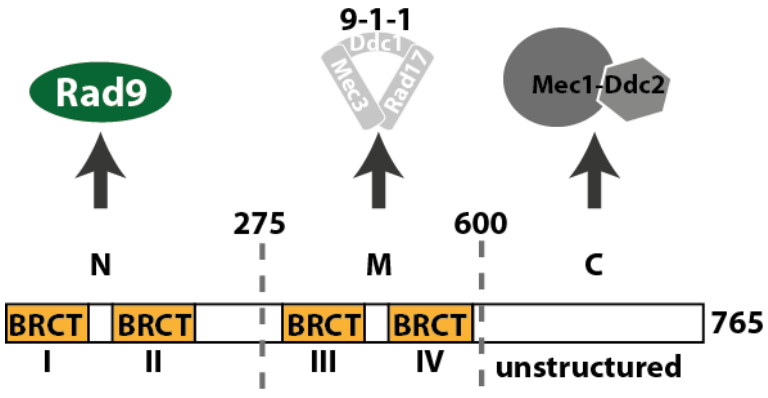

Fig. 4: domains and interactors of Dpb11. Schematic diagram of Dpb11 domains and interactors involved in the DNA damage checkpoint. the four BRCT repeat domains are marked as yellow boxes. The BRCT repeats I and II in the N-terminal domain of Dpb11 mediate interaction with Rad9, BRCT repeats III and IV in the middle domain bind to the Ddc1 subunit of the 9-1-1 clamp and the unstructured C terminus binds to Mec1-Ddc2.

2.4.3 Rad9/Crb2/53BP1

Budding yeast Rad9 was the first DNA damage checkpoint gene identified (45). It is a critical mediator protein required for proper activation of the DNA damage response to a variety of genotoxins and in all cell cycle phases (27, 180). Rad9 (homologous to S.pombe Crb2 and human 53BP1) functions as molecular adaptor that recruits proteins to sites of damage and mediates the PIKK-dependent phosphorylation of downstream substrates (44)

Rad9 and its orthologs play a dual role in the DNA damage response: they mediate the signal transduction in the DNA damage checkpoint (33) and control DNA end resection (115). To fulfil these two functions, Rad9 engages in several protein-protein interactions on damaged chromatin (143, 175, 181-184).

As checkpoint signaling mediator, Rad9 acts as a molecular scaffold and links the signal transduction from the apical kinase Mec1 to the effector kinase Rad53 (185-190). In unperturbed cells Rad9 exists in large complexes containing Ssa1 and Ssa2 chaperone proteins that ensure complex stability (191, 192). In G1 and G2/M-phases a fraction of Rad9 is also found at chromatin, bound to modified histones. This low, constitutive association of Rad9 with chromatin is suggested to enhance the efficiency of reponse to DNA damage signals (175, 183). Rad9 is recruited to sites of DNA damage and is hyperphosphorylated by the PIKKs on S/TQ sites, in particular those that form the S/TQ Cluster Domain or SCD (186, 189). The hyperphosphorylated SCD provides a docking site for the FHA domain of Rad53 (185, 187, 188, 190, 192, 193). Thus Rad9 provides a docking site for Rad53 in close proximity to Mec1 allowing efficient Mec1-dependent phosphorylation of Rad53. Overall, Rad9 therefore provides a mechanism of transient Rad53 recruitment and activation, which allows subsequent Rad53 dissociation and activation of the global DNA damage response.

Rad9 is also an inhibitor of DNA end resection (157, 194-196). The lack of Rad9 increases the resection efficiency of otherwise wild-type cells (157, 194) and suppresses the resection defect of Sae2-deficient cells, which show higher amount of Rad9 binding close to the DSBs ends (196, 197). Several studies indicate that Rad9 acts as a barrier toward DSB ends processing enzymes by restricting DNA end resection (196, 197). Furthermore an antagonistic relationship between Rad9 and the resection-promoting nucleosome remodeller Fun30 has been demonstrated (179, 198). Elimination of Fun30 increases accumulation of Rad9 at DSBs suggesting that Fun30 can counteract the resection barrier posed by chromatin-bound Rad9 (154, 198, 199).

Rad9 functions in resection and the checkpoint require its chromatin association. In order to interact with nucleosomes, Rad9 acts as a bivalent histone binder (Fig. 5A). On the one hand, it uses its Tudor domain to interact with K79-methylated histone H3 (H3-K79^{me}), a widespread modification of chromatin introduced by the methyltransferase Dot1 (184, 200). After DNA damage, Rad9 additionally engages in a second interaction via the tandem-BRCT domain, which binds to histone H2A in its S129-phosphorylated form (γ H2A), (183, 201) a DNA-damage-specific chromatin mark introduced by the apical checkpoint kinases Mec1 and Tel1 (202). The lack of H3-K79 methyltransferase Dot1 or mutation of serine 129 on H2A histone increase the resection efficiency (194, 154, 203). This Rad9 feature as a bivalent

nucleosome binder is conserved among Rad9 orthologs, even though different histone marks are being recognized (204-208)

A second pathway of Rad9 recuritment to DNA damage sites involves the interaction of Rad9 with the scaffold protein Dpb11 (143, 175, Fig. 5B). This interaction involves BRCT I and II of Dpb11 and is dependent on Rad9 phosphoryltion. According to the current model, the 9-1-1 clamp can tether Dpb11 to DNA damage sites and Dpb11 can in turn recruit Rad9 (143, 209). Notably, the interaction of Dpb11 with Rad9 depends on Rad9 phosphorylation at S462 and T474 residues (143). Both sites match the minimal consensus (S/TP) for phosphorylation by cyclin-dependent kinase (Cdc28 in *S. cerevisiae*) and consistently a CDK-dependent interaction between Rad9 and Dpb11 can be observed in G2/M arrested cells (143).

Rad9 recruitment to damaged chromatin occurs in all cell cycle phases (181). Previous data led to a model where in G1 only one Rad9 recruitment pathway -via interaction with modified nucleosomes, or the "histone pathway" (181-184, 201) is active, while outside of G1 a second Rad9 recruitment pathway (via Dpb11 and 9-1-1, referred to as the 'Dpb11 pathway') is additionally available (143, 209). However, the meaning of restricting the Rad9-Dpb11 interaction to specific cell cycle phases is currently not understood.

The existence of a second pathway of Rad9 recruitment in G2/M-phase is indicated by the fact that loss of either Rad9-binding histone modification does not perturb the G2/M checkpoint activation (181, 184, 200). First evidence of an alternative Rad9 recruitment pathway came from studies in *S. pombe*, where recruitment of the Rad9 ortholog Crb2 to sites of damage is also mediated by two partially redundand pathways (206). Analogous to Rad9 recruitment mechanisms, Crb2 binding to chromatin is regulated by γH2A and H4-K20^{me} (there is no report of H3-K79^{me} in *S. pombe*) and the interaction between Crb2 and histones is mediated by its Tudor and BRCT domains, binding to H4-K20^{me} and γH2A respectively (206-208, 210-212). The second pathway is again independent of histone modifications and requires phosphorylation of CDK consensus site on T215 of Crb2 (206). It therefore seems to be an evolutionary conserved feature in the DNA damage response that Rad9 and its homologs bind damaged chromatin via two distinct mechanisms, which are post-translationally regulated.

Also mammalian 53BP1 functions as molecular scaffold at sites of damage, facilitating phosphorylation of ATM downstream targets like CHK2, BRCA1 and SMC1 (213-218). 53BP1 is recruited at chromatin via binding of its Tudor domain to methylated histone H4-K20 and/or methylated histone H3-K79 (219, 208, 220), two histone marks whose recognition by 53BP1 seem to depend on prior RNF8-RNF168-UBC13-mediated polyubiquitination of histone H2A and H2AX (221-225). 53BP1 was indeed demonstrated to recognize mononucleosomes containing both dimethylated H4K20 (H4K20me2) and H2A ubiquitinated on Lys 15 (H2AK15^{ub}), a product of RNF168 action. While the Tudor domain binds to H4-K20^{me2}, the carboxy-terminal extension, termed the ubiquitination-dependent recruitment (UDR) motif, may interact directly with H2AK15^{ub} (226).

Furthermore Although γH2AX is dispensable for the initial recruitment of NBS1 and the putative sc Rad9 orthologs BRCA1 and 53BP1 to DSBs in mammalian cells (227), their accumulation and retention depends on the interaction between MDC1 (another scRad9 ortholog) and γ and, which promotes further recruitment of ATM to the vicinity of the break leading to the spread of γH2AX along chromatin (228, 229). Vertebrate 53BP1 (scRad9) also interacts with TopBP1 (scDpb11). Moreover, TopBP1 is found to colocalize with 53BP1 following IR-induced DNA damage (230, 231). Furthermore, the 53BP1 protein is strongly regulated by CDK activity during the cell cycle: 42 putative CDK sites are present in 53BP1, 27 of which are phosphorylated in vivo (232-239), but the functional relevance of the CDK-dependent phosphorylation of 53BP1 remains to be clarified.

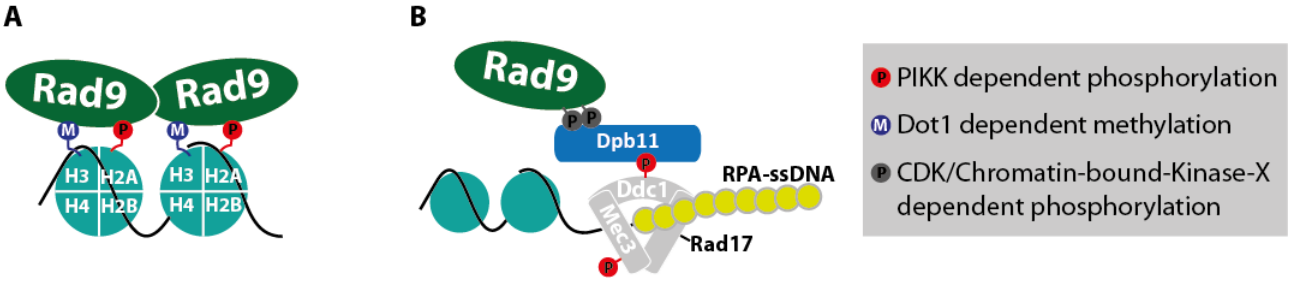

Fig. 5: mechanism of Rad9 recruitment at sites of DNA damage. The two parallel pathways that recruit Rad9 to chromatin following DNA damage are represented separately. **(A)** The histone-dependent pathway requires binding of Rad9 Tudor and BRCT domains to H3-K79^{me} and γH2A respectively. **(B)** The Dpb11-dependent pathway requires prior phosphorylation of Rad9 on residues S462 and T474, which then provide binding sites for BRCT I and II of Dpb11. The phosphorylation of S462 and T474 is dependent on CDK and, upon DNA damage, on an unidentified protein kinase likely to be chromatin-bound.

2.5 Checkpoint effector kinases

Once activated in response to DNA damage the PIKKs promote the activation of downstream effector kinases such as *S. cerevisiae* Chk1 and Rad53, *S. pombe* Chk1 and Cds1 or human CHK1 and CHK2, which target downstream components of the DNA damage response and amplify the DDR signals (42). In *S. cerevisiae* both Rad53 and Chk1 are activated by Mec1/Tel1 (91) while in vertebrates ATM primarily activates CHK2 (scRad53) and ATR activates CHK1 (scChk1) (42). As outlined above, the activation of the effector kinases is dependent on mediator proteins and PIKK activators (44).

Activation of the effector kinases leads to a cell-wide response that includes cell cycle arrest, activation of DNA repair, transcription of damage inducible genes and S-phase specific mechanisms to prevent collapse of replication forks and late origin firing (240, 241).

2.5.1 Rad53/Cds1/CHK2

Rad53 is the main effector kinase in replication and DNA damage checkpoints of budding yeast.

Once recruited to sites of damage, Mec1-dependent phosphorylation of Rad9 facilitates the recruitment of Rad53 and promotes its Mec1-dependent activation (185, 190 , 192) as well as Rad53 in-trans autophosphorylation (192). Vertebrate CHK2 is also known to dimerize and trans-autophosphorylate in an ATM-dependent manner, but the precise role of DNA damage mediators in this activation remains to be investigated (242). Fully activated Rad53 is then released from the hyperphosphorylated Rad9 complex in an ATP-dependent manner (192). Maintenance of Rad53 activation and checkpoint-induced cell cycle arrest is dependent on Rad9 oligomerization which, by promoting its accumulation at sites of damage, allows amplification of the DNA damage signal and sustained activation of Rad53 (243). At the same time a Rad53-mediated negative feedback loop appears to regulate Rad9 oligomerization: fully activated Rad53 phosphorylates the Rad9 tandem BRCT domains attenuating the BRCT-SCD interaction, therfore mediating the turnover of hyperphosphorylated Rad9 by promoting its dissociation from sites of damage and subsequently dampening Rad53 activity (243).

Rad53 is also crucial for the replication checkpoint. Here, Mrc1 is another molecular adaptor that regulates Rad53 activation in response to replication stress. (244).

In response to replication stress and DNA damage in S-phase Rad53 activation blocks origin firing (245). To this end Rad53 phosphorylates and inhibits replication initiation protein Sld3 and Cdc7/Dbf4 kinase. Moreover, Rad53 stabilizes replication forks by targeting the Exo1 nuclease, known to be recruited to stalled replication forks, where it can induce degradation. Phoshporylation by Rad53 inhibits Exo1-dependent cleavage and also establishes a negative feedback loop that limits checkpoint hyperactivation (245).

When activated in G2/M Rad53 causes cell cycle arrest. In the unperturbed cell cycle, budding yeast securin, Pds1 is degraded at the entry into mitosis after being ubiquitinated by the Anaphase Promoting Complex (APC) in complex with its specificity factor Cdc20. Rad53 promotes Pds1 stability as it specifically blocks the interaction between Pds1 and Cdc20 in vivo (93), thereby blocking sister chromatid separation. Although the exact molecular mechanism is unknown, it has been proposed that one site on Cdc20 is a likely substrate of Rad53 direct phosphorylation (246).

In addition to preventing mitotic entry, Rad53 also stalls mitotic exit by a parallel pathway, mantaining high levels of mitotic CDK activity (91). Following checkpoint activation, Cdc5, a component of the mitotic exit network (MEN) is phosphorylated in a Rad53-dependent manner and therefore inactivated.

Rad53 also regulates transcritpion of DNA repair genes by targeting Dun1, a protein kinase required for transcriptional induction of many DNA-damage-inducible genes and genes encoding ribonucleotide reductase (RNR) subunits involved in the Rad53 modulation of dNTP pools (247, 248).

2.5.2 Chk1/CHK1

In response to DNA damage Rad9 also facilitates activation of the second kinase effector: Chk1 in *S. cerevisiae* (*S. pombe* Chk1 and human CHK1). The Mec1-dependent

activation of Chk1 requires the Chk1 activation domain (CAD) of Rad9 (91, 250). The mechanistic aspects of Rad9-dependent activation of Chk1 are still to be unraveled since interaction between the two proteins has so far been demonstrated only via yeast two hybrid analyses (91, 251). The existence of *chk1* mutants that can be activated in a Rad9-independent manner suggest that Rad9 could be required for conformational changes that facilitate Chk1 activation (252). While Rad53 is activated in response to replication stress via Mec1-dependent phosphorylation mediated by Mrc1, Chk1 only gets activated when replication stress signals are converted into DNA damage signal (245, 253). Chk1 also plays a role in the stabilisation of replication forks in the absence of Rad53, suggesting a degree of redundancy (72). Moreover, both Rad53 and Chk1 function in the G2/M checkpoint response to inhibit anaphase entry and mitotic exit in the presence of DNA damage (91, 95, 254). Chk1-dependent phosphorylation of Pds1 prevents its degradation by the APC/C^{Cdc20} complex, thus inhibiting sister chromatid separation and preventing anaphase entry (91-93). Lastly, Chk1 is also phosphorylated in a DNA-damage-dependent manner in G1-arrested cells (51) suggesting that it may also participate in the G1 checkpoint.

In contrast to *S. cerevisiae* where Rad53 (human CHK2) is the principal effector kinase, in vertebrates CHK1 is the primary effector of both replication stress and DNA damage checkpoint (42). CHK1 activation by ATR is mediated by TopBP1 (scDpb11) and adaptor protein Claspin (scMrc1) (242). Claspin functions by recruiting CHK1 to stalled replication forks, facilitating its ATR-dependent phosphorylation (255-258). In vertebrates, ATR-dependent phosphorylation of S317 and S345 on CHK1 promotes CHK1 activation by inducing a conformational change that relieves the inhibition of the N-terminal kinase domain by the C-terminal regulatory domain (259-262) and stimulates the release of CHK1 from chromatin (263, 264). Activated CHK1 can dissociate from chromatin and phosphorylate its substrates among which Cdc25A, Cdc25C and Wee1 are key regulators of the cell cycle (53, 81, 265). Furthermore, ATR-CHK1 signaling inhibits an interaction between Cdc45 and the Mcm7 subunit of the MCM helicase complex, inhibiting DNA replication initiation via a CDK2-independent mechanism.

AIMS OF THE STUDY

The DNA damage checkpoint is an intricate signaling pathway whose major players and functions are conserved in the eukaryotic kingdoms. This complex pathway is set in motion by the presence of even a single DNA Double Strand Break and it starts with the recruitment and assembly on chromatin of several proteins with disparate functions: DNA damage sensors, scaffolding factors and signal transducers. At the beginning of my PhD the lack of biochemical characterization of such complexes compelled the use of mass spectrometry techniques in attempt to detect and analyse chromatin-bound checkpoint protein complexes. The goal of such approach was to resolve the exact composition, stoichiometry and spatial arrangement along the chromosomes of such checkpoint complexes.
Another interesting characteristic of the DNA damage checkpoint is that despite more than 20 years of research elucidated its major features and choreography, many aspects like the regulation of the specific protein interactions, signal amplification and specificity still elude understanding. One such missing piece is the regulation and function of the interaction between Rad9 and Dpb11, two proteins that are stably recruited at damaged chromatin and are important for proper signal transduction and activation of the DNA damage response (DDR). Rad9 especially has been the subject of extensive research given its conserved and essential role in the DNA damage response and its engagement in numerous interactions with other DDR proteins and histones. My work focused on revealing the requirements, cell-cycle regulation, and possible functions of the Rad9-Dpb11 interaction in the context of the DNA damage checkpoint response.

4 RESULTS

4.1 Purification of chromatin-associated checkpoint complexes

4.1.1 ChIP-MS of RPA1^{3FLAG} for purification of DNA damage checkpoint proteins assembled on DNA damage sites

Many basic features of the checkpoint signaling have been elucidated using the downstream read-out of checkpoint activation in combination with genetic manipulation. The critical involvement of scaffold proteins such as Dpb11 and Rad9 in the checkpoint suggests that apical checkpoint signaling takes place at DNA damage sites and possibly in checkpoint signaling complexes. However, these complexes have never been purified and characterized, presumably due to their transient nature and their dependency on a chromatin template. Such limitations may be overcome by the use of crosslinking agents. In recent years, several pioneering studies have shown the possibility of employing formaldehyde, a crosslinker widely used in chromatin-immunoprecipitation, purifications and interactomics particularly of chromatin-associated protein complexes (266-272).

In this study I employed formaldehyde crosslinking to create covalent protein-protein and DNA-protein crosslinks in order to purify the checkpoint signaling complexes formed at DNA damage sites *in situ*. To cause DNA damage, I made use of MMS, a DNA alkylating agent which methylates DNA predominantly on N7-deoxyguanosine and N3-deoxyadenosine. MMS causes stalling of replication forks, which eventually leads to DSBs. I then used affinity chromatography directed against ssDNA-binding protein RPA to purify complexes bound at DNA damage sites, and quantitative SILAC-based (stable isotope labeling by amino acids in cultured cells) mass-spectrometry to measure their composition (273, 274) . RPA was chosen as purification target, since RPA-coated single-stranded DNA is found at sites of DNA lesions undergoing repair (for examples DSBs resection). Importantly, RPA-coated ssDNA represents the structure that triggers recruitment of the apical checkpoint kinase Mec1 and consequent DNA damage checkpoint activation (37). I used asynchronous cells of an RPA1^{3FLAG} strain and an untagged control in a SILAC experiment to identify the RPA specific interactors after MMS-induced DNA damage (Fig. 6A, B and C). A total of 1395 proteins were measured, among these, 338 proteins appeared likely to be copurifying with RPA, since they were specifically enriched in the light medium sample expressing RPA1^{3FLAG}. The majority of proteins copurified ith RPA1^{3FLAG} are known to function in DNA damage repair, DNA damage checkpoint, modification/remodelling of chromatin, DNA replication and transcription or are reported to be RPA interactors.

In a different experiment the same workflow was used to identify which proteins were found to interact with RPA specifically under DNA damage conditions (Fig. 7). I therefore used RPA1^{3FLAG} strains and performed pulldowns from asynchronous non-treated and MMS-treated cells in a SILAC experiment. In this experiment, replication proteins

appeared not to be enriched in any of the samples. This indicates that replication proteins will interact with RPA-ssDNA in both normal and DNA damage-conditions.

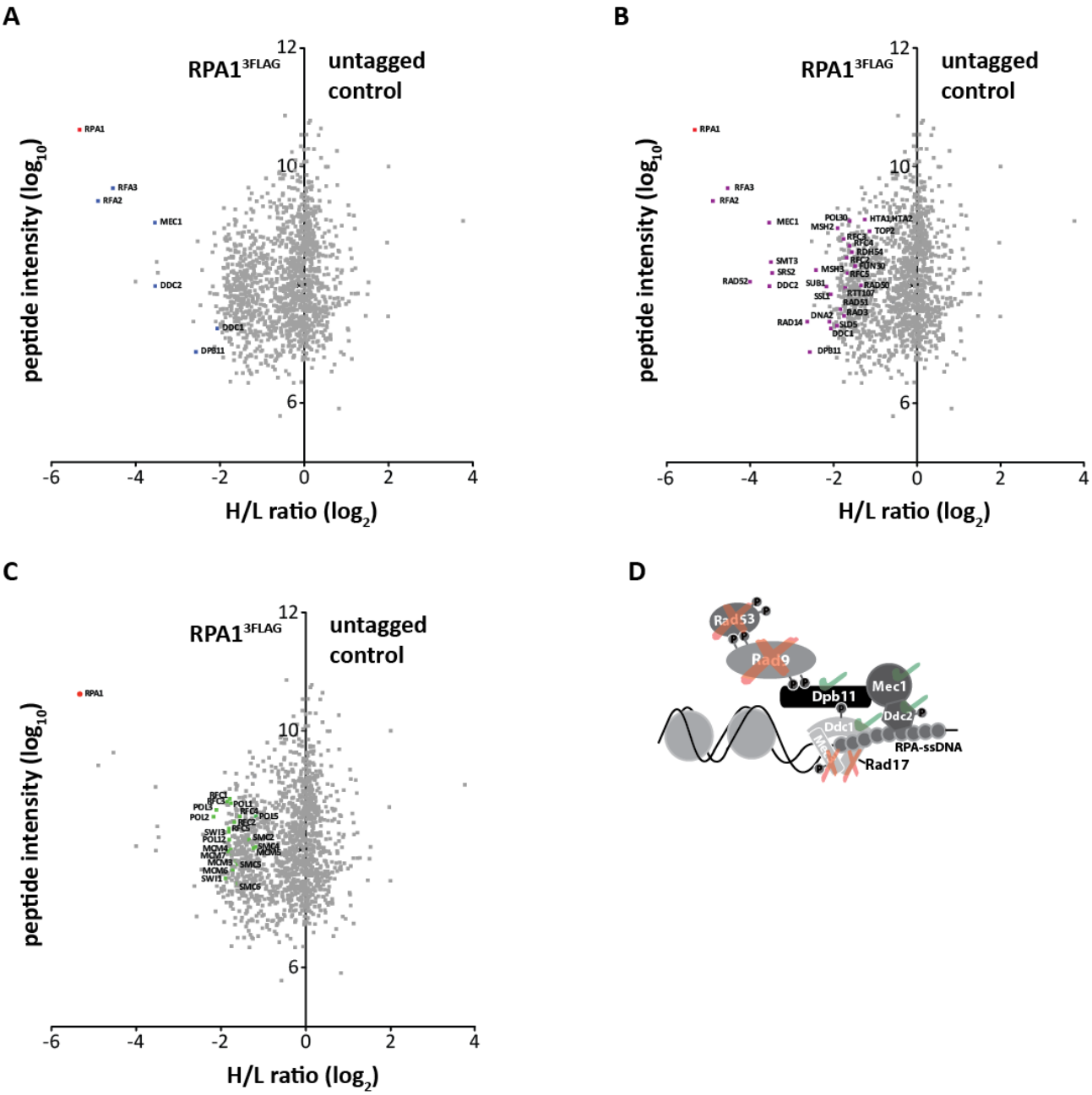

Fig. 6: putative RPA1-specific interactors acting in the DNA damage checkpoint response, DNA repair and replication identified by SILAC after DNA damage. SILAC-based RPA1^{3FLAG} pulldown to detect RPA1-specific interactors after MMS-induced DNA damage. **(A, B, C)** Plotted are SILAC ratios (RPA1^{3FLAG} tagged versus untagged control) for 1395 quantified proteins against the sum of the relevant peptide intensities. Proteins are coloured according to the values of MaxQuant Significance(B) (the measure of the standard deviation from the centre of the distribution, taking into account the dependence of the distribution on the summed protein intensity). **(A)** Blue, putative RPA1 interactors with significance(B)≤0.1 which are involved in the DNA damage checkpoint. **(B)** Purple, putative RPA1 interactors with significance(B)≤0.1 which are involved in DNA damage repair **(C)** Green, putative RPA1 interactors with significance(B)≤0.1 which are involved in DNA replication. **(D)** Depiction of the DNA damage checkpoint proteins recruited at the site of damage on chromatin. Proteins marked in green have been identified in SILAC-based RPA1^{3FLAG} pulldowns, red marks indicate components of the checkpoint complexes which could not be identified with this approach.

This expected outcome is likely due to the usage of MMS, a DNA damaging agent that leads to replication fork stalling and correspondent RPA-containing DNA repair intermediates in S-phase (275-281). On the contrary, DNA damage repair proteins appeared to be specifically enriched in the MMS-treated sample. Interestingly, the proteins showing the strongest enrichment are the KU complex (Yku70 and Yku80) and Rad52, some of the first DNA repair proteins recruited to a DSB.

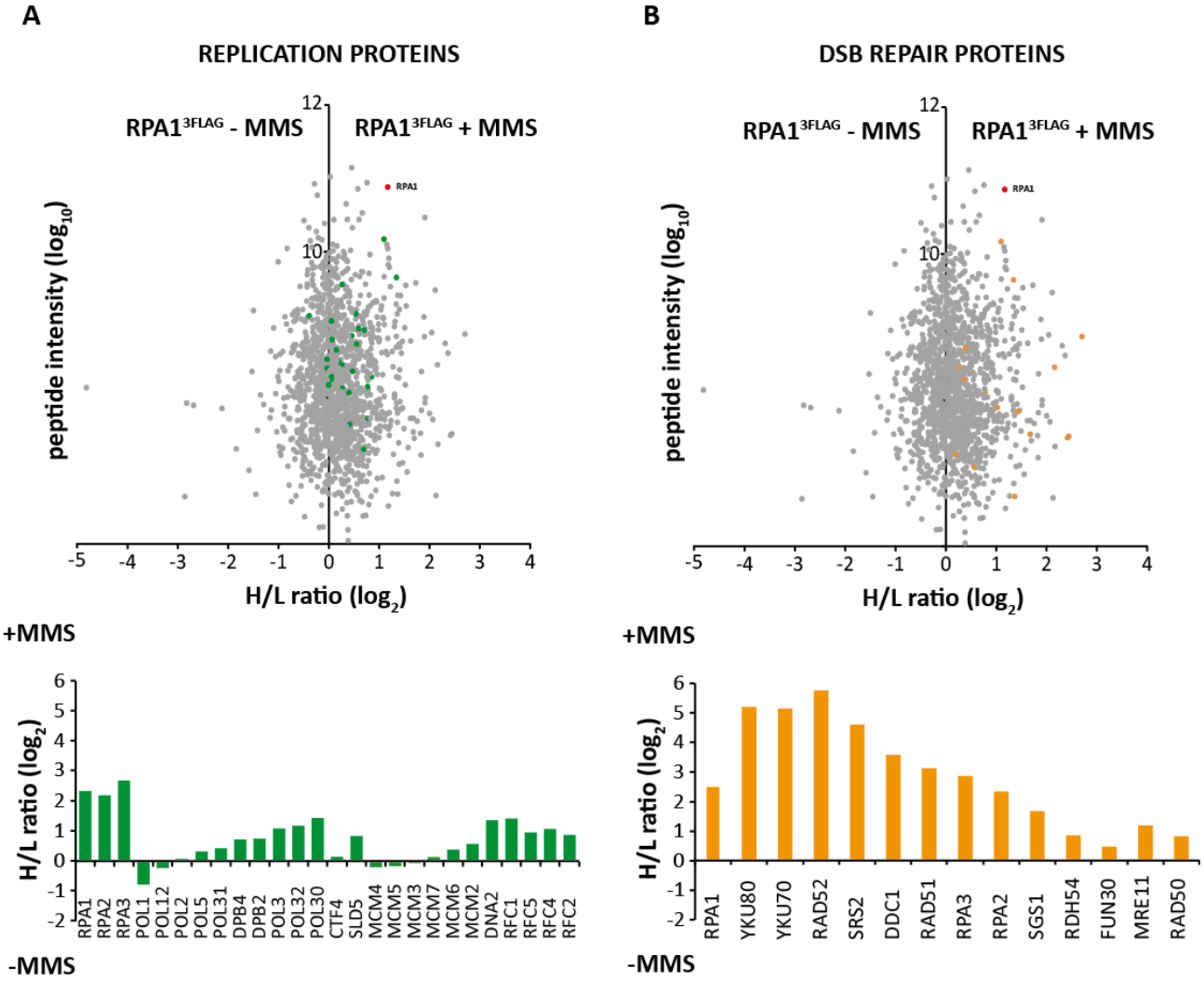

Fig. 7: putative RPA1-specific interactors in presence or absence of MMS-induced DNA damage. SILAC-based quantifications of RPA1^{3FLAG} interactors in MMS-treated and untreated cells. **(A, B)** Plotted are SILAC-ratios (MMS-treated cells versus untreated cells) for 1481 MS-quantified proteins against the sum of the relative peptide intensities. **(A)** Proteins coloured in green (upper panel) are involved in DNA replication. In the Lower panel are the identified DNA replication proteins and their relative SILAC ratios (MMS-treated/ untreated). **(B)** Proteins coloured in orange are involved in DSB repair. In the lower panel are shown the identified DSB repair proteins and their relative SILAC ratios.

Overall, the enrichment of DNA damage proteins in the RPA1^{3FLAG} pulldown performed after MMS treatment was not strong as could be expected, when compared to undamaged conditions. To better appreciate the differences between RPA interactors before and after DNA damage a similar experiment performed in cells synchronised outside of S-Phase,

could be helpful, since this strategy would allow to exclude form the analysis the background of replicative proteins.

Overall, using RPA as bait for pulldowns I was able to purify chromatin-bound proteins and DDR proteins with significant coverage. However, while the described method was able to identify most proteins involved in the formation of DNA damage checkpoint complexes, Rad9 and Rad53, the two most peripheral proteins of the checkpoint signaling complexes were notably absent (Fig. 6D).

4.1.2 ChIP-MS of HTA1^{3FLAG} for purification of DNA damage checkpoint complexes assembled onto intact chromatin

Histones close to DNA damage sites are known to be evicted (282-284). The spreading of checkpoint signals (like γ H2A) into surrounding chromatin and the ability of checkpoint proteins such as Rad9 to bind to modified histones suggests that checkpoint complexes may also be recruited at sites further away from the damage, within intact chromatin. The function of these checkpoint complexes is currently unclear, but they could serve as a way of amplification of the checkpoint signal.

ChIP-MS directed against H2A were performed to elucidate if checkpoint proteins can spread into intact chromatin surrounding DNA damage, and also in order to serve as specificity control for the RPA ChIP-MS experiment. Therfore, I directed my purification towards histone HTA1 using the same experimental design described in 4.1.1. I again employed formaldehyde crosslinking and used affinity chromatography against HTA1^{3FLAG} to purify checkpoint proteins bound to DNA, followed by SILAC-based quantitative mass-spectrometry to measure their composition.

In the experiment shown in figure 8B , asynchronous cells containing either HTA1^{3FLAG} or its untagged wildtype version were used to purify HTA1-specific interactors in presence of the DNA damaging agent MMS. After MS analysis 159 putative HTA1 interactors were identified in flag pulldowns performed after SILAC. The major hits, after the core histones themselves, consisted of a wide population of proteins and protein complexes involved in chromatin functions. Notably, the components of all the major chromatin remodeling complexes were present, like FACT, DSIF, ISWI, RSC SAGA, INO80, Paf1,SWI/SNF, NuA3, as well as histone modifying enzymes (histone chaperones for histone exchange, deacetylases, acetyltransferases), cohesins, RNA Polymerase 2, and transcription factors.

With this approach I aimed to purify proteins bound to a wider chromosomal region than the site of damage itself, and at the same time provide a specificity control for the RPA-pulldown previously described. Interestingly, no DDR proteins were detected in this experiment after mass spectrometry analysis. While this may be seen as an indication that DNA damage repair proteins are absent from undamaged chromatin, it needs to be pointed out that this outcome may also be simply due the low number of proteins identified (only 500 hits were obtained after MS-analysis). Also, another explanation might be that DNA damage specific signals are diluted by an excess of non-damaged chromatin. Lastly, it currently cannot be excluded that 1 h after MMS treatment the majority of repair proteins

are still recruited to the sites close to the damage, limiting their spreading into surrounding chromatin.

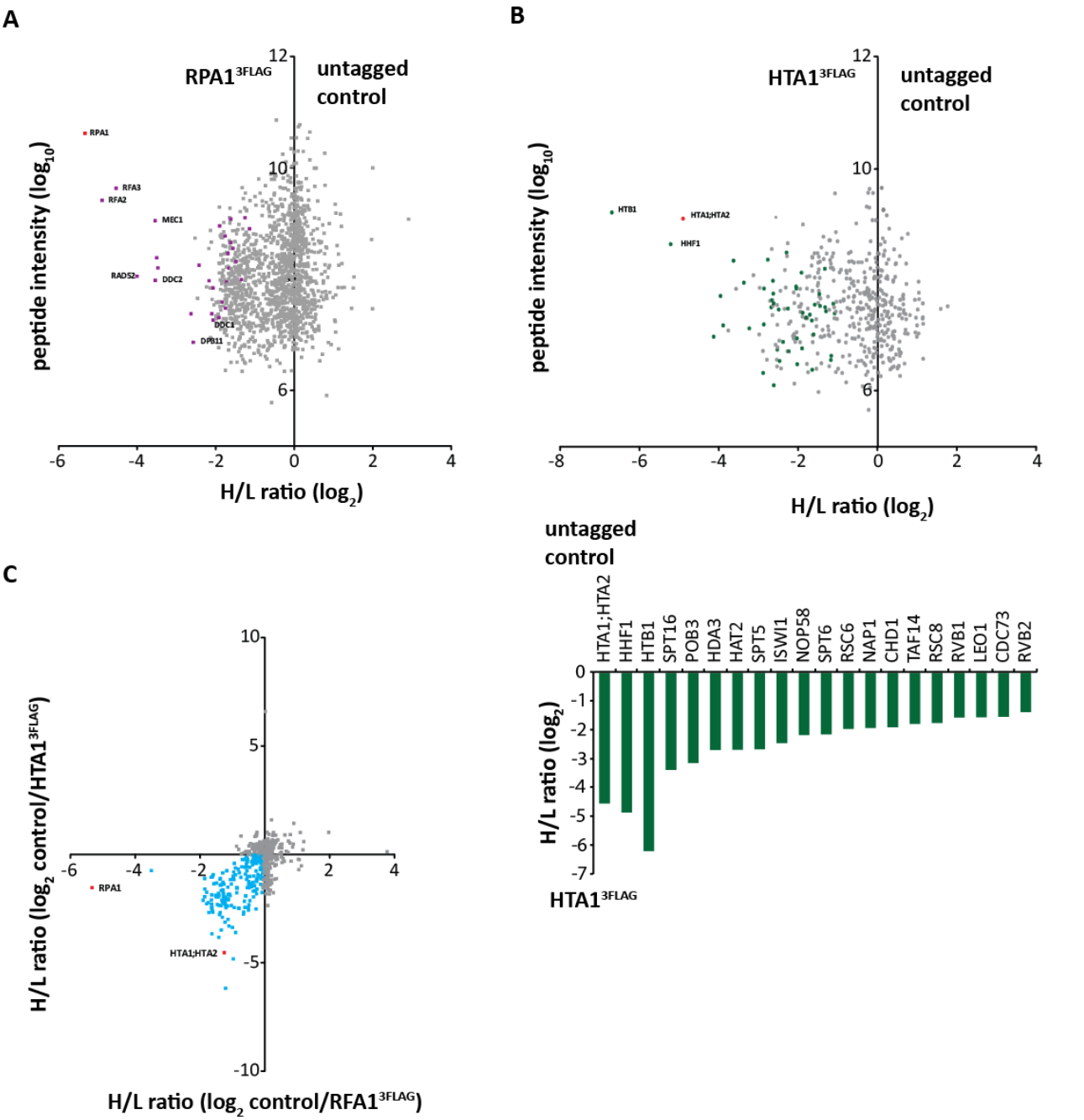

Fig. 8: putative H2A-specific interactors in presence of MMS-induced DNA damage. A comparison between RPA1^{3FLAG} and HTA1^{3FLAG} interactors identified in SILAC-based pulldowns, after MMS-induced DNA damage. **(A)** SILAC ratios (RPA1^{3FLAG} versus untagged control) for 1395 quantified proteins against the sum of the relevant peptide intensities, after RPA1^{3FLAG} pulldown in presence of MMS (see Fig. 6). In purple are the putative RPA1 interactors involved in DNA repair and proteins of the DNA damage checkpoint complexes are labelled. **(B)** SILAC experiment performed to detect H2A-specific interactors in HTA1^{3FLAG} pulldown after MMS-induced DNA damage. Plotted are the SILAC ratios (HTA1^{3FLAG} versus untagged control) for 500 quantified proteins against the sum of the relevant peptide intensities. All putative HTA1-specific interactors with significance(B)≤0.7 are marked in dark green. In the bar graph below are the identified HTA1 interactors that are components of chromatin remodeling complexes, and their relative SILAC ratios. **(C)** SILAC ratios of RPA1^{3FLAG} interactors identified in experiment in figure 6 plotted against SILAC ratios of HTA1^{3FLAG} interactors identified in experiment in **(B)**. The plot shows correlation between the proteins enriched by RPA1^{3FLAG} pulldowns and HTA1^{3FLAG} pulldowns after MMS-induced DNA damage. In blue are proteins enriched in both RPA1^{3FLAG} and HTA1^{3FLAG} pulldowns.

To circumvent these problems the use of specific antibodies for the DNA damage modified form of H2A (γ H2A) might be indicated.

Figure 8C shows the correlation between the proteins enriched by both strategies, (with RPA1^{3FLAG} and with HTA1^{3FLAG} pulldown, represented in the figures 6 and 8B respectively) The 275 proteins enriched by both strategies consist to a large extent of chromatin modifying factors. Specific binding to RPA1^{3FLAG} and HTA1^{3FLAG} appears to weekly correlate, suggesting that also with the RPA1^{3FLAG} strategy a certain amount of surrounding chromatin is enriched. These findings suggest that our ability to specially resolve proteins complexes associated directly with the DNA damage site or with the surrounding chromatin is limited.

In conclusion, I was able to develop a ChIP-MS for DNA damage sites. So far with this technique I was able to enrich many proteins recruited to sites of damage via the RPA1 pulldowns. However, recruitment to distal regions under DNA-damage conditions via HTA1^{3FLAG} pulldown only showed chromatin-associated factors, but not those involved in the DNA damage response.

4.2 DNA-damage induced interaction of Rad9 and Dpb11 in G1

4.2.1 DNA damage induces phosphorylation of Rad9 S/TP sites and binding of Rad9 to Dpb11

Orthologs of Rad9 and Dpb11 are known to interact in different organisms (143, 175, 206, 231). In budding yeast the two proteins were initially found to interact exclusively in the M-phase of the cell cycle (143). The interaction appeared to be strictly cell-cycle regulated and under normal conditions it relies on a CDK-dependent phosphorylation of two residues on Rad9-S462 and -T474. After being phosphorylated these S/TP sites provide a binding surface for BRCT domains I and II of Dpb11. In S. cerevisiae Cdc28 is the essential CDK regulating the entire cell cycle progression and will be referred to as CDK hereafter.

During this study I found a second, DNA-damage-dependent mode of interaction between Rad9 and Dpb11. Specifically I observed that Rad9^{9myc} from cell extracts of cells treated wit the DNA-damaging agent MMS showed increased interaction with ^{GST}Dpb11 in pull-down experiments (Fig. 9A). Strikingly, the DNA damage treatment with the DSBs-inducing agent phleomycin resulted in an increased interaction of Rad9^{9myc} with ^{GST}Dpb11 even in G1-arrested cells which is not observed under non-damaging conditions (Fig. 9A and 9B). After phleomycin treatment Rad9 undergoes a DNA-damage-dependent phospho-shift (186, 188-190) and Dpb11 associates with this hyperphosphorylated form of Rad9 (Fig. 9A). In contrast, in M-phase cell extracts Rad9^{9myc} was able to interact with ^{GST}Dpb11 even in the absence of DNA damage treatment (Fig. 9B), consistent with previous result on the CDK regulation of Rad9.

In order to test whether the DNA-damage triggered interaction was depending on phosphorylation of the same S/TP motives on Rad9, we made use of previously generated

phospho-specific antibodies directed against the Rad9-epitopes containing phosphorylated forms of S462 and T474 (143). I performed Rad9 immunoprecipitation from extracts of cells arrested in G1 or G2/M phase respectively (Fig. 10A) and observed that, while in G2/M arrested cells the two S/TP sites were phosphorylated in both damaged and undamaged cells (consistent with these sites being modified by CDK), in the case of G1 arrest, cells displayed the Rad9 phosphorylation only when treated with phleomycin (note that anti-Rad9-T474^{P} is highly specific for the phosphorylated form, while anti-Rad9-S462^{P} retains some binding to the unmodified form).

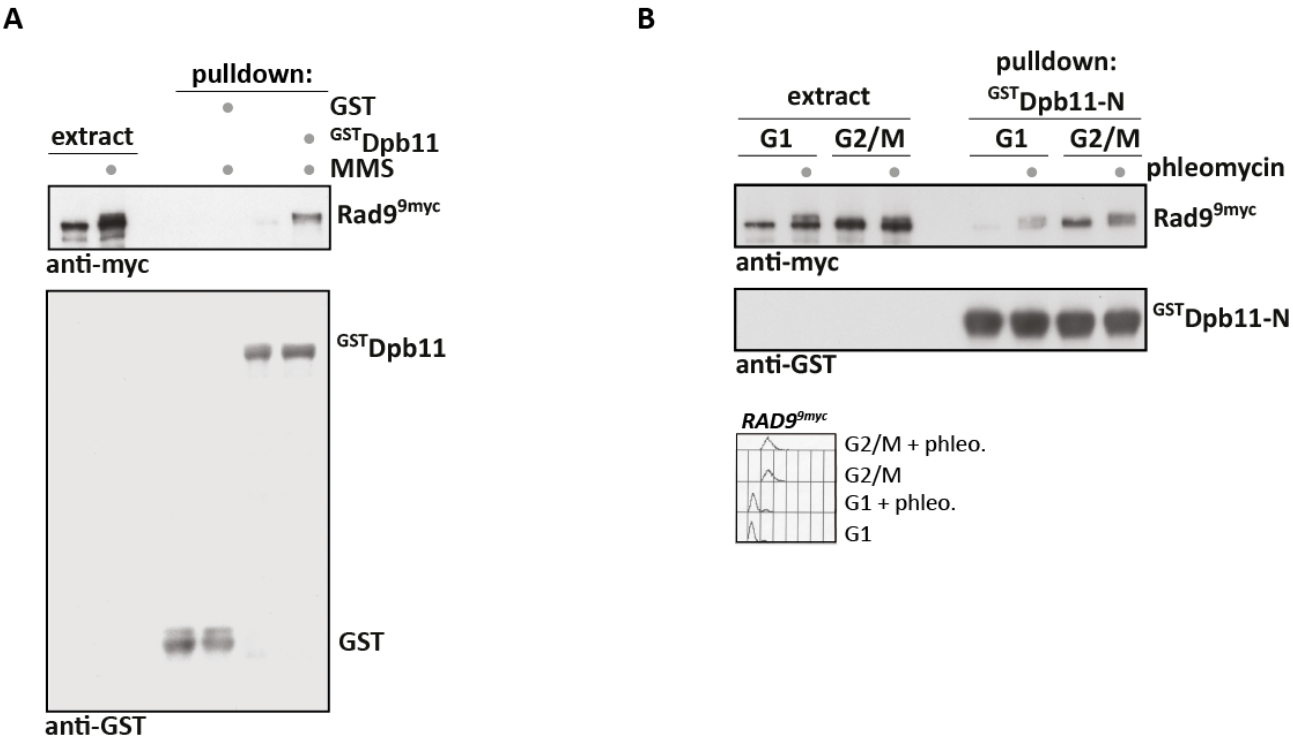

Fig. 9: DNA-damage-induced interaction of Dpb11 and Rad9. DNA damage stimulates the Rad9-Dpb11 interaction in cell extracts. **(A)** Pulldown with recombinant ^{GST}Dpb11 and extracts of asynchronous cells after MMS treatment shows damage-induced interaction of Rad9 and Dpb11. **(B)** GST pulldown experiment with ^{GST}Dpb11-N (contains BRCT I and II, which is the Rad9 interaction site) and extracts from Rad9^{9myc} expressing cells arrested in G1 (α -factor arrest) or M phase (nocodazole arrest) and treated with phleomycin or mock treated. FACS profiles are shown below.

The anti-Rad9-T474^{P} antibody can also detect Rad9 S/TP phosphorylation from cell extracts. In figure 10B we used this antibody to detect Rad9-T474 phosphorylation in extracts from G1 or G2/M arrested cells, before and after damage. Alongside with wild type cells we tested a strain containing the *rad9-ST462,474AA* mutant as a specificity control for the antibody, and as previously observed in the Rad9 pulldowns I could detect Rad9-T474 phosphorylation in undamaged M-phase cells, as well as damaged G1- and M-phase cells, but not in undamaged G1-cells; moreover cells expressing the *rad9-ST462,474AA* variant (referred to as *rad9-AA* hereafter) did not show any reactivity with the Rad9-T474^{P} antibody, confirming specificity (Fig. 10B)

Taken together these results suggest that there are two scenarios in which Rad9 and Dpb11 interact: in the first scenario the interaction follows the cell cycle and depends on CDK, given the high CDK activity, in G2/M phase Rad9 is phosphorylated on the S/TP motives and binds to Dpb11 constitutively. In the second scenario DNA damage can trigger the same phosphorylation on Rad9 independently of CDK, therefore Rad9 and Dpb11 can interact in G1 phase only after DNA damage.

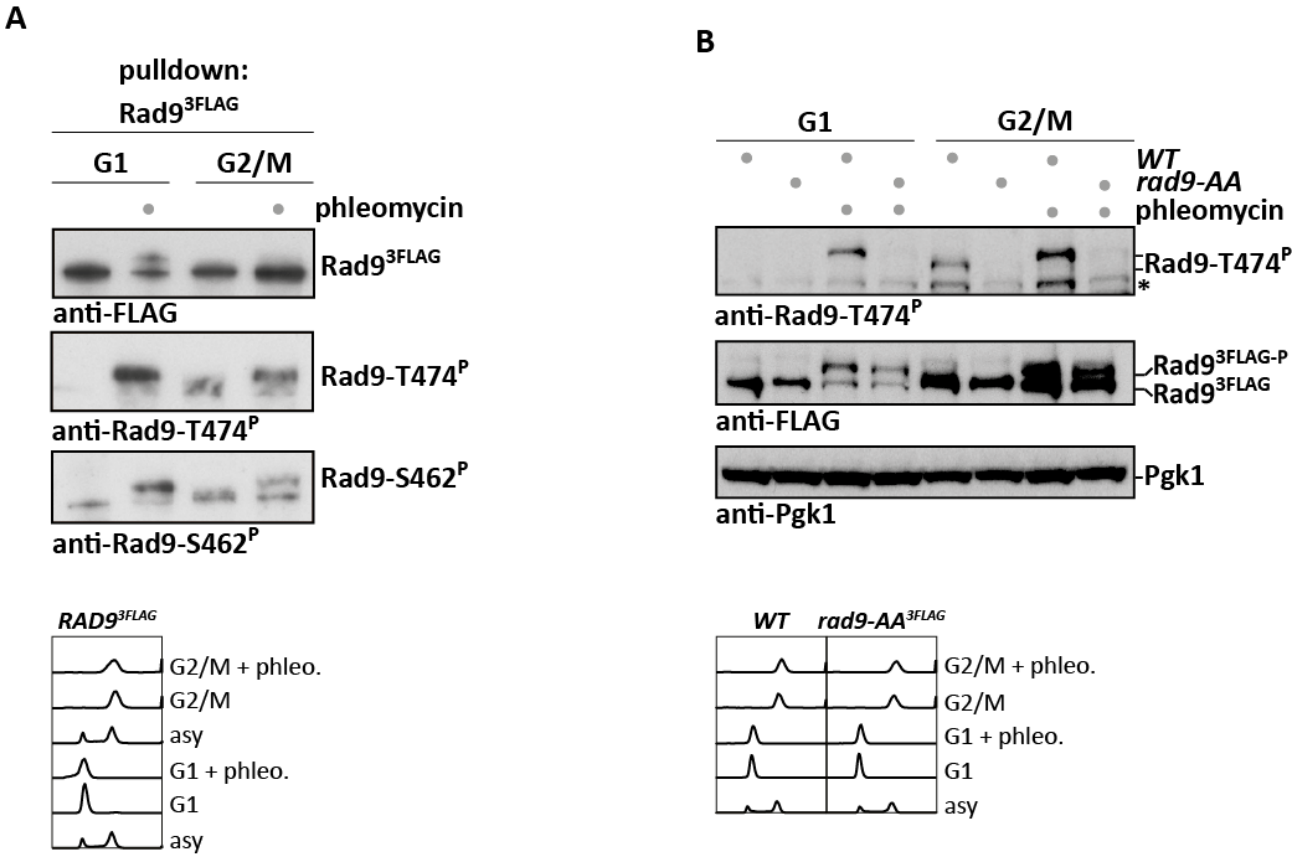

Fig. 10: phosphorylation of Rad9-S462 and -T474 is stimulated by DNA damage. DNA damage induction via phleomycin treatment results in Rad9-S462 and –T474 phosphorylation in extracts from G1-arrested cells. **(A)** Rad9^{3FLAG} was purified by FLAG-IP from cells arrested in G1 (α-factor arrest) and treated with phleomycin or mock treated. Phosphorylation of Rad9 S/TP sites was determined using Rad9-S462^{P} and Rad9-T474^{P} phosphorylation-specific antibodies. FACS profiles are shown below. **(B)** Cells arrested in G1 (α-factor arrest) or G2/M (nocodazole arrest) and treated with phleomycin or mock treated were used to prepare whole cell extract, which was probed with the Rad9-T474^{P} phosphorylation-specific antibody. The *rad9-AA* mutant strain was used as specificity control. A Pgk1 immunoblot serves as loading control. The asterisk denotes a crossreactive band. FACS profiles of the respective experiments are shown below.

The CDK activity in G1 phase is nearly absent, nonetheless, to completely rule out involvement of CDK in the DNA-damage-dependent phosphorylation of these S/TP sites in G1 I used a strain containing the *cdc28-as1* mutant allele, which is inactivated by treatment with the ATP analog 1-NM-PP1. As shown in figure 11A when CDK was inactivated in G1-arrested cells there was no loss of the Rad9-T474 phosphorylation after treatment with phleomycin, while in undamaged G2/M arrested cells the CDK-dependent phosphorylation of Rad9-T474 was effectively inhibited, in line with previous results (Fig. 11B, 143). Interestingly phleomycin treatment triggered phosphorylation of Rad9 in M-phase-arrested

cells even after CDK inhibition (Fig. 11B), it can be therefore concluded that the damage-induced phosphorylation of the Rad9 S/TP sites is independent of the cell cycle phase and CDK activity.

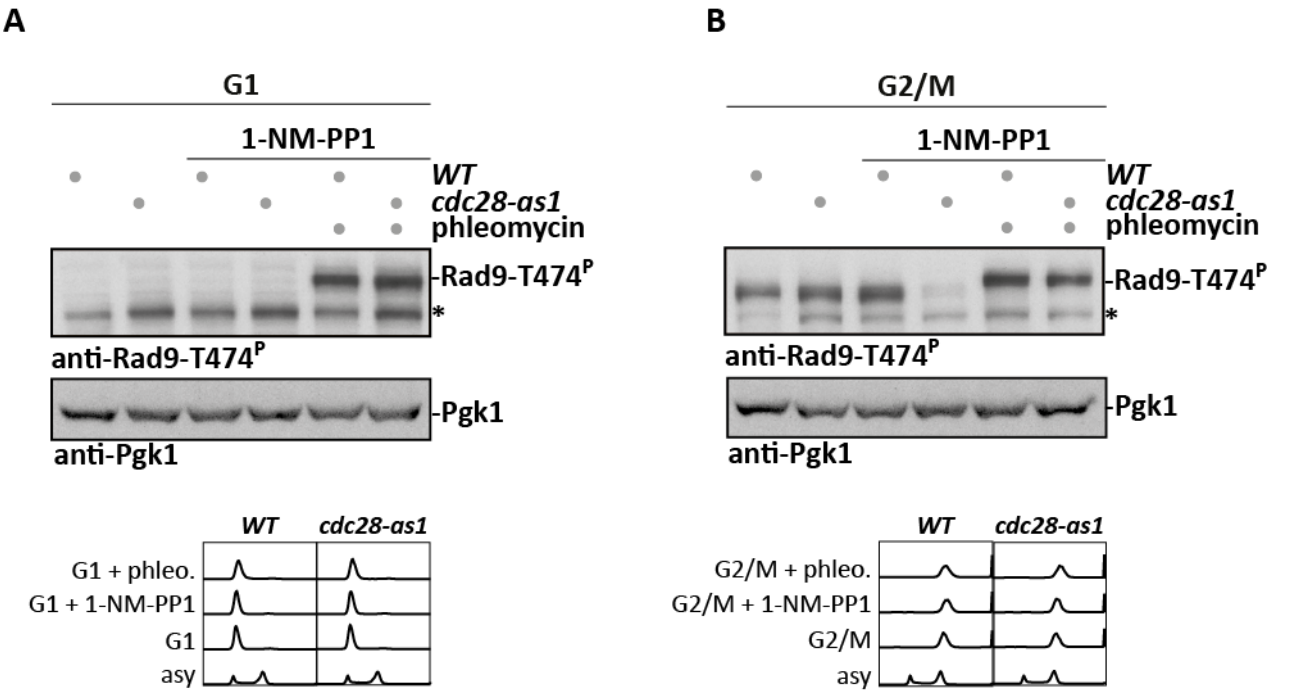

Fig. 11: **CDK inhibition does not affect DNA-damage-induced Rad9 S/TP phosphorylation.** Inhibition of an analogue-sensitive mutant of Cdc28 did not affect the DNA-damage-dependent phosphorylation of Rad9-T474 in cell extracts from G1- or G2/M-arrested cells **(A)** 1-NMPP1 was used to inhibit CDK in G1-arrested *cdc28-as1* cells, but this did not affect Rad9-T474 phosphorylation after DNA damage. Pgk1 immunoblot serves as loading control. The asterisk denotes a crossreactive band FACS-based DNA content measurement are shown below. **(B)** As in **(A)**, but with G2/M-phase arrested cells. 1-NM-PP1 treatment abolished T474 phosphorylation in undamaged cdc28-as1 cells, demonstrating that CDK is effectively inhibited. In contrast, after phleomycin treatment Rad9-T474 is efficiently phosphorylated, even in the absence of active CDK. Pgk1 immunoblot serves as loading control. The asterisk denotes a crossreactive band. FACS-based DNA content measurement are shown below.

4.2.2 DNA-damage-induced phosphorylation of the Rad9 S/TP sites depends on the apical checkpoint kinases Mec1 and Tel1 and the Rad9 SCD

When DNA damage occurs, DNA damage checkpoint kinases Mec1 and Tel1 target several S/TQ motives on Rad9 (186, 189, 190), which are clustered in the S/TQ cluster domain or SCD. Given the proximity of the S/TP sites to the SCD, I tested whether these sites could be phosphorylated by Mec1 and Tel1 in response to DNA damage. As can be seen in figure 12A, Rad9-T474 phosphorylation in G1-arrested, phleomycin treated cells was reduced in *mec1Δ* and *tel1Δ* mutant cells and completely abolished in a *mec1Δ tel1Δ* double mutant. In contrast, when deletions of the effector kinases Rad53 and Chk1 were used (alone or in combination) this had no effect on the DNA-damage-dependent phosphorylation of the S/TP sites in G1 (Fig. 12B).

These data suggest that, in addition to hyperphosphorylating Rad9 in the SCD cluster, Mec1 and Tel1 could also target Rad9 S/TP sites. However, from *in vitro* tests with purified Rad9 and Mec1 containing extracts, I could not gather evidence for a direct action of the

Mec1 kinase on Rad9 S/TP sites (data not shown), therefore I proceeded to test the possibility of an indirect effect of the apical checkpoint kinases: for example the Mec1/Tel1-dependent phosphorylation of the SCD could be a priming event for the S/TP phosphorylation, alternatively, Mec1 and Tel1 could promote the chromatin recruitment of a factor involved in the S/TP site phosphorylation, such as the kinase acting on Rad9 or Rad9 itself.

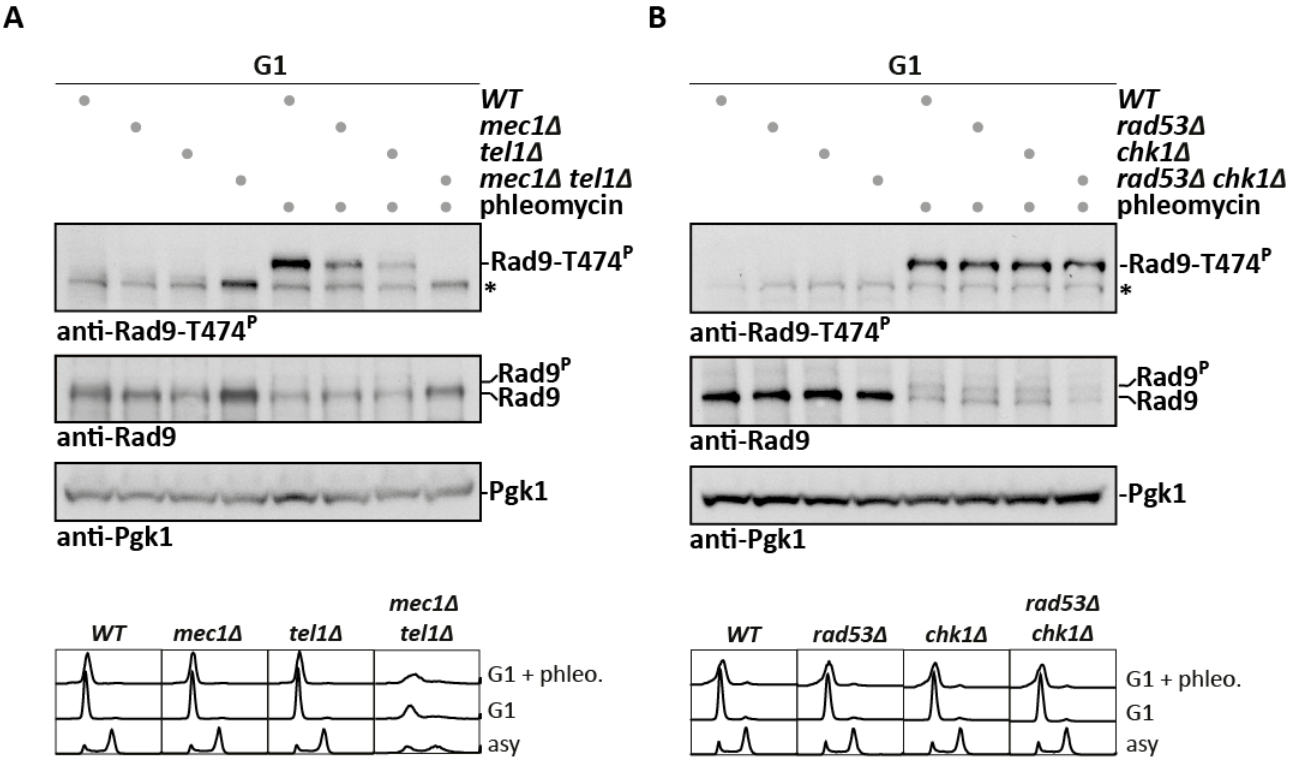

Fig. 12: Mec1 and Tel1 are required for Rad9 S/TP phosphorylation after DNA damage. Rad9-T474 phosphorylation after DNA damage depends on the apical checkpoint kinases Mec1 and Tel1. **(A)** G1-arrested cells with indicated genotypes were treated with phleomycin, Rad9-T474 phosphorylation was visualized by immunoblotting. Pgk1 immunoblot serves as loading control. An asterisk denotes a crossreactive band. FACS-based DNA content measurement are shown below.**(B)** Rad9-T474 phosphorylation after DNA damage is independent of checkpoint effector kinases Chk1 and Rad53. G1-arrested cells with indicated genotypes were treated with phleomycin and subjected to analysis with immunoblots for detection of Rad9-T474 phosphorylation. Pgk1 immunoblot serves as loading control. An asterisk denotes a crossreactive band. FACS-based DNA content measurement are shown below.

In order to corroborate this hypothesis I tested the phosphorylation of a Rad9 mutant harboring six S/T to A exchanges in the S/TQ cluster domain (SCD) (*rad9-6AQ*, 190), as seen in figure 13A, this mutant abolished phleomycin-induced phosphorylation of Rad9 S/TP sites in G1. In contrast, CDK-dependent phosphorylation of these sites in M-phase was unaffected by the *rad9-6AQ* mutant (Fig. 13B).

In addition I also tested the Rad9- S1129A mutant, as previous work had suggested that phosphorylation of the SCD would induce Rad9 dimerization (243), however the dimerization-defective *rad9-S1129A* variant showed normal phosphorylation of Rad9-T474 both in G1 after DNA damage and in G2/M-phase (Fig. 13A and 13B).

These data reveal the importance of the apical checkpoint kinases and the SCD phosphorylation as an event necessary for the S/TP phosphorylation and consequently the DNA-damage-dependent interaction of Rad9 and Dpb11.

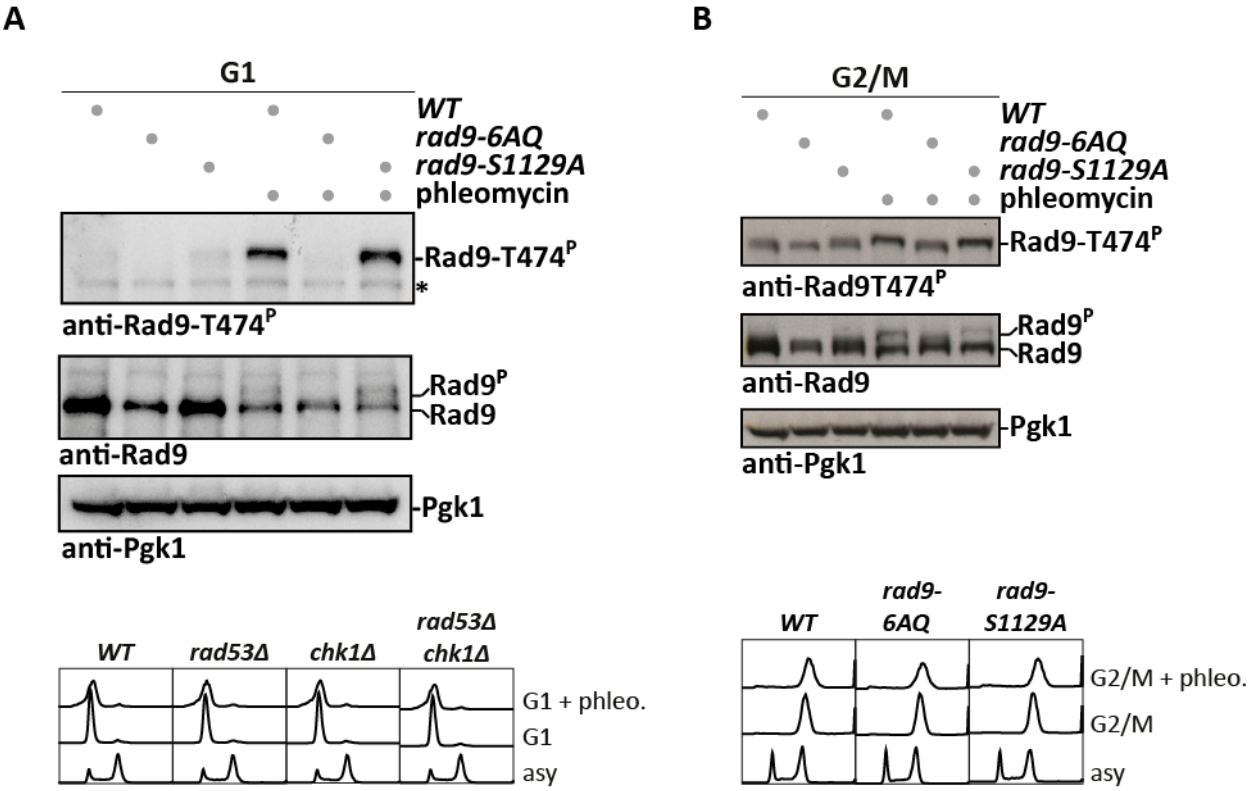

Fig. 13: integrity of the Rad9 SCD domain is important for DNA-damage-induced Rad9 S/TP phosphorylation. Phosphorylation of the Rad9 SCD domain is required for damage-induced phosphorylation of Rad9-T474 **(A)** Phelomycin treatment and immunoblotting of WT, *rad9-6AQ* and *rad9-S1129A* strains arrested in G1. Rad9-T474 phosphorylation was visualized by immunoblotting. Pgk1 immunoblot serves as loading control. An asterisk denotes a crossreactive band. FACS profiles are shown below. **(B)** Cell extracts of G2/M arrested cells treated as in **(A)** were probed with indicated antibodies. Pgk1 immunoblot serves as loading control.FACS-based DNA content measurements are shown below.

4.2.3 Chromatin-recruitment of Rad9 is required for phosphorylation of the Rad9 S/TP sites

According to previous studies Rad9 can be recruited to chromatin via two different pathways, commonly referred to as the "histone pathway" (181-184, 284) and the "Dpb11 pathway" (143, 209). While the "histone pathway" is believed to be active throughout the cell cycle, it was suggested that the "Dpb11 pathway" is confined to the G2/M- or S-phases given the requirement for resected DNA, a process known to be limited in G1, and CDK phosphorylation of Rad9. Given our findings I decided to investigate the possible role of the "histone pathway" and the "Dpb11 pathway" in the recruitment of Rad9 to chromatin, and its phosphorylation on the S/TP sites following DNA damage in G1.

One way in which Rad9 is recruited to chromatin via the "histone pathway" is through interaction of its Tudor domain with methylated form of H3-K79 (181, 184). This modification is carried out by the histone methyltransferase Dot1 (200). I tested the recruitment of Rad9 to damaged chromatin in presence or absence of Dot1 via ChIP, using

the GAL-HO system to induce a site-specific, non-repairable DSB at the MAT locus (285). I observed that while Rad9 became enriched in the chromatin region surrounding the DSB in WT cells, Rad9 enrichment was strongly decreased in *dot1 Δ* cells (Fig. 14).

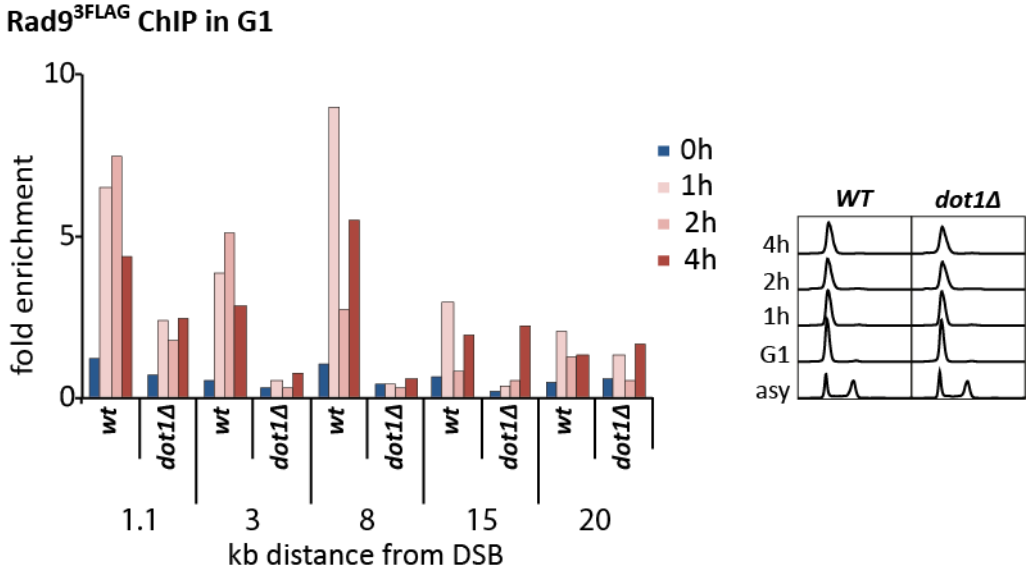

Fig. 14: Dot1 promotes Rad9 association with damaged DNA (DSB). Rad9 recruitment at a DSB is impaired in *dot1Δ* cells. Induction of an irreparable DSB at MAT locus was achieved using galactose-induced HO endonucleas. ChIP was performed against $Rad9^{3FLAG}$ to regions located from 1.1 kb to 8 kb distal of the DSB site and 1, 2 and 4 h after DSB induction. On the right are shown FACS-based DNA contents.

Consistent with a lack of Rad9 recruitment to damaged chromatin, I also found that deletion of Dot1 caused a strong reduction of Rad9-T474 phosphorylation in phleomycin-treated G1 cells (Fig. 15A).

To make sure that reduction in the S/TP sites phosphorylation was due to the strong decrease in Rad9 recruitment at damaged chromatin in *dot1Δ* cells (so to a defect in the "histone pathway"), I introduced the corresponding H3-K79-binding-defective mutation in the Rad9 Tudor domain (*rad9-Y798Q,* 181) and I observed a very similar reduction in S/TP sites phosphorylation in *rad9-Y798Q* cells.

Importantly the effects of both *dot1Δ* and *rad9-Y798Q* backgrounds were specific for the DNA-damage-dependent phosphorylation of the Rad9 S/TP sites, since neither a *dot1Δ* nor a *rad9-Y798Q* mutation diminished CDK-dependent phosphorylation of Rad9-T474 in M-phase (Fig. 15B and 15C).

Given the lack of S/TP phosphorylation of Rad9 in the *dot1Δ* background, I expected Rad9 to be unable to bind Dpb11 under these conditions. Indeed when I induced the Rad9-Dpb11 interaction with phleomycin treatment in G1-arrested cells, I observed a reduced association of Rad9 in ^{GST}Dpb11 pulldowns in the absence of Dot1 (Fig. 16A).

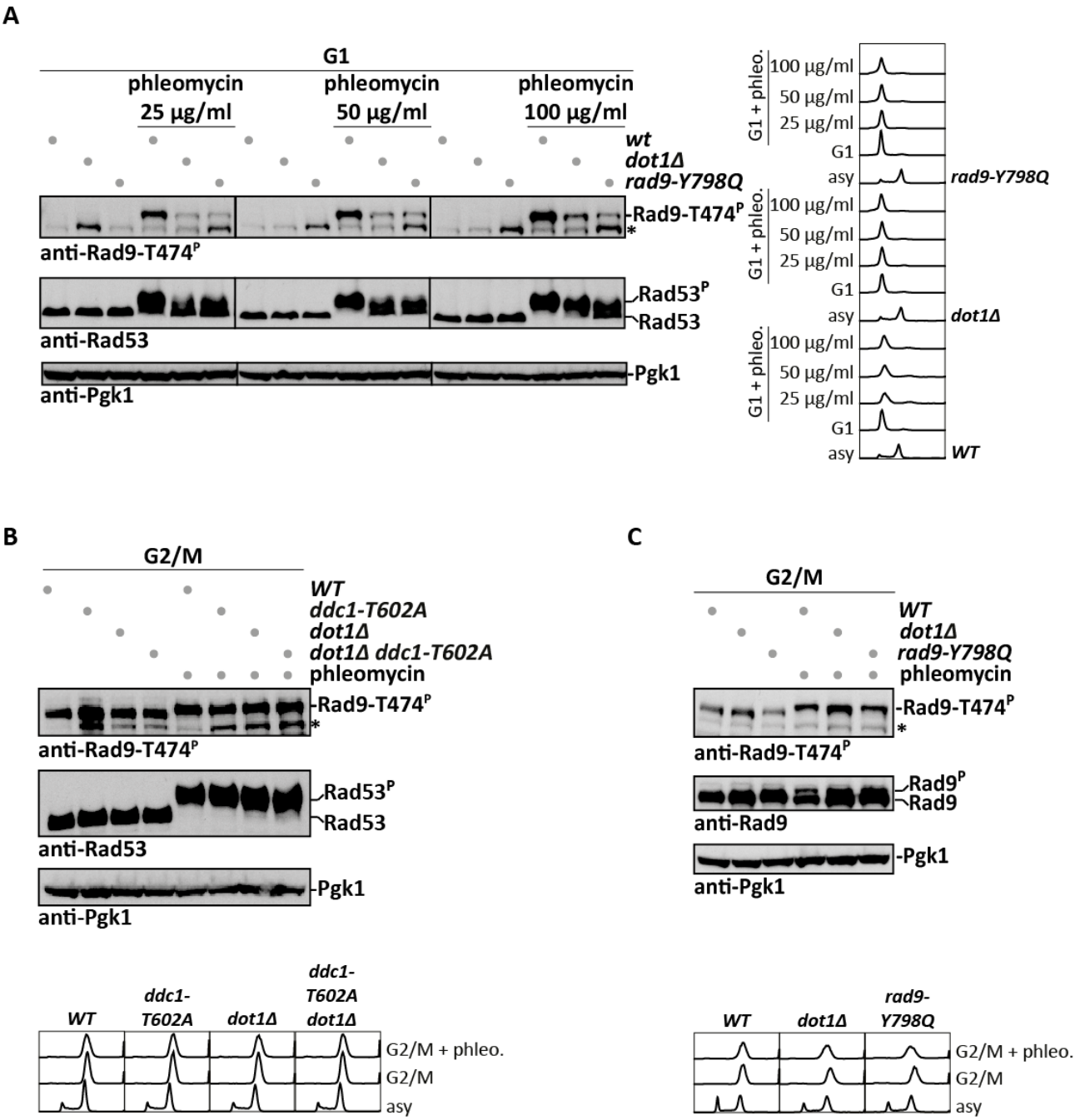

Fig. 15: Involvement of Dot1 and Rad9 recruitment pathways in Rad9-T474 phosphorylation. The DNA-damage-dependent phosphorylation of Rad9-T474 is dependent on Dot1 and the Tudor domain of Rad9 in G1 but not in G2/M phase **(A)** G1-arrested cells with indicated genotypes were treated with phleomycin, Rad9-T474 phosphorylation was visualized by immunoblotting. RAD9 mutant conditions that impair Rad9 recruitment to chromatin (*dot1Δ* and *rad9-Y798Q*) lead to defects in Rad9-T474 phosphorylation and Rad53 phosphorylation, when arrested in G1 in a manner dependent on phleomycin dosage. Phleomycin concentrations tested were 50 µg/ml (standard concentration), 25 µg/ml and 100 µg/ml. Rad53 activation was measured by detecting its phospho-shift on 10% SDS-gels using anti-Rad53 antibodies. Pgk1 immunoblot serves as loading control. An asterisk denotes a crossreactive band. On the right are shown FACS-based DNA content measurements. **(B)** *dot1Δ* cells retain S/TP phosphorylation of Rad9 in G2/M. Extracts from G2/M-arrested and phleomycin-treated cells of the indicated mutant background were probed with the indicated antibodies. Pgk1 immunoblot serves as loading control. An asterisk denotes a crossreactive band. FACS-based DNA content measurement are shown below. **(C)** A defect in the Rad9 Tudor domain (*rad9-Y798Q*) does not abolish Rad9-T474 phosphorylation S/TP phosphorylation in G2/M cells after DNA damage. Extracts from G2/M-arrested and phleomycin-treated cells of the indicated mutant background were probed with the indicated antibodies. Pgk1 immunoblot serves as loading control. An asterisk denotes a crossreactive band. FACS-based DNA content measurement are shown below.

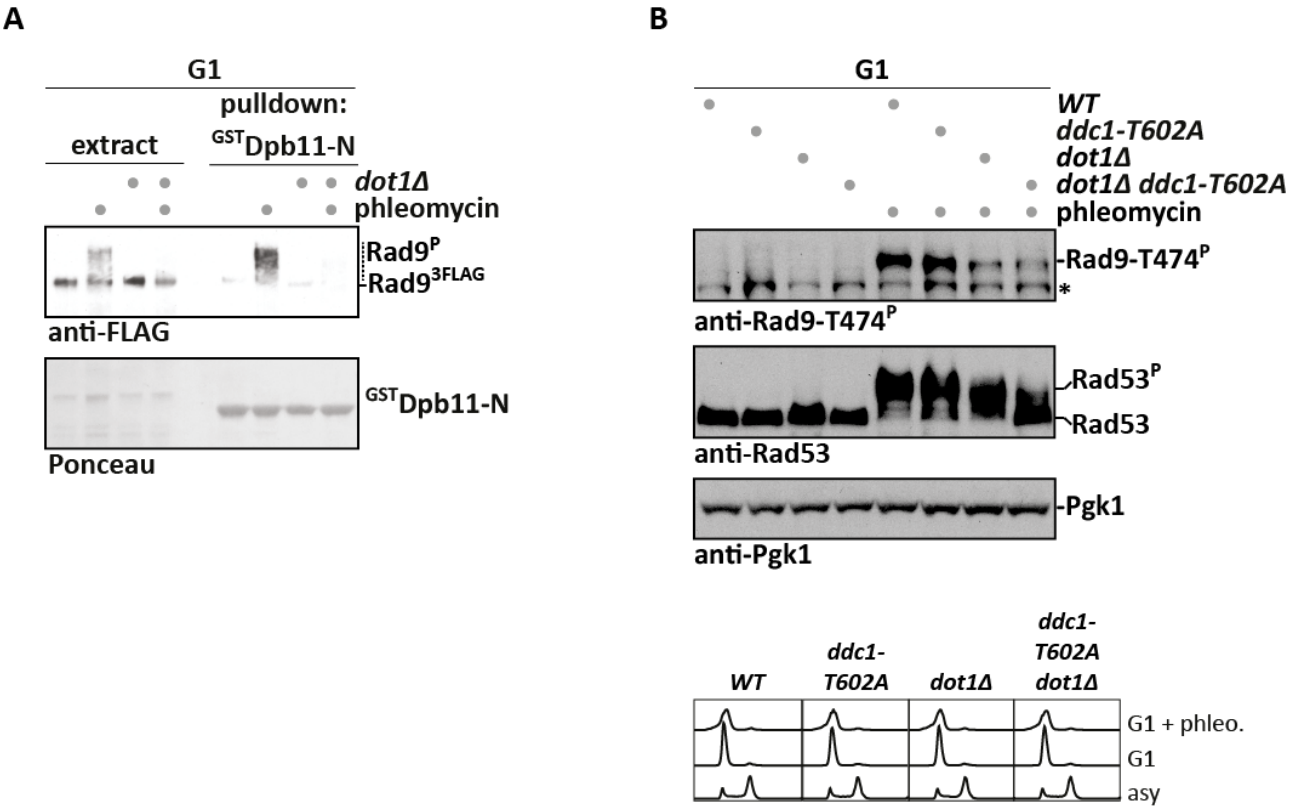

Fig. 16: **Dot1 is required for DNA-damage-induced interaction with Dpb11.** Dot1 is important for Rad9-Dpb11 binding and Rad9 S/TP phosphorylation in G1 after DNA damage **(A)** GST pulldown experiment with ^{GST}Dpb11-N (contains BRCT I and II, which is the Rad9 interaction site) and extracts from cells expressing Rad9^{3FLAG} in a WT or *dot1Δ* background, arrested in G1 (α-factor arrest) and treated with phleomycin or mock treated. **(B)** G1-arrested cells with indicated genotypes were treated with phleomycin and Rad9-T474 phosphorylation was visualized by immunoblotting. Pgk1 immunoblot serves as loading control. An asterisk denotes a crossreactive band. FACS-based DNA content measurement are shown below.

Although strongly reduced compared to wild-type cells, some residual DNA-damage-dependent Rad9-T474 phosphorylation can be observed in *dot1Δ* and *rad9-Y798Q* cells in G1. Moreover, the residual phosphorylation seemed to augment with increasing dosage of phleomycin (Fig. 15A). Since M-phase cells could compensate a defect in the "histone pathway" by Dpb11-dependent Rad9 recruitment ("Dpb11 pathway"), I tested if the "Dpb11 pathway" would be responsible for the residual phosphorylation of Rad9. However, when I introduced the Dpb11-binding deficient *ddc1-T602A* allele either alone or in combination with *dot1Δ* I did not observe any additional defect in Rad9-T474 phosphorylation in G1 (Fig. 16B).

From these results I could conclude that in G1, the DNA-damage-dependent phosphorylation of Rad9 on S/TP sites and its consequent interaction with Dpb11 are dependent on the "histone pathway".

4.2.4 Forced Rad9 recruitment to damaged chromatin allows efficient Rad9 S/TP sites phosphorylation

The data so far described suggested that Rad9 needs to localize to damaged chromatin in order for the DNA-damage-induced Rad9 S/TP phosphorylation to occur. I therefore created a cellular scenario in which Rad9 localization at chromatin is forced, so bypassing the requirement for the "histone pathway".

It was previously shown that covalent protein fusions containing the BRCT III and IV domain of Dpb11 localized efficiently and cell cycle-independently to damaged chromatin (179) therefore I used a *RAD9-DPB11 ΔN* fusion protein, (referred to as Rad9-Dpb11 fusion) known to hyperactivate the DNA damage checkpoint signaling (143). To ascertain that this fusion acts by forcing Rad9 localization to damaged chromatin, we measured inhibition of DNA end resection by Rad9 as a read-out of Rad9 function (194, 195). To this end I performed ChIP against the ssDNA binding protein RPA to measure the extent of resection from an HO-induced, non-repairable DSB at the MAT locus using the Gal-HO system. As can be seen in figures 17 and 18 in presence of the Rad9-Dpb11 fusion the association of RPA to sites distal to the DSB strongly diminished compared to wild-type in both G1- and G2/M-phase indicating that resection was inhibited in this background.

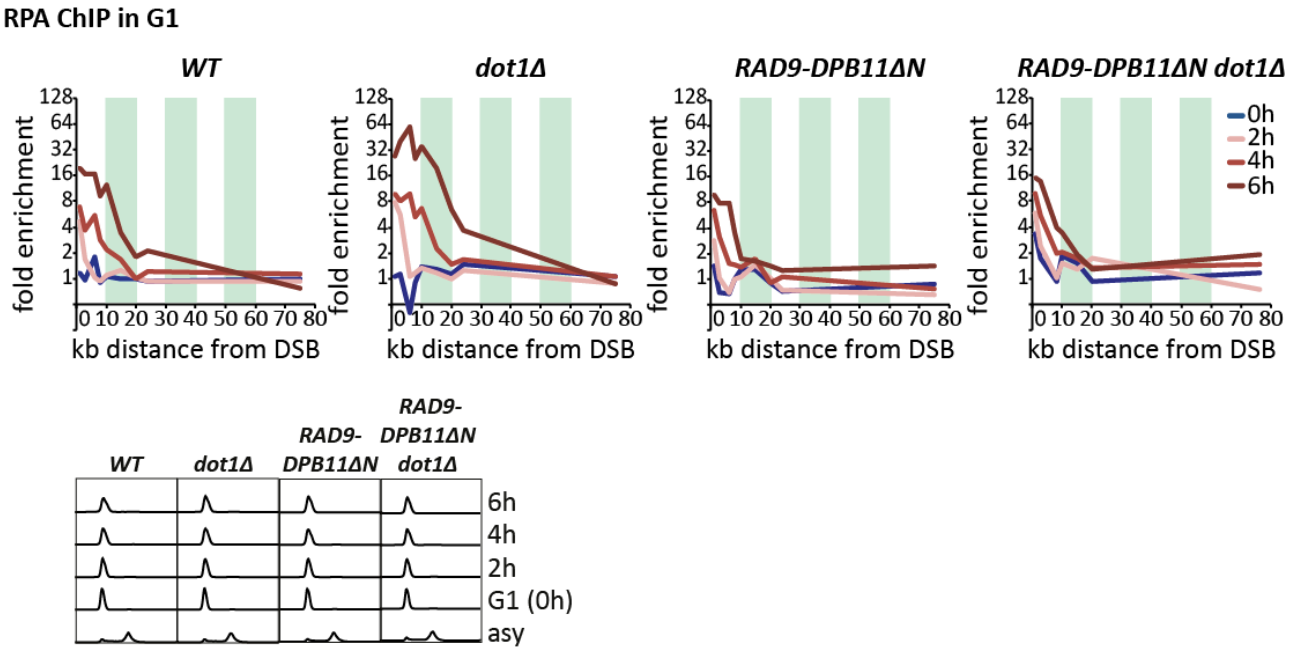

Fig. 17: a Rad9-Dpb11 fusion functions independently of the "histone pathway". A Rad9-Dpb11 fusion forces Rad9 recruitment to DSBs independently of Dot1. The Rad9-Dpb11 fusion blocks resection in G1, also in the absence of Dot1. RPA-ChIP at the indicated distances from an HO-induced DSB (0, 2, 4 and 6 h after HO induction) in WT, *dot1 Δ*, *RAD9-DPB11 ΔN* and *RAD9-DPB11 ΔN dot1 Δ* is taken as proxy for DNA end resection. FACS-based DNA content measurements is shown below.

These data are consistent with a model in which a Rad9-Dpb11 fusion forces Rad9 recruitment to damaged chromatin, and this has a hyperactivating effect on the checkpoint as well as an inhibitory effect on resection spreading, in agreement with previous results (143, 286).

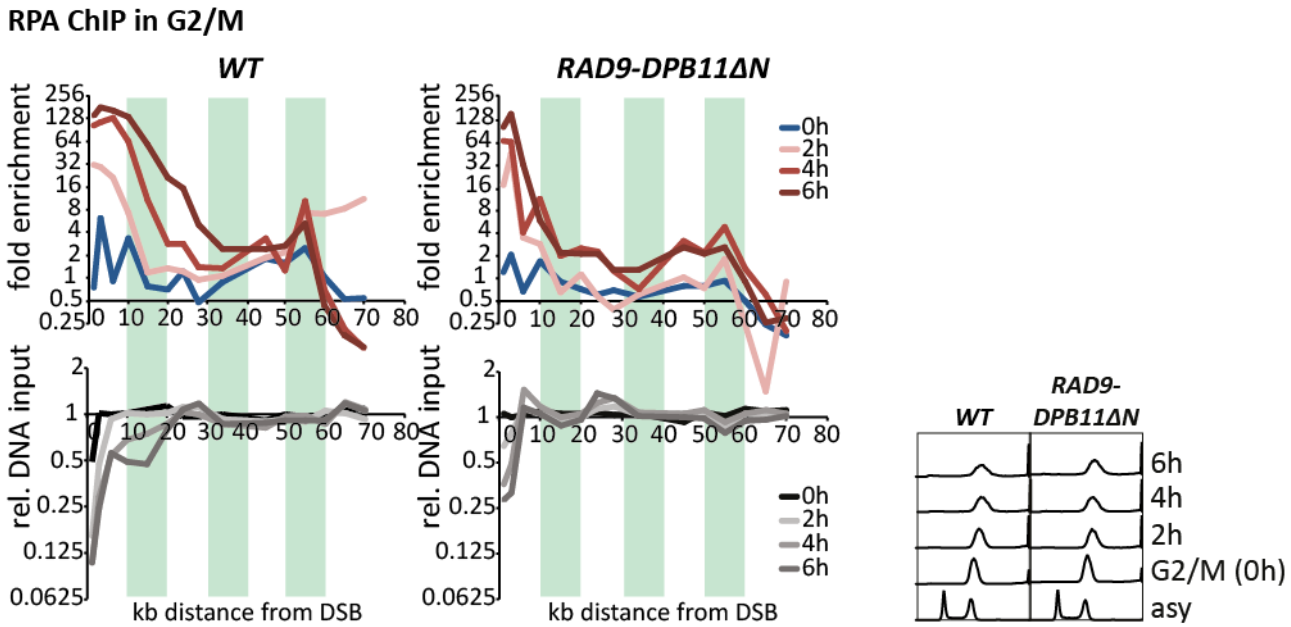

Fig. 18: a Rad9-Dpb11 fusion inhibits resection in G2/M. RPA ChIPs demonstrate inhibition of resection in the presence of the RAD9-DPB11 fusion. RPA recruitment was measured at positions spanning 1.1 to 70 kb from an HO-induced DSB at the indicated timepoints in G2/M arrested cells. In the lower panel DNA loss is visualized by ChIP DNA inputs (Input DNA at each position relative to controls outside of the affected region). On the right are shown the FACS-based DNA content measurements.

Since Rad9-Dpb11 fusion proved to force an enhanced Rad9 chromatin localization I decided to test whether such fusion could also influence the DNA-damage-dependent Rad9 phosphorylation in G1, which itself is dependent on the recruitment of Rad9 to chromatin via the "histone pathway" (as suggested from the data obtained with the *dot1 Δ* and *rad9-Y798Q* mutants).

After DNA damage induction with phleomycin Rad9-T474 phosphorylation was enhanced in a Rad9-Dpb11 fusion background and was even present to low levels without the induction of exogenous damage (Fig. 19A and 19B). Importantly, in this mutant background Rad9-T474 phosphorylation was also largely independent of Dot1 (Fig. 19A), while it still showed dependency on the apical kinases Mec1 and Tel1 (Fig. 19C). Overall, these data suggest that the function of the "histone pathway" in damage-induced Rad9 S/TP phosphorylation lies entirely in the recruitment of Rad9 to damaged chromatin.

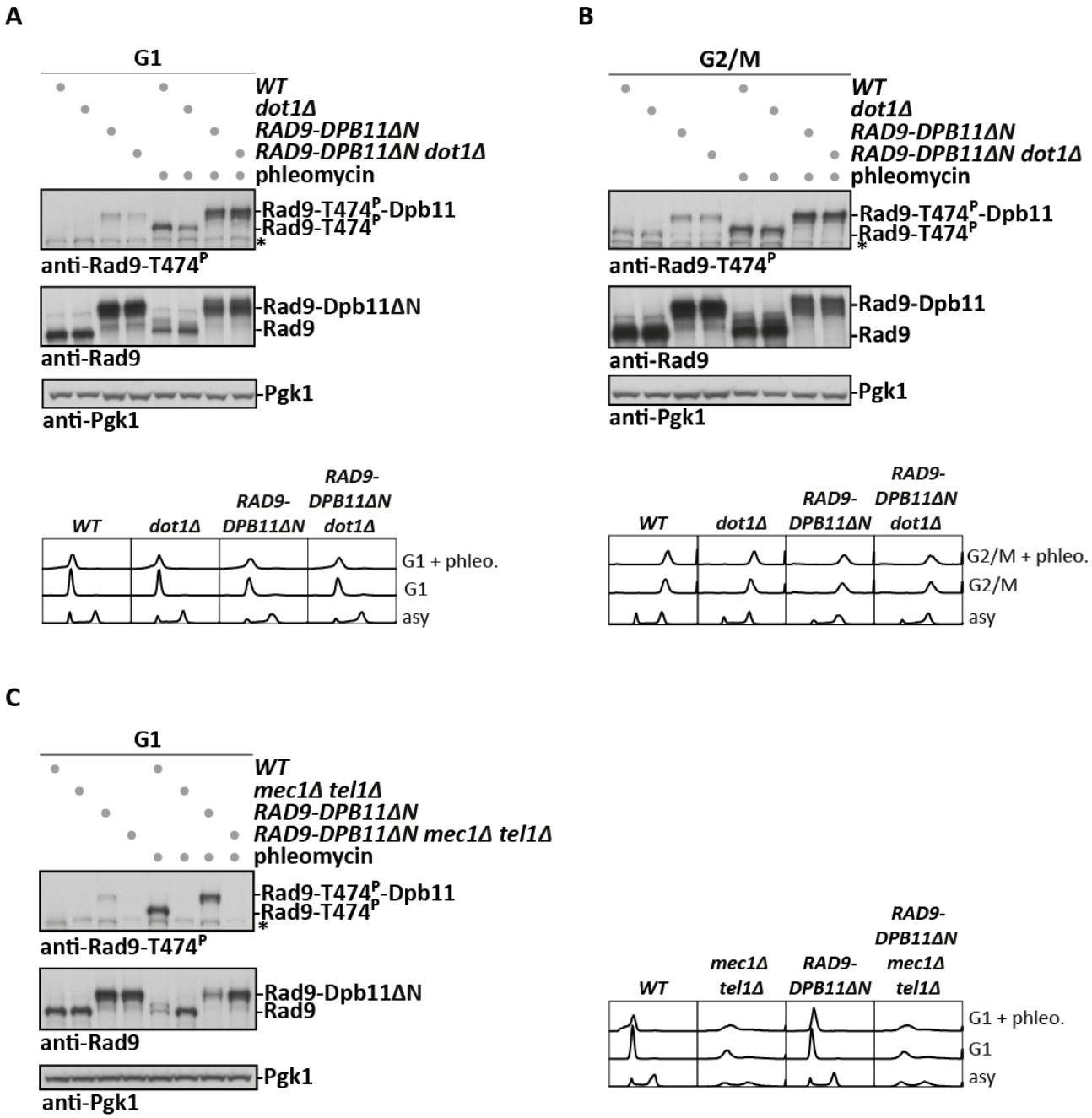

Fig. 19: **the Rad9-Dpb11 fusion bypasses the requirement for Dot1, but not for Mec1 and Tel1.** A Rad9-Dpb11 fusion shows Rad9 T-474 phosphorylation even in absence of Dot1 but not in absence of Mec1 and Tel1 **(A)** Measurement of Rad9-T474 phosphorylation using Rad9-T474^{P} phosphorylation-specific antibodies to probe whole cell extracts of cells expressing the Rad9-Dpb11 fusion in *WT* and *dot1 Δ* mutant background. The cells were G1-arrested and treated with phleomycin or mock treated. An asterisk denotes a crossreactive band. FACS-based DNA content is shown below. **(B)** Experiment as in **(A)**, but in G2/M-arrested cells. S/TP phosphorylation of Rad9 occurs in G2/M arrested cells independently of *RAD9-DPB11 ΔN*. FACS based DNA content measurements are shown below. **(C)** Measurement of Rad9 T474 phosphorylation in G1-arrested cells expressing the Rad9-Dpb11 fusion in *WT* and *mec1 Δ tel1 Δ*. Pgk1 immunoblot serves as loading control. An asterisk denotes a crossreactive band. On the right are shown FACS based DNA content measurement.

4.2.5 Rad9 S/TP phosphorylation in G1 is dispensable for DNA end resection and the DNA damage checkpoint

The CDK-dependent phosphorylation of Rad9 allows the recruitment of Rad9 to chromatin via a pathway alternative to the "histone pathway" (143). According to our data, however, the DNA-damage-dependent Rad9 S/TP phosphorylation in G1 is downstream the Rad9 recruitment to chromatin, suggesting other functions for this particular phosphorylation (Fig. 15, 16).

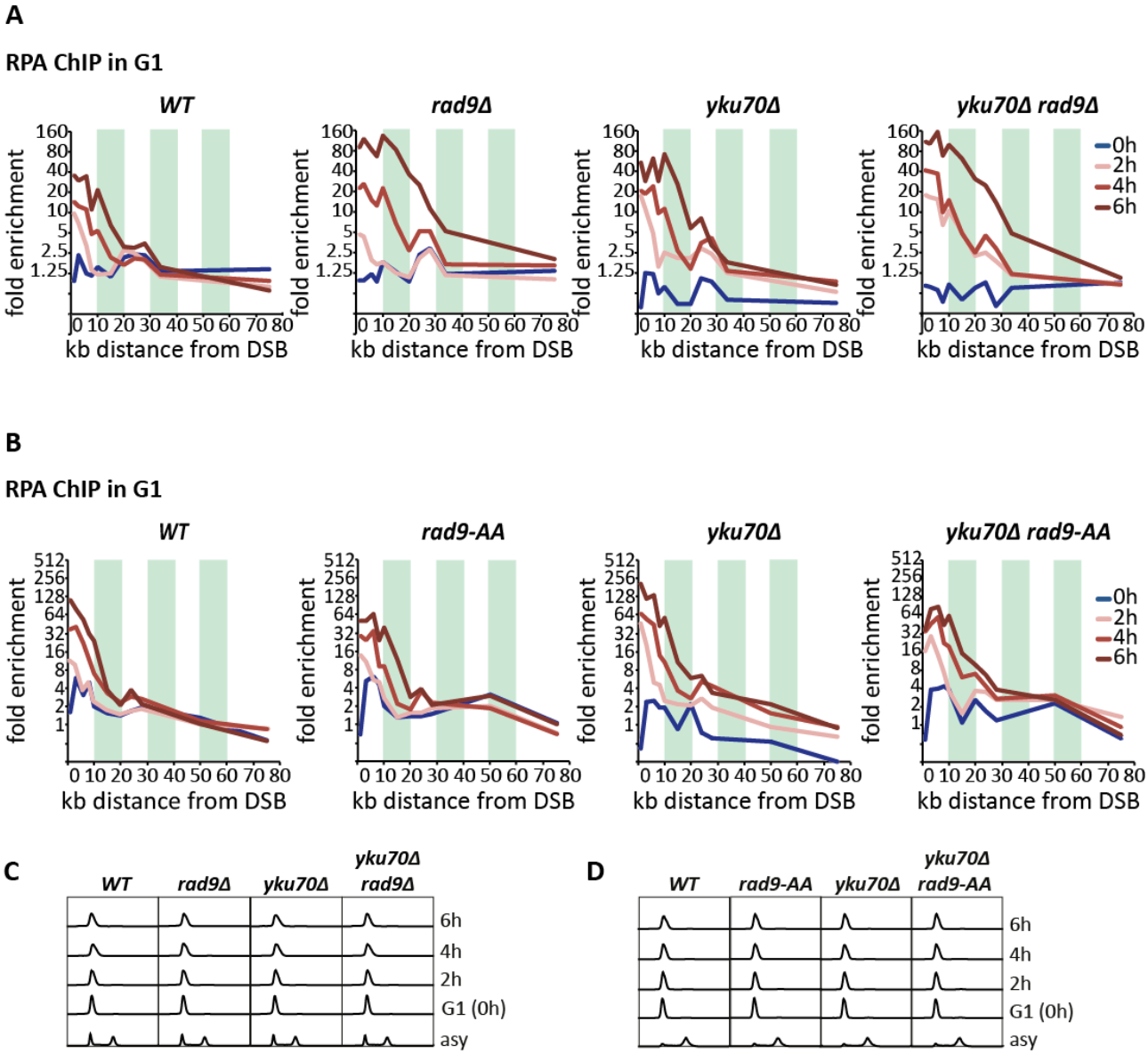

Fig. 20: lack of DNA-damage-induced Rad9 S/TP phosphorylation does not affect DNA end resection in G1. The *rad9-AA* mutant – in contrast to the *rad9 Δ* mutant – does not induce hyper-resection in G1-arrested cells. **(A,B)** A site-specific DSB was induced at the MAT locus using GAL-induced HO endonuclease in G1-arrested cells. DNA end resection is measured by ChIP against RPA at 0, 2, 4 and 6 h after HO induction and within 0 – 80 kb distance to the DSB. **(A)** Resection was measured in *WT, rad9 Δ, yku70 Δ* and *rad9 Δ yku70 Δ* strains. FACS based DNA content measurements are in **(C). (B)** as in **(A)**, but with *WT, rad9-AA, yku70AA* and *rad9-AA yku70Δ* strains. FACS based DNA content measurements are shown in **(D).**

The known functions of Rad9 in the context of the DNA damage response are two-fold: (A) inhibition of DNA end resection and (B) DNA damage checkpoint activation. I therefore tested if a *rad9-AA* mutant would show a G1-specific defect in any of these functions.

To measure changes in DNA-end resection I again made use of ChIP against RPA in G1-arrested cells after induction of a non-repairable DSB using the Gal-HO system. I observed that in the *rad9 Δ* and *dot1 Δ* strains the spreading of RPA signal from the site of DSB induction is strongly increased, indicating hyperactivation of resection in absence of chromatin-bound Rad9 (Fig 17 and 20A, consistent with previous data in 194, 195). On the contrary no hyperactivation of resection was detected when I used the *rad9-AA* variant, not even in combination with a *yku70 Δ* background (Fig. 20B), suggesting that the Rad9-Dpb11 interaction is not involved in regulating DNA end resection in G1 after DNA damage.

It was previously shown that the *rad9-AA* mutant is not causing any measurable modification in the DNA damage checkpoint activation, indeed this mutant alone could not induce any defects in the phosphorylation of the effector kinase Rad53 in G1 arrested cells (143, see also Fig. 21). This suggests that other factors might compensate for a defect in the Rad9 S/TP phosphorylation. Following this hypothesis we tested for compensation by the 9-1-1 complex since both Rad9 and 9-1-1 can bind to and therefore in principle recruit Dpb11 to sites of DNA damage. I therefore combined the *rad9-AA* mutant with the *ddc1-T602A* mutant, which is known to abolish the 9-1-1-Dpb11 interaction. However, while the *ddc1-T602A* mutation strongly reduced the Dpb11 association with a site-specific DSB in G1-arrested cells, the *rad9-AA* mutant did not induce a measurable defect (Fig. 22). Consistently, checkpoint activation was still largely unaffected in the *rad9-AA* mutant, even in the *ddc1-T602A* background (Fig. 21).

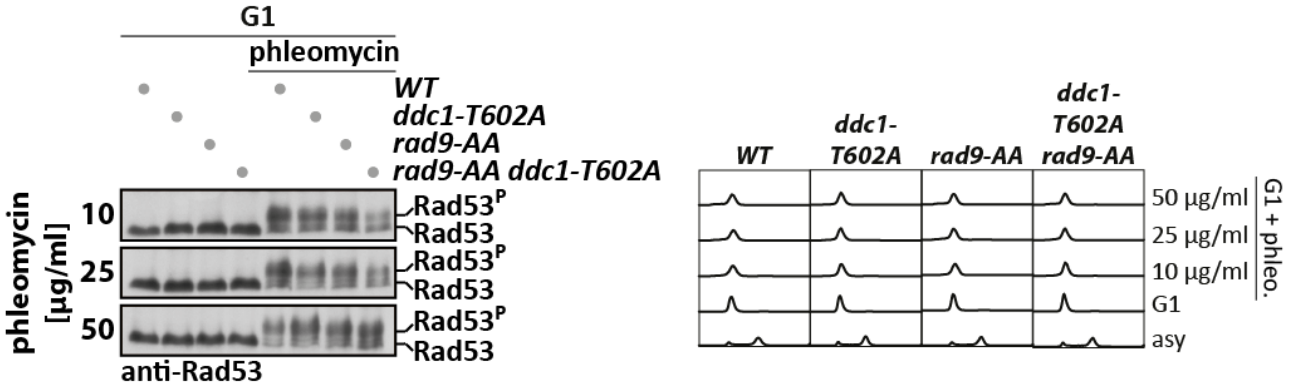

Fig. 21: lack of DNA-damage-induced Rad9 S/TP phosphorylation does not affect checkpoint signaling in G1. The *rad9-AA* mutant does not induce apparent defects in checkpoint activation in G1 even in background of the *ddc1-T602A*. Hyperphosphorylation of Rad53 induced by different concentrations of phleomycin is used as measure of checkpoint activation. On the right are shown FACS based DNA content measurements.

Overall the function of the DNA-damage-induced Rad9 phosphorylation and Rad9-Dpb11 interaction in G1 remains unclear. Given the high redundancy of the DNA damage checkpoint network it is highly likely the presence of other factors that can compensate for a

defect caused by a *rad9-AA* mutation, or alternatively that other S/TP sites in Rad9 can be phosphorylated and elicit the same response as phosphorylated S462 and T474.

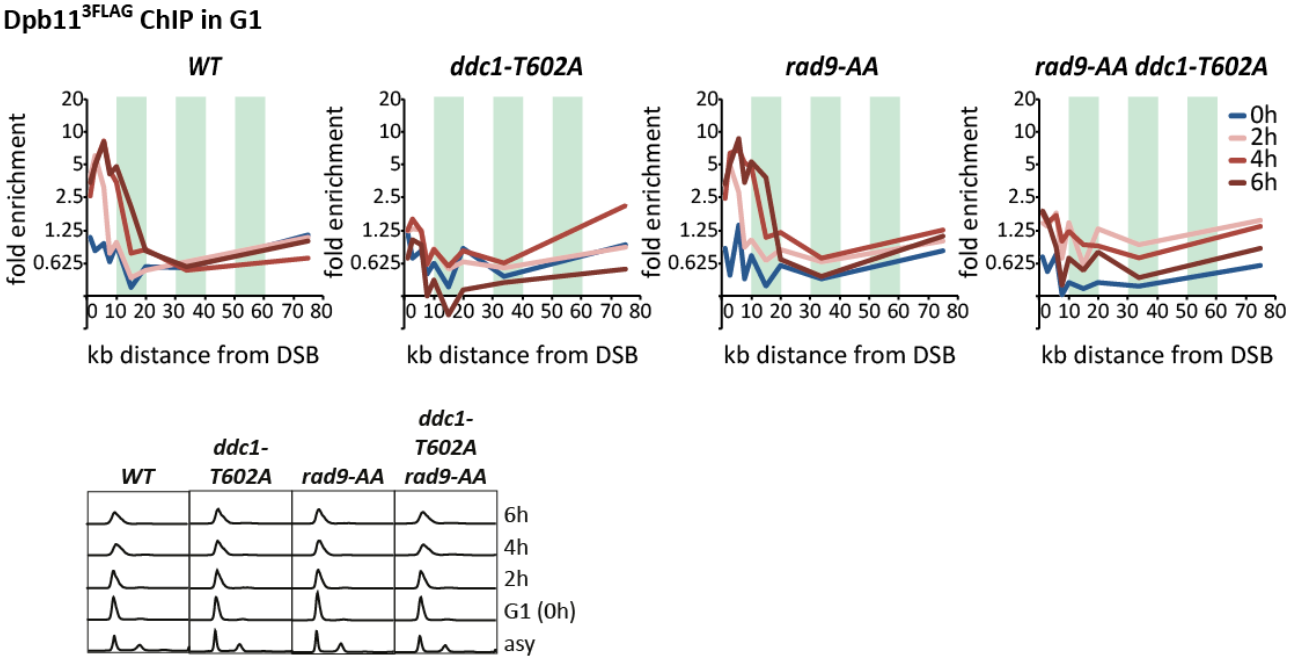

Fig. 22: lack of DNA-damage-induced Rad9 S/TP phosphorylation does not affect recruitment of Dpb11 to DNA damage sites in G1. Dpb11 is efficiently recruited at a DSB even when it cannot interact with Rad9. Dpb11 binding to DSBs in G1 as visualized by Dpb11^{3FLAG} ChIPs is abolished in *ddc1-T602A* cells, but not in *rad9-AA* cells. Dpb11 enrichment and spreading was measured starting from 1.1 kb until 75 kb away from an HO-induced DSB at the indicated time-points. FACS-based DNA content measurement are shown below.

4.2.6 Identification of the kinase responsible for Rad9 DNA-damage-dependent CDK sites phosphorylation in G1

CDK is the responsible kinase for the phosphorylation of ST/P sites on Rad9 in G2/M (143), but not required for ST/P site phosphorylation of Rad9 in response to DNA damage (see figures 11A and 11B). I therefore aimed to identify the kinase responsible for the Rad9 S/TP site phosphorylation in G1. To this end, I used two approaches: first, an unbiased approach where individual kinase deletion strains were separately tested via immunoblotting using our anti-Rad9-T474^{P} and anti Rad9-S462^{P} antibodies, and a second, candidate-directed approach.

For the unbiased approach, I made use of a library of haploid deletion strains available to us from the Saccharomyces genome deletion project (287, 288). This library contains all viable deletion mutants and overall, covered 99 out of 110 known S/TP kinases in budding yeast. Out of these I selected 56 candidates from various kinase families. From each single kinase deletion strain I prepared whole cell extracts after treatment with phleomycin and probed it with the anti-Rad9-T474^{P} antibody. All the deletion strains tested with this method retained phosphorylation of Rad9 on the T474 residue, therefore, none of the candidates tested seems to be directly responsible for the G1 phosphorylation of Rad9 ST/P sites after DNA damage in non-redundant fashion. In the appendix are summarized the tested kinases.

For the subsequent candidate-directed approach, I reasoned that the kinase phosphorylating S/TP sites after DNA damage should bear similarity to CDK as it is able to

target similar sites. CDKs are proline-directed serine/threonine-protein kinases with some preference for the S/T-P-X-K/R consensus and their broad family is traditionally subdivided in cell-cyle and transcriptional CDKs. Since phosphorylation of Rad9 ST/P sites after DNA damage occurs only when Rad9 is recruited to chromatin via the Dot1 pathway (see Fig. 15 and 16), I reasoned that the responsible kinase is likely chromatin-localized. This suggested the transcriptional kinases, belonging to the CDK family, as potential candidates: *SSN3, CTK1, KIN28* and *BUR1*. Compared to other cell-cycle-related subfamilies, transcriptional CDKs are more conserved, both in sequence and function and are typically directed to S/TP sites found on the CTD of the largest subunit (Rpb1) of RNAPII. The cyclin subunits of transcriptional CDKs do not show significant oscillations in protein levels during the cell cycle, therefore they are regulated rather by protein-protein interactions. Also, the requirement for the basic residue in the +3 position is not maintained transcriptional CDKs, which display a less-stringent S/T-P-X consensus (289). In order to deregulate Ssn3, Ctk1 and Kin28 I used deletion mutants of *SSN3* and *CTK1*, as well as an analog sensitive allele of the essential kinase *KIN28* (*kin28-as1*). However all mutants tested retained normal T474 phosphorylation of Rad9 after phleomycin treatment in G1 (data not shown). All transcriptional CDKs contain regulatory cyclin subunits. Interestingly, I found that in a deletion mutant of Bur2 (the Bur1 kinase cyclin) Rad9-T474 phosphorylation after phleomycin treatment was strongly reduced (Fig. 23).

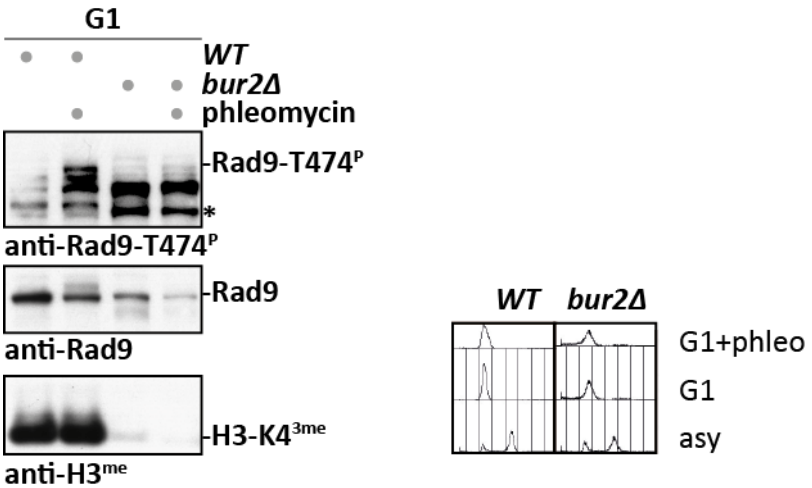

Fig. 23: deletion of Bur2 cyclin causes lack of Rad9 S/TP phosphorylation in G1. The Bur1 kinase cyclin Bur2 influences the Rad9-T474 phosphorylation after DNA damage in G1. Whole cell extracts from *WT* or *bur2 Δ* cells were prepared after G1 arrest and phleomycin treatment or mock treatment, and probed with Rad9-T474^{P} phosphorylation-specific antibodies. An asterisk indicates a crossreactive band. On the right are FACS-based DNA content measurements. H3-K4^{3me} was used as control for the *bur2 Δ*.

In order to test, whether Bur1-Bur2 was directly involved in Rad9 phosphorylation, I performed Rad9 pulldowns in G1-arrested cells before and after phleomycin treatment to test for possible interaction between Rad9 and Bur1-Bur2. I was able to detect co-purification of Bur1 with Rad9 using a Bur1 specific antibody, however the interaction did not depend on DNA damage and background binding of Bur1 could be detected in the untagged control strain (Fig. 24A). A possible explanation is that while Bur1 is able interact with Rad9 once this is recruited at the damaged chromosome, it can only phosphorylate its S/TP sites after Rad9 SCD domain is previously phosphorylated by the DNA-damage-activated checkpoint kinases Mec1 and Tel1.

Notably, *bur1 Δ* cells are inviable, while *bur2 Δ* cells are viable although with a severely impaired proliferation rate (290). In order to deregulate Bur1, I therefore used a *bur1-ts* (temperature-sensitive allele) and a *bur14x-AID* degron fusion. Surprisingly, both mutants did not show reduced Rad9 S/TP site phosphorylation after induction of DNA damage (Fig. 24B and 24C). The inconsistency of the results obtained with the *bur2 Δ* and the two Bur1 mutants may indicate that Bur1 is either not the kinase responsible for the DNA-damage-dependent phosphorylation of Rad9 S/TP sites in G1, but that the effects of the *bur2Δ* mutation is rather indirect. Alternatively, it is possible that residual Bur1-Bur2 activity retained in the Bur1 mutants tested is sufficient to achieve phosphorylation of Rad9-S462 and –T474.

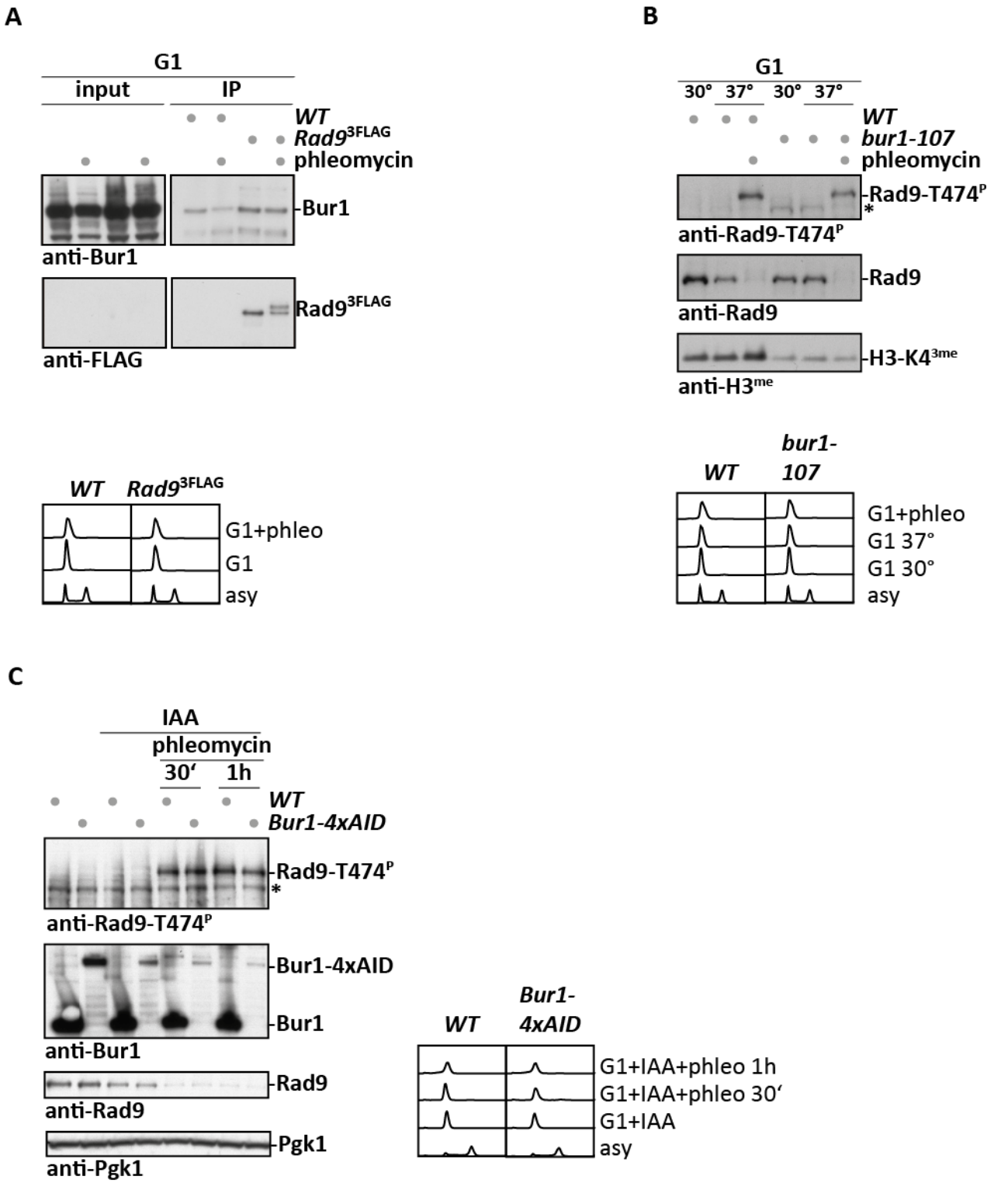

Fig. 23: Bur1 is a candidate Rad9 S/TP kinase but different bur1 mutations do not affect the DNA-damage-dependent Rad9-T474 phosphorylation in G1. Kinase Bur1 co-purifies with Rad9 in immunoprecipitation experiments but bur1 temperature-sensitive and degron mutants were both proficient for Rad9 S/TP phosphorylation after DNA damage in G1 (**A**) Rad9^{3FLAG} was purified from G1-arrested cells treated with phleomycin by FLAG-IP. Co-purification of Bur1 was detected by using anti-Bur1-C antibodies. FACS profiles are shown below. (**B**) Extracts prepared from G1-arrested, phleomycin-treated cells expressing either wildtype or a temperature sensitive mutant of bur1 (*bur1-107*) were probed with the Rad9-T474^{P} phosphorylation-specific antibody. FACS-based DNA content measurements are shown below. (**C**) Rad9-T474^{P} phosphorylation-specific antibody was used to probe extracts from cells treated like in (**B**), expressing either wildtype Bur1 or the degron-mutant *bur1-4xAID*. The anti-Bur1-C antibody was used to monitor the depletion of *bur1-4xAID*. On the right are FACS-based DNA content measurements. An asterisk in (**B**) and (**C**) indicates a crossreactive band. IAA: Indole-3-acetic acid.

5 DISCUSSION

5.1 A DNA damage-induced mode of Rad9 S/TP phosphorylation

Rad9 is an important DNA damage checkpoint factor. It is recruited to chromatin following DNA damage (184, 185, 203) where it acts as a scaffold protein that brings the DNA damage checkpoint effector kinase Rad53 in close proximity of the damage site, thereby facilitating Rad53 autophosphorylation and activation (186, 193). In order to act as a checkpoint mediator Rad9 engages in different protein-protein interactions. Some of these interactions involve modified histones: Rad9 is known to bind to phosphorylated histone H2A (γH2A) via its phospho-protein-binding BRCT repeats. In yeast, γH2A is generated by the DNA damage-activated kinases Mec1 and Tel1 and known to spread from the site of DNA damage up to 50 kb away along the chromosome. A second histone modification recognized by Rad9 is histone H3 in its K79-methylated form (H3-K79^{me}). The H3 methylation is created by the methyltransferase Dot1, whereupon Rad9 can bind this modification via its Tudor domain. H3-K79^{me} appears to be a constitutive, DNA damage-independent marker of chromatin.

Besides mediating DNA contact via specific interaction to modified histones, Rad9 has also been found to associate with the scaffold protein Dpb11, which itself is recruited to sites of DNA damage via binding the 9-1-1 complex on chromatin. Previous work has shown that Rad9 specifically interacts with Dpb11 in cells arrested in M phase, but not in cells arrested in G1 (143). Additionally, cell cycle regulation of this interaction was shown to be achieved by CDK-dependent phosphorylation of two S/TP motifs on Rad9 (S462 and T474), which are recognized by the BRCT I and II domain of Dpb11 (143).

In this study I elucidated the presence of two different modes of Rad9 S/TP phosphorylation: mode 1, which is cell-cycle-regulated and depends on CDK, and mode 2, which is independent of the presence of CDK, but DNA damage-dependent. In accordance with previous studies on the CDK regulation of Rad9, I observed a CDK-dependent Rad9-Dpb11 interaction in pulldown experiments from M phase cells, even in the absence of DNA damage (mode 1) (143). Strikingly, however, I was additionally able to observe increased interaction of Rad9 with Dpb11 when cells were arrested in G1, but only after treatment with the DNA-damaging agents MMS or phleomycin (mode 2).

Interestingly, I was able to establish that the DNA damage-dependent Rad9-Dpb11 interaction relied on the same two Rad9 phospho-sites. Therefore, our previously generated phospho-specific antibodies revealed that the Rad9 residues S462 and T474 were not only phosphorylated in M phase-arrested cell extracts (in the presence or absence of DNA damage), consistently with these sites being modified by CDK, but also in G1-arrested cells after induction of DNA damage with phleomycin. Furthermore, the DNA damage-induced phosphorylation of Rad9 in G1 is CDK-independent, as shown by the *cdc28-as1* mutant strain, which was proficient in damage-induced Rad9-T474 phosphorylation even after CDK inhibition by 1NM-PP1. I could therefore conclude that this new damage-induced

phosphorylation mode of the Rad9 S/TP sites occurs independently of the cell cycle phase and CDK activity.

5.2 Role of the "histone pathway" in targeting Rad9 to chromatin during the DNA damage response

As mentioned above the crucial step of Rad9 recruitment to chromatin depends on two domains on Rad9: The Tudor domain and the tandem BRCT domain. Furthermore, Rad9 engages in the binding to the Rad53 checkpoint effector kinase, and to the Dpb11 scaffold protein.

The interactions of Rad9 with the modified histones H3-K79^{me} and γH2A and with the protein scaffold Dpb11 are, according to current models, two parallel pathways acting to recruit Rad9 to the chromatin during the DNA damage response (143, 175). These pathways are referred to as the "histone pathway" and the "Dpb11 pathway", respectively and while the "histone pathway" is ubiquitous, the "Dpb11 pathway" is considered as a redundant Rad9 recruitment mechanism that acts during G2/M phase, when CDK activity is available (143). Relying on histone modifications, the "histone pathway" is believed to act at all stages of the cell cycle: H2A phosphorylation occurs upon DNA damage in G1, S and G2/M phase cells, and Dot1-dependent methylation of histone H3 is thought to be a constitutive modification (181, 219). The "Dpb11 pathway" on the contrary, is believed to be exclusively active in the G2/M phase of the cell cycle, given the requirement for CDK activity (143). In this context, CDK is not only involved in Rad9 phosphorylation on the S/TP residues necessary for Dpb11 binding, but CDK has also been demonstrated to positively regulate DNA end resection (278, 280, 282), which is a prerequisite of Dpb11 association with DNA damage sites. Therefore, CDK activity also indirectly enhances Rad9 recruitment to chromatin through resection

In my study, I uncovered a G1-specific and DNA damage-dependent Rad9-Dpb11 interaction, which does not rely on CDK activity and does not serve as a Rad9 recruitment mode, but in fact is dependent on recruitment of Rad9 by the "histone pathway" (as will be discussed in section 5.4).

In response to DNA damage Rad9 is known to undergo hyperphosphorylation due to the action of the DNA damage checkpoint kinases Mec1 and Tel1, which target multiple S/TQ motifs on Rad9 in the so called SCD (S/TQ Cluster Domain) (187, 190). Importantly, this phosphorylation critically requires prior chromatin recruitment of Rad9 via the "histone pathway". In this study I uncovered that phosphorylation of Rad9 S/TP sites requires the "histone pathway" as well. It is dependent on the binding of Rad9 to H3-K79^{me} and both deletion of the methyl-transferase Dot1 and mutation of the Rad9 Tudor domain abolished DNA damage-dependent phosphorylation of Rad9. Therefore DNA damage induced S/TP phosphorylation has the identical requirements as DNA damage induced S/TQ phosphorylation, suggesting a similar mechanisms; furthermore, its dependency on Rad9 recruitment to chromatin suggests that, similarly to the S/TQ phosphorylation scenario, a

chromatin-bound kinase might be responsible for S/TP site phosphorylation after DNA damage.

5.3 The kinase involved in the DNA damage-dependent phosphorylation of Rad9 S/TP sites

Currently, the identity of the kinase phosphorylating Rad9 after DNA damage is unknown. In undamaged G2/M-arrested cells these Rad9 S/TP sites are phosphorylated by CDK. However, I could rule out an involvement of CDK after DNA damage based on two pieces of evidence: first, the damage-induced Rad9 S/TP phosphorylation occurs in G1 where CDK is inactive, second, efficient inhibition of CDK using the *cdc28-as1* mutant and 1NM-PP1 treatment did not affect the damage-induced Rad9 S/TP phosphorylation.

In order to find the kinase responsible for the Rad9 S/TP sites phosphorylation after DNA damage, candidate mutant strains were tested for their ability to phosphorylate Rad9-T474 *in vivo*. The two most striking requirements for this mode of Rad9 phosphorylation are a dependency on DNA damage and on Rad9 chromatin recruitment. I therefore reasoned that a likely candidate would be a kinase which is activated by DNA damage and/or is recruited to chromatin after DNA damage.

Given the similarity of damage-induced Rad9 S/TP to the S/TQ phosphorylation I first tested the damage-induced kinases of the DNA damage checkpoint, starting with the PIKKs Mec1 and Tel1. These kinases are involved in the DNA damage-dependent hyperphosphorylation of Rad9 by targeting its SCD (187, 190), the S/TQ cluster which is located proximal to the residues S462 and T474. Moreover, Mec1 and Tel1 are stably recruited to chromatin after DNA damage (36-38). Indeed, I observed that single *mec1Δ* and *tel1Δ* mutations reduced damage-induced Rad9 S/TP phosphorylation and the *mec1Δ tel1Δ* double mutation completely abolished it. However, this effect could be indirect. Mec1 and Tel1 are S/TQ directed kinases (187, 190, 291), therefore bearing a consensus sequence which differs from the S/TP motifs, and currently there is no report of Mec1 or Tel1 phosphorylating S/TP sites. Furthermore, I could not obtain *in vitro* evidence for Mec1 directly targeting Rad9 S/TP sites. Lastly, using the *rad9-6AQ* mutant I found that Rad9 S/TP phosphorylation is dependent on SCD phosphorylation by Mec1 or Tel1, suggesting an indirect mechanism, by which the PIKKs could influence Rad9 S/TP phosphorylation after DNA damage.

There are different possible scenarios in which Mec1 and Tel1 could indirectly affect phosphorylation of Rad9 S/TP domains in G1. For example, It is possible that the hyper-phosphorylation of the Rad9 SCD causes a structural change in Rad9 that uncovers S/TP sites. Alternatively, Rad9 SCD phosphorylation could provide a docking site for the S/TP kinase or another factor involved in the S/TP site phosphorylation. A similar mechanism has been described for other DNA damage-activated phosphorylation events, like the checkpoint effector kinase Rad53, which binds to Rad9 once it is hyperphosphorylated by Mec1 and Tel1 (186, 188, 189, 190, 193). A last mechanism, by which Mec1 and Tel1 could contribute to Rad9 S/TP sites phosphorylation could involve the activation of the

responsible Rad9 S/TP kinase, or chromatin recruitment of Rad9 itself (via γH2A) or of the kinase.

The checkpoint effector kinases Rad53 and Chk1 appeared to be further potential candidates for Rad9 S/TP phosphorylation. Rad53 contains two phospho-protein binding FHA domains (188) and like Rad9 it contains an S/TQ cluster domain or SCD (291), which is a Mec1 and Tel1 target and participates in its activation following DNA damage. The FHA domains are involved in the binding of Rad53 to the phosphorylated SCD of Rad9, an event which leads to Rad53 recruitment and accumulation at chromatin, and in direct phosphorylation of Rad53 by Mec1 (193). I tested *rad53Δ sml1Δ* cells, but found them proficient for the Rad9-T474 phosphorylation after DNA damage induction *in vivo* In order to rule out a possible redundant effect, Chk1, the second kinase effector activated by the DNA damage checkpoint cascade, was also tested, alone and in combination with *rad53Δ*, but both single and double mutants did not show an influence on the Rad9 S/TP sites phosphorylation *in vivo*.

Another class of kinase candidates for Rad9 phosphorylation are Mitogen Activated Kinases (MAPKs). MAPKs are serine/threonine protein kinases that belong to the CMGC group and preferentially phosphorylate ST/P sites (292, 293). *S. cerevisiae* contains six MAPKs active in five functionally distinct signalling cascades: Fus3 mediates cellular response to peptide pheromones. Kss1 permits adjustment to nutrient-limiting conditions. Hog1 is necessary for survival under hyperosmotic conditions. Slt2/Mpk1 is required for repair of injuries to the cell wall. Smk1 along with another, more divergent MAPK-related kinase, Ime2, regulates spore wall assembly during meiosis and sporulation, a developmental response of MATa/MATα diploid cells to acute nutrient deprivation (293). These kinases regulate a multitude of cellular functions but despite their importance many MAPK substrates are yet to be identified. I therefore decided to unbiasedly test single knock-out strains of six MAPKs (Fus3, Kss1, Hog1, Slt2, Smk1 and Ime2), but in none of these strains, I could observe a deficiency for Rad9-T474 phosphorylation (data not shown). While it is possible that the different MAPKs act redundantly on Rad9, I consider this as a relatively unlikely scenario, given the distinct functions that MAPKs play in normal physiology.

In yeast, three kinases belonging to the CDK family are involved in phosphorylation of the C-terminal repeat domain (CTD) of RNA PolII: Bur1, Ctk1 and Kin28 (294-296). Additionally, the CDK-like kinase Ssn3 is part of the RNA PolII holoenzyme and is also involved in the CTD phosphorylation (297). These kinases act on chromatin where they bind to RNA polymerase and phosphorylate S5 or S2 residues on the CTD. Bur1 and Ctk1 are the major S2 kinases, while Kin28 targets S5 residues. Given their chromatin localization ability, the similarity to CDK and their S/TP consensus site, I decided to test this subgroup of the CDK family as well as Ssn3. In particular Bur1 was reported to interact via its C-terminal domain with RPA, and *bur1ΔC* mutants showed a deregulated DNA damage response and increased sensitivity to DNA damage and replication stress (298). Bur1 is an essential kinase, which associates with its cognate cyclin Bur2 (although Bur2 is named a cyclin by homology,

its expression does not fluctuate during the cell cycle). While a *bur2Δ* strain showed reduced Rad9 S/TP phosphorylation *in vivo*, I did not observe a similar effect when I used temperature-sensitive and degron mutants to deregulate Bur1 itself. This suggests that the residual activity Bur1 in those mutant cells was still sufficient, alternatively, it could mean that Bur1 is not involved in the DNA damage-dependent Rad9 S/TP phosphorylation, in which case the effect observed in the *bur2Δ* mutant could be rather indirect as *bur2Δ* cells show a severe growth defect. It is therefore not entirely unlikely that Bur2 has a cellular function upstream of the Rad9 S/TP sites regulation. Ctk1 is the second major S2 kinase together with Bur1 (299), but also in this case the deletion mutant *ctk1Δ* did not influence the Rad9 S/TP phosphorylation after treatment with phleomycin *in vivo*. Finally, Kin28 is the third kinase targeting RNA-PolII CTD on S5 residues (300). Like Bur1, it is an essential kinase, but a *kin28-as1* analog-sensitive allele did not cause any reduction in the Rad9 S/TP phosphorylation *in vivo*.

This candidate approach did not allow me to conclude on the identity of the kinase responsible for the DNA damage-induced phosphorylation of the Rad9 S/TP residues in G1. Also, an unbiased approach, which took advantage of the yeast knock-out library from which 61 Serine/Threonine kinase candidates from various kinase families were tested (listed in the Appendix), did not lead to the identification of the kinase. However, except for the DNA damage checkpoint kinases, only single mutants were taken into consideration. At this point of the study I therefore cannot exclude the possibility of redundancy, i.e. that different kinases might act on the same substrate or that kinases involved in the same pathway might suppress the effect of single mutants by taking over the phosphorylation of Rad9 S/TP sites.

Lastly, the PIKKs Mec1/Tel1 may play additional roles on top of Rad9 SCD phosphorylation and Rad9 chromatin recruitment. It would therefore be interesting to establish whether the PIKKs, so far classified as strictly S/TQ-directed kinases, are actually able to regulate S/TP sites on Rad9 and possibly other DDR proteins in response to DNA damage in order to facilitate their activities in the absence of CDK.

5.4 Potential functions of the DNA damage-dependent Rad9-Dpb11 interaction in G1

Several studies have suggested a CDK regulation of Rad9 recruitment and activation in both budding and fission yeast (143, 301). According to this model the function of the Rad9-Dpb11 interaction in the DNA damage checkpoint is merely to recruit Rad9 to damaged chromatin. As such it would be similar to the "histone pathway", with the difference that the "histone pathway" is not restricted to a specific cell cycle phase while the "Dpb11 pathway" can only function from S to M phase.

In this study I showed that the Rad9-Dpb11 interaction can take place in G1 and is specifically triggered by DNA damage. However, these new findings do not contradict the model of Rad9 chromatin recruitment in G1 that is mediated by the "histone pathway", since the Dot1-mediated recruitment of Rad9 to chromatin is necessary in order to achieve Rad9

S/TP sites phosphorylation and consequent binding to Dpb11. Figure 24 depicts an holistic view of the "Histone pathway and the "Dpb11 pathway" of Rad9 recruitment to chromatin

Previous results have shown that protein-fusions containing the BRCT III and IV domain of Dpb11 localized efficiently and cell-cycle-independently to damaged chromatin (179). Fusing Rad9 to the Dpb11 BRCT III and IV domain (Rad9-Dpb11ΔN) causes hyperactivation of DNA damage checkpoint signaling (143). Here, I confirmed that the Rad9-Dpb11 fusion functions by forcing Rad9 localization to damaged chromatin and therefore allows damage-induced Rad9 S/TP phosphorylation, bypassing the requirement for Dot1-dependent Rad9 chromatin recruitment.

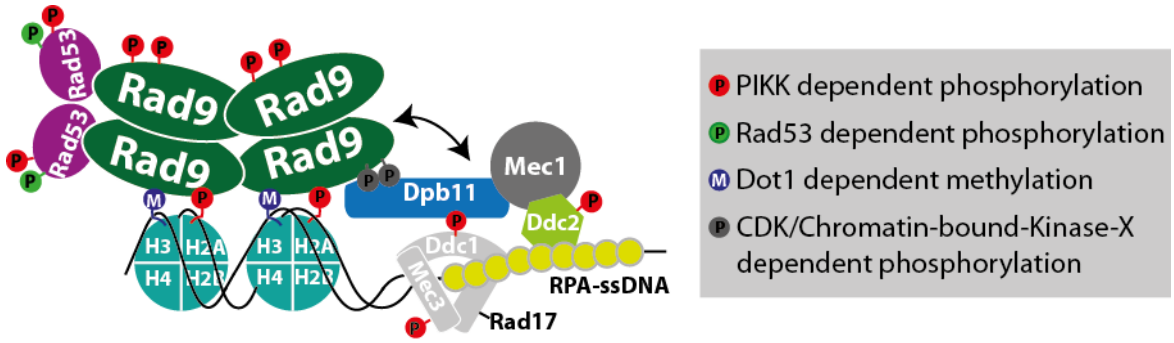

Fig. 24: model of Rad9-Dpb11 module in checkpoint signalling. Holistic view of the "histone pathway" and the "Dpb11 pathway" for the recruitment of Rad9 to damaged chromatin. Binding of Rad9 to modified histones, (H3-K79 methylated and H2A-S129 phosphorylated) localizes Rad9 to DNA damage sites. Rad9 also interacts with Dpb11, which is bound to sites of DNA damage via its interaction with Ddc1 subunit of the 9-1-1 clamp. In G1 the "Dpb11 pathway" does not play a role in Rad9 recruitment, but is dependent on the "histone pathway", indeed the Rad9 S/TP site phosphorylation and consequent binding to Dpb11 is dependent on the Dot1-mediated recruitment of Rad9. This suggests that the Rad9-Dpb11 interaction in G1 could function to aid Dpb11 recruitment at the damage site via Rad9. The Mec1 kinase activity is stimulated by the Dpb11 AAD domain and by the Ddc1 subunit of the 9-1-1 complex.

These findings suggest that the damage-induced S/TP phosphorylation of Rad9 is not involved in recruitment of Rad9 to damaged chromatin. Consistently, our results did not show any role of Dpb11 in recruiting Rad9 to chromatin in G1. Here I used the extend of DNA end resection as proxy Rad9 recruitment, as Rad9 is a well-characterized inhibitor of DNA end resection. To measure DNA end resection, ChIP experiments were performed against RPA performed in the background of the *rad9-AA* mutant (defective for Dpb11 binding), but resulted in wild-type levels of resection in G1, suggestting normal chromatin recruitment and functiom of Rad9-AA. Furthermore, in line with previous studies (144, 215) lack of the Rad9-Dpb11 interaction did not influence the activation of Rad53 in G1.

Given that the binding of Rad9 to Dpb11 requires Rad9 chromatin recruitment and S/TP site phosphorylation, an alternative function of this interaction could be to aid Dpb11 recruitment at the damage site via Rad9. A previously described recruitment pathway for Dpb11 to damaged chromatin is via interaction with the Mec1-phosphorylated Ddc1 subunit of the 9-1-1 clamp (209, 215). When I tested Dpb11 recruitment in ChIP experiments, I observed normal recruitment of Dpb11 to DSBs in a *rad9-AA* mutant background, while conversely Dpb11 recruitment was strongly reduced in the *ddc1-T602A* mutant of the 9-1-1 complex (defective in Dpb11 binding). Alltogether, the function of a Rad9-bound Dpb11 in G1

remains unclear since a *rad9-AA* mutant alone or combined with a *ddc1-T602A* mutant did not have any effect on Rad53 activation, suggesting that even the absence of a Dpb11-Rad9 interaction does not hamper efficient DNA damage checkpoint activation.

Using the *ddc1-T602A* and *dot1Δ* mutants I tried to uncover possible redundancies in the Dpb11 and Rad9 recruitment, but these mutant backgrounds did not reveal any defects. The Rad9 S/TP phosphorylation and the Rad9-Dpb11 interaction do not appear essential for efficient recruitment of either Rad9 or Dpb11 scaffolds at chromatin in response to the DNA damage. This interaction does also not affect the regulation of resection, a process of which Rad9 is a known negative regulator. Taken together, these results suggest that the Rad9 S/TP phosphorylation induced by DNA damage could act redundantly with currently unknown factors or mediate an entirely new function.

5.5 Evolutionary conservation of the Rad9-Dpb11 interaction

Seveal eukaryotic orthologs of Rad9 were found to be recruited to chromatin in response to DNA damage by similar mechanisms, involving interaction with modified histones (204-209, 213, 220, 221). In humans, 53BP1 specifically interacts with two histone marks: it binds specifically to histone H2A ubiquitinated on residue K15 through a peptide segment called the ubiquitination-dependent recruitment motif (UDR), and simultaneously via its tandem Tudor domain to histone H4 dimethylated on lysine 20 (H4-K20^{me2}). In fission yeast, the Rad9 ortholog Crb2 is targeted to damaged chromatin by preferentially binding the dimethylated H4-K20 residue, and disruption of this interaction results in the loss of Crb2 localization to double-strand breaks and in impaired checkpoint function (206-208, 211-213). Furthermore, both Crb2 and 53BP1 were found to interact with the respective Dpb11 orthologs (206, 231). Studies with fission yeast gave a very similar picture to the situation in budding yeast. Parallel to the interaction with modified histones, an alternative pathway for Crb2 recruitment to DSBs requires a cyclin-dependent kinase phosphorylation site in Crb2 (206). This phosphorylation mediates association with the BRCT-domain-containing protein Cut5 (Dpb11 homolog), which also accumulates at HO-induced DSBs.

In human cells, the BRCT IV and V domains of TopBP1 (Dpb11 homolog) interact with 53BP1. Interestingly, however, this interaction was found to occur in G1 phase (231), suggesting that the interaction is independent of CDK activity, and to be specifically triggered by DNA damage as described in the present work for the budding yeast ortholog. Similarly to the damage-induced Rad9-Dpb11 interaction, the exact mechanism by which TopBP1 exerts a checkpoint function in G1 phase remains to be determined. Also, phosphorylation sites on 53BP1 responsible for the interaction with TopBP1 are yet to be ascertained.

The mode of Rad9 recruitment to chromatin in response to DNA damage and the interaction between Rad9 and Dpb11 in proximity of damage sites appear to be evolutionary conserved in eukaryotes. Additionally, findings in human cells also suggest conservation of a CDK-independent and DNA damage-dependent interaction of these two proteins in G1. In this context, a G1-specific role for 53BP1 has been described in human cells. These studies

revealed that in G1, 53BP1 accumulated at DSB sites promotes NHEJ and opposes HR in part by blocking DNA end resection via a mechanism that requires ATM-dependent phosphorylation of the 53BP1 N-terminal region. This in turn promotes the recruitment of PTIP and RIF1, two factors independently involved in blocking DNA end resection (302-304). Therefore, it would be important to elucidate if also the Rad9-Dpb11 interaction in yeast plays a role in the G1-specific DNA damage response as was shown in human cells, or if it even mediates further functions in other processes of DNA repair.

5.6 Regulation of S/TP and S/TQ sites on DNA Damage Repair Proteins

Cyclin-dependent kinases (CDKs) are involved in the regulation of all the major events in the eukaryotic cell division and can target many substrates. Importantly, CDKs have a strong preference to phosphorylate S/TP sites (305). Studies on the CDK-dependent phosphorylation revealed that CDK substrates tend to be phosphorylated at multiple sites and that this often leads to conformational changes likely to modify the function of the substrates by disrupting or generating protein-protein interaction surfaces. Given the specificity of these interactions, the precise position of these phosphorylation sites is often conserved only in closely related species (305). Several DNA damage response proteins have been demonstrated to be regulated by CDK in their role in DNA repair processes. In particular, CDKs are known regulators of DSB end resection (195, 306).

Several yeast proteins like Rad9 require CDK phosphorylation in order to maintain their functions in DNA repair, a characteristic that is often conserved in higher eukaryotes. A key CDK site on the yeast resection factor Sae2 is S267. Lack of S267 phosphorylation by CDK was shown to impair Mec1/Tel1-dependent phosphorylation of two S/TQ sites, S249 and T279 (307). Additionally, mutation of this residue shows reduced rate and extent of DSB resection and an increased sensitivity to DNA-damaging agents (308). Similarly, CDK-dependent phosphorylation of the human ortholog CtIP is a prerequisite for ATM-dependent phosphorylation of its S/TQ sites upon DNA damage, which was shown to be important for efficient end resection in order to activate HR (301). Another yeast endonuclease regulated by cell-cycle-dependent phosphorylation is Slx1-Slx4. The non-catalytic subunit Slx4 is phosphorylated by CDK at S486 and this promotes the Dpb11–Slx4 interaction, implicated in the resolution of DNA repair intermediates (176). The CDK regulation of this interaction is conserved between yeast and humans, since addition of CDK inhibitor roscovitine strongly reduces binding of SLX4 to TopBP1 (176). Another example for a CDK-regulated DNA repair protein in yeast is Xrs2, a component of the MRX (Mre11-Rad50-Xrs2) complex, involved in the initial processing of DSBs (309). Contradictory results have been collected regarding its CDK regulation in both yeast and humans (310-313). However, recent proteomic studies identified three additional S/TP motifs that were phosphorylated in Xrs2, and increasing evidence shows the possibility of this protein being a CDK substrate (314, 315).

Given the abundance of target proteins that are modified at S/TP sites by CDK, S/TP site phosphorylation is often interpreted as phosphorylation by CDK (305); this study shows

however that S/TP sites of Rad9 protein can be targeted by kinases other than CDK and therefore be regulated by signals other than the cell cycle. This suggests that S/TP sites on other proteins could become phosphorylated in a similar fashion, in particular if the proteins become recruited to chromatin, a classical hallmark of DNA damage response proteins. It would therefore be important to establish whether an equivalent CDK-independent S/TP site phosphorylation may as well regulate other DDR proteins like Sae2, Slx4 and Xrs2.

So far, phospho-proteomic studies on the DNA damage-dependent regulation of S/TP sites have been conducted in human cells, but in contrast to our results in budding yeast, DNA damage-inducing treatments such as etoposide addition or γ-irradiation rather caused a general downregulation of the S/TP sites phosphorylation (316). It is important to note however that in human cells CDK1 and CDK2 activity is downregulated in response to DNA damage and, as such, a general reduction of S/TP phosphorylation of DNA damage is not unexpected. Since CDK activity remains unaffected under conditions of DNA damage in *S. cerevisiae*, budding yeast would therefore provide a more suitable system to study how S/TP-sites-containing substrates are differentially modified after DNA damage. While changes in protein phosphorylation in response to DNA damage have already been addressed in *S. cerevisiae* (75), these studies only addressed modification of S/TQ sites. Therefore a systematic investigation of damage-induced S/TP sites changes and the involved kinases is still lacking.

6 MATERIALS AND METHODS

Chemicals and reagents were provided by Amersham-Pharmacia, AppliedBiosystems, Biomol, Biorad, Difco, Fluka, Invitrogen, Merck, New England Biolabs, Promega, Roth, Roche, Riedel de Haen, Serva, Sigma and Thermo Scientific. Standard techniques were used for microbiological, molecular biological and biochemical methods or the instructions of the manufacturer were followed. Deionized sterile water, sterile solutions and sterile flasks were used for the described methods.

6.1 MATERIALS

E. coli strains

Strain name	**genotype**	**source**
BL21-Gold	BF- ompT hsdS (r_B- m_B-) dcm+ Tet^r gal endA Hte	Agilent Technologies
Stellar	F–, endA1, supE44, thi-1, recA1, relA1, gyrA96, phoA,Φ80d lacZΔ M15, Δ (lacZYA - argF) U169, Δ(mrr - hsdRMS -mcrBC), ΔmcrA, λ–	Clontech

E.coli media

LB medium/plates:
1% Tryptone (Difco)
0.5% Yeast extract (Difco)
1% NaCl
(1.5% Agar)
sterilized by autoclaving

SOC medium:
2% Tryptone
0.5% Yeast extract
10 mM NaCl
2.5 mM KCl
10 mM MgCl2
20 mM Glucose
sterilized by autoclavin

S. cerevisiae plasmids

S. cerevisiae plasmid	Purpose	Reference
pYIplac128, pYIplac204	integrative	Gietz and Sugino, 1988
pRS303, pRS304, pRS306	integrative	Sikorski and Hieter, 1989
pNHK53 (Yiplac based)	integrative	Nishimura 2009

S. cerevisiae strains

Strain	Relevant genotype	Reference
W303	MATa leu2-3,112 trp1-1 can1-100 ura3-1 ade2-1 HIS3-11,15 [phi+]	Thomas and Rothstein, 1989
YBP061	MATa RAD9-9myc::hphNT1	Pfander & Diffley, 2011
YBP109	MATa dot1Δ::kanMx4	Pfander & Diffley, 2011
YBP269	MATa ddc1-T602A::HIS3Mx6	Pfander & Diffley, 2011
YBP270	MATa ddc1-T602A::HIS3Mx6 dot1Δ::kanMx4	Pfander & Diffley, 2011
YBP366	MATa rad9Δ::natNT2 TRP1::RAD9-3FLAG::HISMx6 pep4::hphNT1	Pfander & Diffley, 2011
YBP388	MATa pep4Δ::LEU2	Pfander & Diffley, 2011
YBP390	MATa bar1Δ::TRP1	Pfander & Diffley, 2011
YBP403	MATa rad9Δ::natNT2 TRP1::rad9-3FLAG::HIS3Mx6 pep4 Δ ::LEU2 dot1 Δ::kanMx4	Pfander & Diffley, 2011
YBP406	MATa rad9Δ::NATNT2 TRP1::rad9AA-3FLAG::HIS3Mx6 pep4Δ::LEU2	Pfander & Diffley, 2011
YBP3616	MATa Lys2::NATNT2 arg4:: hphNT1 HTA1-3flag:: KanMX4	This study
YDG003	MATa Lys2::NATNT2 arg4:: hphNT1 RFA1-3flag::KanMX4	This study
YGD016	Mat a bur1-107::LEU2	Strasser et al 2010
YGD017	Mata bur2Δ::hphNT1 bar1 Δ ::TRP1	This study
YGD019	MATa ura3::pADH1-OsTIR1-9myc::URA3 bur1-4xAID-9myc::HIS3Mx6 bar1 Δ::hphNT1	This study
YGD030	MATa rad9Δ::NATNT2 bar1 Δ ::HISMX6 trp1::RAD9-DPB11ΔN::TRP1	This study

Strain	Relevant genotype	Reference
YGD031	MATa RAD9-3FLAG::hphNT1 hml::pRS hmr::pRS bar1Δ::TRP1 pGal-HO::ADE3	This study
YGD032	rad9Δ::hphNT1 hml::pRS hmr::pRS bar1 Δ::TRP1 pGal-HO::ADE3	This study
YGD034	MATa rad9 Δ ::hphNT1 LEU2::RAD9AA-3FLAG hml::pRS hmr::pRS bar1::TRP1 pGal-HO::ADE3	This study
YGD035	MATa RAD9-3FLAG::hph dot1 Δ::kanMX4 hml::pRS hmr::pRS bar1 Δ ::TRP1 pGal-HO::ADE3	This study
YGD036	MATa rad9Δ::NATNT2 trp1-1::RAD9-DPB11ΔN::TRP1 mec1Δ::LEU2 tel1Δ::hphNT1 bar1Δ::HISMX6 sml1Δ::URA3	This study
YGD037	MATa trp1-1::RAD9-DPB11::TRP1 mec1Δ::LEU2 bar1Δ::HISMX6 rad9Δ::NATNT2 sml1Δ::URA3	This study
YGD038	MATa mec1 Δ ::LEU2 tel1 Δ ::NATNT2 bar1 Δ ::TRP1 sml1Δ::URA3	This study
YGD039	MATa rad53 Δ :: kanMX4 chk1 Δ ::NatNT2 bar1 Δ ::TRP1 sml1::URA3	This study
YGD040	MATa yku70::NAT rad9 Δ ::hphNT1 hml::pRS hmr::pRS bar1 Δ ::TRP1 pGal-HO::ADE3	This study
YGD041	MATa yku70::NATNT2 dot1 Δ ::kanMX4 hml::pRS hmr::pRS bar1 Δ ::TRP1 pGal-HO::ADE3	This study
YGD042	MATa RAD9-DPB11ΔN-3FLAG::hphNT1 hml::pRS hmr::pRS bar1 Δ ::TRP1 pGal-HO::ADE3	This study
YGD043	MATa RAD9-DPB11ΔN-3FLAG::hphNT1 dot1 Δ ::kanMX4 hml::pRS hmr::pRS bar1 Δ ::TRP1 pGal-HO::ADE3	This study
YGD044	MATa rad9Δ::hphNT1 leu2-3::Rad9AA-3FLAG::LEU2 yku70Δ::NATNT2 hml::pRS hmr::pRS bar1 Δ ::TRP1 pGal-HO::ADE3	This study
YGD045	MATa hml::pRS hmr::pRS bar1 Δ ::TRP1 pGal-HO::ade3 dpb11-3FLAG::kanMX4 rad9-AA::NATNT2	This study
YGD046	MATa hml::pRS hmr::pRS bar1 Δ ::TRP1 pGal-HO::ADE3 ddc1-T602A::hphNT1 DPB11-3FLAG::kanMX4 rad9-AA::NATNT2	This study
YKR112	MATa cdc28-F88G	Reusswig et al., 2016
YKR139	MATa ura3::pADH1-OsTIR1-9myc::URA3	Reusswig et al 2016
JPY923	MATa FLAG-rad53::LEU2 bar1 Δ::hisG cdc13-1 cdc15-2	Usui et al., 2008
JPY993	MATa FLAG-rad53::LEU2 bar1 Δ ::hisG cdc13-1 cdc15-2 rad9S1129A::URA3	Usui et al., 2008
JPY3344	MATa FLAG-rad53::LEU2 bar1 Δ ::hisG cdc13-1 cdc15-2 rad9-6AQ	Usui et al., 2008
YSB095	MATa mec1 Δ ::LEU2 bar1 Δ ::TRP1 sml1Δ::URA3	This study
YSB096	MATa rad53 Δ ::hphNT1 bar1 Δ ::TRP1 sml1Δ::URA3	This study

Strain	Relevant genotype	Reference
YSB097	MATa tel1 Δ ::NATNT2 bar1 Δ ::TRP1	This study
YSB098	MATa chk1 Δ ::NATNT2 bar1 Δ ::TRP1	This study
YSB189	MATa rad9 Δ ::NATNT2 pep4 Δ ::kanMX4 leu2-3::rad9-Y798Q-3FLAG::LEU2	This study
YSB517	MATa hml::pRS hmr::pRS bar1Δ::TRP1 pGal-HO::ADE3	Bantele et al 2017
YSB812	MATa hml::pRS hmr::pRS bar1Δ::TRP1 pGal-HO::ADE3 dpb11-3FLAG::kanMX4	This study
YSB816	MATa hml::pRS hmr::pRS bar1Δ::TRP1 pGal-HO::ADE3 ddc1-T602A::hphNT1	This study

PCR screening of genomic recombination events

PCR reaction mix:
2 µl template DNA
2.5 µl 10x ThermoPol buffer
0.9 µl dNTPs (10mM)
1.6 µl primer I (10 µM)
1.6 µl primer II (10 µM)
0.25 µl Taq DNA polymerase
16.15 µl dH2O
25 mM EDTA, pH 8.0

Cycling parameters (30 amplification cycles):

PCR step	°C	Time	
Initial denaturation	94	5 min	
denaturation	94	30 s	30 cycles
annealing	50	30 s	
enlongation	72	1 min/kb	
Final enlongation	72	10 min	
Cooling	4	∞	

Amplification of genomic DNA fragments

PCR reaction mix:
200 ng Genomic DNA
10 µl 5x GC buffer
1.75 µl dNTP-Mix (10 mM each; NEB)
3.2 µl Forward primer (10 µM)
3.2 µl Reverse primer (10 µM)
1 µl DMSO
1 µl $MgCl_2$ (50 mM)
0.5 µl Phusion DNA polymerase
adjust to 50 µl with dH_2O

Cycling parameters (30 amplification cycles):

PCR step	°C	Time	
Initial denaturation	98	4 min	
denaturation	98	30 s	30 cycles
annealing	50	30 s	
enlongation	72	1 min/kb	
Final enlongation	72	10 min	
Cooling	4	∞	

Amplification of chromosomal targeting cassettes

PCR reaction mix:
100 ng plasmid DNA
10 µl HF buffer
1.75 µl dNTP-Mix (10 mM each; NEB)
3.2 µl Forward primer (10 µM)
3.2 µl Reverse primer (10 µM)
0.5 µl Phusion DNA polymerase
adjust to 50 µl with dH2O

Cycling parameters (30 amplification cycles):

PCR step	°C	Time	
Initial denaturation	98	4 min	
denaturation	98	30 s	30 cycles
annealing	50	30 s	
enlongation	72	1 min/kb	
Final enlongation	72	10 min	
Cooling	4	∞	

Site-directed mutagenesis

PCR reaction mix:
50-100 ng plasmid DNA
2.5 µl 10x Pfu buffer
0.63 µl Forward primer (10 µM)
0.63 µl Reverse primer (10 µM)
0.63 µl dNTPs (10mM)
0.5 µl Pfu Turbo DNA polymerase
adjust to 25 µl with dH_2O

Cycling parameters (20 amplification cycles):

PCR step	°C	Time	
Initial denaturation	95	3 min	
denaturation	95	30 s	20 cycles
annealing	55	60 s	
enlongation	68	2 min/kb	
Final enlongation	72	10 min	
Cooling	4	∞	

6.1.3 Molecular biology buffers and solutions

TE buffer:	10 mM Tris-HCl, pH 8.0 1 mM EDTA sterilized by autoclaving
TBE buffer 5x:	90 mM Tris 90 mM Boric acid 2.5 mM EDTA, pH 8.0 sterilized by autoclaving
DNA loading buffer 6x:	0.5% SDS 0.25% (w/v) Bromophenol blue 0.25% Glycerol
Breaking buffer:	2% Triton X-100 1% SDS 100 mM NaCl 10 mM Tris-HCl, pH 8.0 1 mM EDTA, pH 8.0

6.1.4 Biochemistry buffers and solutions

HU sample buffer:	8 M Urea 5% SDS 1 mM EDTA 1.5% DTT 1% Bromphenol blue
MOPS running buffer:	50 mM MOPS 50 mM Tris base 3.5 mM SDS 1 mM EDTA
SDS-PAGE running buffer:	25 mM Tris base 192 mM Glycine 0.1% SDS

Transfer buffer:	250 mM Tris base 192 mM Glycine 0.1% SDS 20% Methanol
TBST:	25 mM Tris-HCl, pH 7.5 137 mM NaCl 2.6 mM KCl 0.1% Tween 20
Co-IP Lysis buffer :	200mM KAc 100mM Hepes-KOH pH 7.6 0.1% NP-40 10% glycerol 2mM β-mercaptoethanol 10mM NaF 20mM β-glycerophosphate protease inhibitors ocadaic acid
IP lysis buffer:	500mM NaCl 100mM Hepes-KOH pH 7.6 10% glycerol 0.1% NP-40 2mM β-mercaptoethanol 1mM EDTA 10mM NaF 20mM β-glycerophosphate protease inhibitors ocadaic acid

Antibodies for western blot analyses

Antibody	Antigen	Source
Mouse anti-Pgk1	Pgk1	Invitrogen
Rabbit anti-Rad9	Rad9	Lowndes F, EMBO J. 1998
Rabbit anti-Rad9-S462P	Rad9 S462P peptide	Pfander B & Diffley J, EMBO J. 2010
Rabbit anti-Rad9-T474P	Rad9 T474P peptide	Pfander B & Diffley J, EMBO J. 2010
Rabbit anti-Rad53	Rad53	Abcam
Rabbit anti-RPA	Rfa1, Rfa2, Rfa3	Agrisera
Rabbit anti-FLAG	containing synthetic FLAG peptide DYKDDDDK-GC	Sigma
Mouse anti-myc	myc aa 410-420	Millipore
Rabbit anti-GST-Dpb11	GST-Dpb11 555-C	Pfander B & Diffley J, EMBO J. 2010
Rabbit anti-Bur1	Bur1 C-terminus	Clausing E, JBC 2010

6.1.5 Chromatin Techniques Buffers and solutions

FA lysis buffer:
50 mM Hepes-KOH, pH 7.5
150 mM NaCl
1 mM EDTA
1% (v/v) Triton X-100
0.1% (w/v) Deoxycholic acid, Na-salt
0.1% (w/v) SDS

FA lysis buffer 500 (high salt):
50 mM Hepes-KOH, pH 7.5
500 mM NaCl
1 mM EDTA
1% (v/v) Triton X-100
0.1% (w/v) Deoxycholic acid, Na-salt
0.1% (w/v) SDS

ChIP wash buffer:
10 mM Tris-HCl, pH 8
250 mM LiCl
1 mM EDTA
0.5% (v/v) NP-40

	0.5% (w/v) Deoxycholic acid, Na-salt
TE:	10 mM Tris-HCl, pH 8
	1 mM EDTA
ChIP elution buffer:	50 mM Tris-HCl, pH 7.5
	10 mM EDTA
	1 % (w/v) SDS

ChIP primers

Name	**Sequence**	**Position/distance from HO break**
BP2509	TGGTCTGAGTTTCCAGTTCTTTGGT	Ctrl fw chrom I
BP2510	AGCGTCCAAACTAAATGAGCAGTCT	Ctrl re chrom I
BP2507	TGATAGCTTCTGCAATCGTAGGGC	Ctrl fw chrom V
BP2508	TGGATCACGGTGCTAAGGAGGTTA	Ctrl re chrom V
BP2505	CTAAACGTGGCCGCATTTGGTAAG	Ctrl fw chrom VI
BP2506	ATCATCGCCGATTGGATAAGGGTG	Ctrl re chrom VI
BP2503	ACTGCAACAAGACCTTCACTCAACT	Ctrl fw chrom XV
BP2504	GCAGGATGGTTTTCTGGTGAGGA	Ctrl re chrom XV
BP1266	CTCGGCATATTTGTATTAACCCACT	1.1 kb fw
BP1267	GTCCTCCGTCCAATCTGTGC	1.1 kb re
BP1268	GATATTGGCCTAGAACTGCCGG	3 kb fw
BP1269	GCATGGGCACTTGCTAACCAAT	3 kb re
BP2186	CTTCATCTCATGCAAAGTGC	4.7 kb fw
BP2187	GGGGCAATTGGTAAATTGCG	4.7 kb re
BP2188	CACTGCCTACTGTTGCCCC	6 kb fw
BP2189	GCCTATTGGGGTAATAGAC	6 kb re
BP2190	CACCAAGAGGTAGTGTGAC	7.6 kb fw
BP2191	AGCCTTCTACGCCAAACCAG	7.6 kb re
BP1270	GATGTTTACACAGGGCCCCC	8 kb fw
BP1271	CGTTCTTAGTGGTCTGGAGTTC	8 kb re
BP1272	GAAGGAGACAGAGACAGAGGG	10 kb fw
BP1273	GAAGGGAGGCAAAGACAAGGAG	10 kb re
BP1274	GTGGAGTTTGATGGTATCGACATC	15 kb fw
BP1275	CGTTGGAACCATCTTGAGCCTC	15 kb re
BP1276	CATCGTTCTCTTCGTTCTCTTCG	20 f kb w
BP1277	CACAAATATCTCTTCTCGACGGC	20 kb re
BP2511	CTCTGTGGGTATTTCCGTG	24 kb fw
BP2512	CTTGGCGCTACGATGTGC	24 kb re

BP2513	CTGTGCTGTCTGCGCTGCATT	28 kb fw
BP2514	GACGAAGGAGACGAAAACCTCTTC	28 kb re
BP2515	GGATGGATGGTTATGTTTCGGAAGG	34 kb fw
BP2516	CACCAGCAACTCTATCTTCGTTG	34 kb re
BP4204	TCCAGTCGTCCAACTCTTGCC	45 kb fw
BP4205	CAAGATATTGAGCCTGGATGC	45 kb re
BP4206	CATGTGGAGATTTCAGGAGAGG	50 kb fw
BP4207	GAAGAAAGTCGATCTGTTCC	50 kb re
BP4208	AATAATGTCTGCCAGCAACGC	55 kb fw
BP4209	TGATGGATGTATGGACCAGAG	55 kb re
BP4210	AGATCTATCTAATGAGCCGG	60 kb fw
BP4211	GATGGTGTTACCACCGTCGCTG	60 kb re
BP4212	TCTTCCCGTGTTAACGACAAC	65 kb fw
BP4213	CAGAACTAGGATCAATCTTGG	65 kb re
BP4214	AGCCCAGTAGTACTACCTCTC	70 kb fw
BP4215	ACAAACCTGTCAACACTGCG	70 kb re
BP874	CCCAAGCTCACAAATTAATATGGC	75 kb fw
BP875	GCATCTGTAGTACCACTGCTCTTTG	75 kb re
BP1280	GTGGCATTACTCCACTTCAAGTAAGAG	HO intact fw
BP1281	CTT CCC AAT ATC CGT CAC CAC G	HO intact re

RT-PCR reaction mix:

2 µl Sample DNA
10 µl SYBR Green I Master Mix
1.2 µl Forward primer (10 µM)
1.2 µl Reverse primer (10 µM)
5.6 µl dH2O

Light cycler program

95°C	**10 min**
Then 45 cycles	
95°C	10 s
55°C	10 s
72°C	16 s
Melting curve analysis	
4°C	∞

6.1.6 Mass Spectrometry Buffers and solutions

Sorbitol buffer:	25 mM HEPES 7.6 1 M sorbitol
Lysis buffer	200 mM KOAc, 10 mM HEPES 7.6 0.1% NP-40 10% glycerol 1 mM ßME 20 mM ß-glycerophosphate 10 mM NaF
Laemmli buffer (2X)	4% SDS 20% Glycerol 120 mM TrisHCl pH 6.8 1% Bromophenol blue

6.2 METHODS

6.2.1 Computational analyses

For DNA and protein sequence search and comparison, protein physical and genetic interactions, mutant phenotypes, scientific literature search electronic services were applied using Saccharomyces Genome Database (http://www.yeastgenome.org/) and Information of National Center for Biotechnology (http://www.ncbi.nlm.nih.gov/). DNA Star software (EditSeq, SeqBuilder, SeqMan) was used for the DNA restriction enzyme maps, DNA sequencing analysis and primer design.

Quantification of the PFGE signal was performed using ImageJ software (http://rsb.info.nih.gov/ij/). Microsoft Office package 2008 (Microsoft Corp.) and Adobe Photoshop (Adobe Systems Inc.) were used for the presentation of text, tables, graphs and figures.

6.2.2 Microbiological and genetic techniques

I E. coli techniques

Cultivation and storage of E. coli cells

LB media was used to grow liquid cultures at 37°C with constant shaking. Cultures on solid media were incubated at 37°C. Ampicillin concentration of 50 µg/ml in the media was used for selection of transformed E. coli. Cultures on solid media were stored at 4°C for no longer than 5 days.

Transformation of plasmid DNA into competent E. coli cells

Competent E. coli cells were thawed on ice shortly before transformation. For transformation of DL21-Gold cells 50 µl of competent cells were mixed with 0.5-2 µl of ligation sample or 10 ng of plasmid DNA and incubated on ice for 15 min. Next, the heat-shock was performed for 45 s and the transformation mixture was placed for 2 min on ice. Then, the cells were resuspended in 1 ml LB media without antibiotics and recovered at 37°C on a shaker for 1 h. After incubation, cells were plated on the solid media containing ampicillin and incubated overnight at 37°C. For transformation of Stella cells, 50 µl of competent cells were mixed with 5 ng of DNA and incubated for 30 min on ice. Heat-shock was performed for 45 s at 42°C. Then, cells were kept for 5 min on ice. Prewarmed SOC medium was added to final volume of 500 µl and cells were incubated by shaking at 37°C for 1 h. Next, cells were plated on selective media and incubated overnight at 37°C.

II S. cerevisiae techniques

S. cerevisiae plasmids

In this study, site-directed mutagenesis with specific primers was used to introduce mutations. For all PCR reactions Phusion and Pfu Turbo highfidelity polymerases were used, and restriction enzymes were provided by NEB.

Integrative plasmids were based on Yiplac and pRS vectors. In order to express proteins at their endogenous levels, the full-length ORFs surrounded by the upstream promoter and downstream terminator were amplified and cloned into integrative plasmids

S. cerevisiae strains

All yeast strains are based on W303 (317). Chromosomally tagged yeast strains and mutants used in this study were constructed by PCR-based, genetic crossing and standard techniques (318; 319).

Cultivation and storage of S. cerevisiae

Yeast liquid cultures were inoculated with a single colony from freshly streaked plates and grown overnight. From this preculture yeast was re-inoculated in the main culture to an OD600 of 0.1 and incubated in baffle-flasks (size ≥ 5x liquid culture volume) on a shaking platform (150-220 rpm) at 30ºC until mid-log phase growth had been reached (equals OD600 of 0.6-0.9). The culture density was determined with a photometer (OD600 of 1 is equal to 1.5x107 cells/ml). Cultures on agar plates were stored at 4°C up to 2 weeks. For long-term storage, stationary cultures were frozen in 15% (v/v) glycerol solutions at –80°C.

III Genetic manipulation of S. cerevisiae

Preparation of competent yeast cells

Competent cells for transformations were prepapred by harvesting 50ml of a mid-log phase culture (500g, 3min, room temperature) and subsequent washing, first with 25ml sterile water and then with 25ml SORB. The pellet was resuspended in 360µl SORB + 40µl carrier DNA (salmon sperm DNA, 10mg/ml, Invitrogen). Competent cells were stored at –80°C in 50µl aliquots.

Transformation of competent yeast cells

For transformation, 200ng of circular or 2 μg of linearized plasmid DNA or PCR product were incubated with 10µl or 50µl of competent yeast cells, respectively. Then, six volumes of PEG solution were added and the cell suspension was incubated for 30 min at 30°C. DMSO (10% final concentration) was added and the transformation mixture was heatshocked at 42°C for 15 min (the duration of the heat shock was adjusted depending on the mutant strain used, for example for temperature sensitive mutants the incubation was reduced to 5 min). Cells were centrifuged (500 g, 3 min, room temperature), resuspended in 100µl sterile water and plated on the appropriate selective plates. If antibiotics were used for selection, the transformed cells were incubated for 3 h in 5 ml liquid YPD medium prior plating. Plates were incubated at 30°C for 2-3 days after to allow growth of transformants. If necessary, replica-plating on fresh selective media plates was performed to remove the background of false-positive colonies.

The YIplac and pRS vector series were used for stable integration of DNA into the yeast genome. Only stably integrated vectors are propagated in yeast since YIplac and pRS plasmids do not contain autonomous replication elements. The ORFs of the respective genes were cloned into YIplac and pRS vectors including the endogenous promoter and terminator. A restriction enzyme that specifically cuts within the auxotrophy marker gene was used to linearize vectors before transformation. These linearized plasmids were then integrated into the genome by homologous recombination with the endogenous locus of the marker gene.

Deletion mutants (as well as chromosomally tagged strains) were constructed by a PCR-based strategy (318; 319). Briefly, PCR products used for transformation contained the selection marker (and epitope tag) being flanked on both sides by genomic targeting sequences. Stable and correct integration by homologous recombination was subsequently checked by yeast colony PCR. If applicable, successful epitope tagging or gene knockout was additionally confirmed in western blot analysis.

The *rad9-AA* mutant strains were constructed by site-directed mutagenesis where a PCR-based protocol with mutagenic oligonucleotides was used. All RAD9 mutations were targeted to the endogenous RAD9 locus. Correct integration and presence of genomic Rad9 mutation was confirmed by sequencing of the Rad9 locus.

The Bur1 degron mutants were constructed using the AID-degron system (326).

PCR screening of genomic recombination events

For the verification of chromosomal gene disruptions, correct recombination events, "yeast colony-PCR" was used. The screening strategy is based on oligonucleotide probes, which anneal upstream/downstream of altered chromosomal locus (primer I) and within the introduced selection marker gene (primer II). To prepare for PCR, a single yeast colony from a selective media plate was resuspended in 50 μl of 0.02 M NaOH and incubated at 95°C for 5min with rigorous shaking (1400 rpm). Then, the solution was briefly centrifuged (13000 rpm, room temperature) and 2µl of supernatant was directly used as a template for PCR. For PCR DNA oligonucleotides were custom-made by Eurofins MWG Operon.

Mating, sporulation and tetrad analysis

Freshly streaked haploid strains of opposite mating type (MATa, MATα) were mixed on a YPD plate and allowed to mate for 10-15 h at 30ºC. For diploid selection, a patch of cells was restreaked on double-selection plates. Diploid yeast cells were streaked on rich sporulation media plates and incubated for 3 days at 30°C. Sporulation efficiency was assessed microscopically, after this, yeast cells were mixed with water and 10 µl of this mixture was added to 10 µl Zymolase 100T solution and incubated at room temperature for 10 min. Tetrads were dissected with a micromanipulator (Singer MSM System) and grown on YPD plates at 30°C for 2-3 days. tetrads were analyzed genotypically by replica-plating on selective media plates.

Synchronization by alpha-factor (G1 arrest) and nocodazole (G2/M arrest)

Treatment of Mat **a** cells with the alpha-factor pheromone or microtubule inhibitor nocodazole results in cell cycle arrest at G1- and G2/M-phase, respectively. For such cell cycle synchronization, mid-log phase cell MAT a BAR1 cell cultures were supplemented with 5-10 µg/ml alpha-factor (stock solution in water) or 5 µg/ml nocodazole (stock solution in DMSO). Cells were typically allowed to arrest for one generation time (2-4 h depending on

the genetic background) and the arrest confirmed microscopically (typically >90%) and later also by flow cytometry (see below). For MAT a bar1Δ cells, alpha-factor was used at 200 nM.

Phenotypic analysis of yeast mutants, growth and cell survival assays

Nonessential gene knockout strains and mutants were tested for growth impairments and DNA damage sensitivity by spotting equal amounts of cells in serial dilutions onto solid YPD media containing DNA damage inducing agents such as MMS.

FACS analysis

$1x10^7$ - $2x10^7$ cells were harvested by centrifugation and resuspended in 70% ethanol + 50 mM Tris pH 7.8. After centrifugation cells were washed with 1 ml 50 mM Tris pH 7.8 (Tris buffer) followed by resuspending in 520 µl RNase solution (500 µl 50 mM Tris pH 7.8 + 20 µl RNase A (10 mg/ml in 10 mM Tris pH 7.5, 10 mM $MgCl_2$) and incubation for 4 h at 37 °C. Next, cells were treated with proteinase K (200 µl Tris buffer + 20 µl proteinase K (10 mg/ml in 50% glycerol, 10 mM Tris pH 7.5, 25 mM $CaCl_2$) and incubated for 30' at 50 °C. After centrifugation cells were resuspended in 500 µl Tris buffer. Before measuring the DNA content, samples were sonified (5''; 50% CYCLE) and stained by SYTOX solution (999 µl Tris buffer + 1 µl SYTOX). Measurement was performed using FL1 channel 520 for SYTOX-DNA on a BD FACSCalibur system operated via the CELLQuest software (Becton Dickinson). Data was quantitatively analyzed with FlowJo (Tree Star).

6.2.3 Molecular biology techniques

General molecular biology and cloning techniques including DNA amplification/site-directed mutagenesis by PCR, restriction digest, ligation or analysis of DNA by agarose gel electrophoresis were performed according to standard (321) or manufacturer's protocols.

I Isolation of DNA

Isolation of plasmid DNA from E. coli

A single E. coli colony carrying the DNA plasmid of interest was inoculated to 5 ml LB medium containing ampicillin and incubated overnight at 37°C. Plasmids were isolated using the AccuPrep plasmid extraction kit (Bioneer Corp.) according to the manufacturer's instructions. NanoDrop spectrophotometer was used to determine the yield of isolated DNA.

Isolation of chromosomal DNA from S. cerevisiae

Yeast genomic DNA was isolated for further use as a template for amplification of genes via PCR. A stationary culture cells from 10 ml were centrifuged (1500g, 5min), washed in 0.5 ml water and resuspended in 200 µl breaking buffer. Next, 200

µlphenol/chloroform/isoamyl alcohol (24:24:1 v/v/v) and 300 mg acid-washed glass beads (425-600 µm; Sigma) were added and the mixture was vortexed for 5 min. The lysate was mixed with 200 µl TE buffer, centrifuged (14000 rpm, 5 min, room temperature) and the supernatant was transferred to a new microcentrifuge tube.

Precipitation of DNA was carried by adding 1 ml ethanol (absolute) and centrifugation (14000 rpm, 3 min, room temperature). The pellet was resuspended in 0.4 ml TE buffer and RNA contaminants were destroyed by treatment with 30 µl of DNase-free RNase A (1 mg/ml) for 5 min at 37°C. Then, 10 µl ammonium acetate (3 M) and 1 ml ethanol (absolute) were added to precipitate DNA. After brief centrifugation (14000 rpm, room temperature), the pellet was resuspended in 100 µl TE buffer.

Precipitation of DNA

For ethanol precipitation, 1/10 volume sodium acetate (3 M, pH 4.8) and 2.5 volumes ethanol (absolute) were added to the DNA solution and incubated at -20°C for 30 min. Then, the mixture was centrifuged (13000 rpm, 15 min, room temperature) and the pellet was washed with 0.5 ml ethanol (70%). The DNA pellet was air-dried and resuspended in sterile water.

Determination of DNA concentration

The DNA concentration was photometrically determined by measuring the absorbance at a wavelength of 260 nm (OD260) using the NanoDrop ND-1000 spectrophotometer (PeqLab). An OD260 of 1 equals to a concentration of 50 µg/ml double-stranded DNA.

II Molecular cloning

Digestion of DNA with restriction enzymes Standard protocols (321) and the instructions of the manufacturer (NEB) were used to perform the sequence-specific cleavage of DNA with restriction enzymes. In general, 5 to 10 units of the respective restriction enzyme were used for digestion of 1 µg DNA. Normally, the restriction reaction samples were incubated for 2 h in the recommended buffers (NEB) and at the permissive temperature. To avoid re-ligation of linearized vectors, the 5' end of the vector was dephosphorylated by adding 1 µl of Calf Intestinal Phosphatase (CIP; NEB) and incubating at 37°C for 1 h.

Separation of DNA by agarose gel electrophoresis

To isolate DNA fragments, DNA samples were mixed with 6x DNA loading buffer and subjected to electrophoresis using 1% agarose gels containing 0.5 µg/ml ethidium bromide at 120V in TBE buffer. Since ethidium bromide intercalates to DNA, an UV transilluminator (324 nm) was used to visualize separated DNA fragments. The size of the fragments was estimated according to standard size DNA markers (1 kb DNA ladder, Invitrogen).

Isolation of DNA fragments from agarose gels

After separation by gel electrophoresis, DNA fragments were excised from the agarose gel using a sterile razor blade. Then, QIAquick Gel Extraction Kit (Qiagen) according to manufacturer's instructions was used to extract DNA from the agarose block. DNA was eluted with an appropriate volume of sterile water.

Ligation of DNA fragments

The amounts of the linearized vector and insert required for the ligation reaction were measured by NanoDrop ND-1000 spectrophotometer (PeqLab). For the ligation reaction, a ratio of 1:3 to 1:10 of vector to insert was used. The 10 μl ligation reaction sample contained 100 ng of vector DNA and 10 units of T4 DNA ligase (NEB). The ligation reaction was performed at 16°C for 4 to 12 h.

Sequence- and ligation-independent (SLIC) cloning

For the SLIC reaction, 10-200 ng (<0.5 kb: 10-50 ng; 0,5 to 10 kb: 50-100 ng; >10 kb: 50-200 ng) purified PCR fragment and 50-200 ng (<10 kb: 50-100 ng; >10 kb: 50-200 ng) linearized vector were used. The 10 µl SLIC reaction sample contained 1 µl 5x In-Fusion HD Enzyme Premix (Clontech). The total reaction volume was adjusted to 10 μl using dH2O and the reaction was mixed. After incubation for 15 min at 50°C, then the sample was placed on ice and used for the transformation procedure. For long-term storage SLIC reaction sample can be stored at -20°C.

DNA sequencing

The Core Facility of the Max Planck Institute of Biochemistry carried out the DNA sequencing reactions using the ABI-Prism 3730 DNA sequencer (Applied Biosystems Inc.). The 7.5 µl sequencing samples contained 300 ng DNA and 2 µl primer (10 µM). The sequencing reactions and the subsequent sample preparation steps were done with the DYEnamic ET terminator cycle sequencing kit (GE Healthcare), according to the manufacturer's instructions.

III Polymerase chain reaction

To specifically amplify DNA fragments from small amounts of DNA templates the polymerase chain reaction (PCR) technique was used. For amplification of DNA fragments for subsequent cloning, amplification of yeast targeting cassettes (e.g., for chromosomal gene disruption), screening/sequencing of genomic recombination events and site-directed mutagenesis, PCR was applied.

Amplification of genomic DNA fragments

For the generation of genomic DNA fragments for subsequent cloning, direct yeast transformation and sequencing, full-length ORFs or selected sequences were amplified from genomic DNA using the Phusion High-Fidelity DNA polymerase (NEB). PCR reactions in a volume of 50 µl were prepared in 0.2 ml tubes (Biozym) on ice. A PCR Mastercycler (Eppendorf) was used for the reaction.

Amplification of chromosomal targeting cassettes

A PCR strategy based on the targeted introduction of heterologous DNA sequences into genomic locations via homologous recombination was used to perform chromosomal gene deletions, epitope tagging and other alterations of the yeast genome (318, 319). Targeting cassettes were amplified by PCR using primers containing homology to the genomic target locus. The 50 μl PCR reactions were prepared and cycling conditions were used as described above (Amplification of genomic DNA fragments). After amplification, PCR products were concentrated by ethanol precipitation, dissolved in 10 μl sterile water and used directly for the transformation of competent yeast cells or stored at -20°C.

Site-directed mutagenesis

To introduce specific point mutations in plasmid DNA sequences, a PCR-base strategy according to the Quick-change protocol (Strategene) was used. This method is based on two complementary oligonucleotide primers with the codon to be mutated in the middle of the sequence flanked by at least 15-20 additional nucleotides, each corresponding to the target sequence. The Pfu Turbo DNA polymerase (Strategene) has proven to be the enzyme of choice for this technique. DNA oligonucleotides for PCR were custom-made by Eurofins MWG Operon.

To eliminate template plasmid DNA that does not contain the mutation, 25 μl of the PCR reaction were treated with 1 μl of DpnI endonuclease for 1-2 hours at 37°C. DpnI endonuclease is specific for methylated and hemimethylated DNA. Since most plasmid DNA from E. coli is methylated, DpnI treatment of the PCR product leads to the selective digestion of the parental DNA template. After digestion, the PCR product was directly used for E. coli transformation. DNA sequencing was performed to identify mutated plasmids.

6.2.4 Biochemistry techniques

Preparation of denatured protein extracts (TCA-precipitation)

In most cases yeast cells were lysed under denaturing conditions to preserve post-translational modifications. For preparation of denatured protein extracts for every time point, $2x10^7$ cells were harvested and frozen in liquid nitrogen. Cells were suspended in 1 ml water and 150 μl 1.85 M NaOH/7.5 % β-mercaptoethanol was added. After 15 min

incubation on ice, 150 µl 55% TCA was added and incubated for 10 min. Proteins were pelleted by centrifugation (13000 rpm, 4°C, 2 min) and suspended in 50 µl HU-buffer. The samples were boiled at 65 °C for 10 min and used for analysis by Western blot or stored at -20°C.

Preparation of native protein extracts (co-immunoprecipitation)

Native protein extracts were used for co-immunoprecipitation (co-IP) studies. To avoid protein degradation and loss of PTMs, the samples were handled as close to 4ºC as possible and protease inhibitors were used: 2 µg/ml aprotinin, 10mM benzamidine, 10 µg/ml leupeptin, 10 µg/ml pepstatin, PMSF 1mM as well as 1mg/ml Pefabloc SC and EDTA-free complete cocktail (Roche).

Typically 200 OD of log-phase yeast culture was pelleted by centrifugation (5000 rpm, 5min, 4ºC), washed once in ice-cold PBS or 1M sorbitol, 25mM Hepes-KOH pH7.6, and resuspended in an equal volume of Co-IP lysis buffer and prepared for lysis using Spex Sample Prep cryo mill (6 cycles, 2' grinding). The lysates were quickly thawed alternating incubation on ice and cool waterbath, transferred in eppendorf tubes and cleared by centrifugation (20000 g, 4°C ,5 min). The supernatant served as input for subsequent immunoprecipitations using 30 µl (bed volume) of FLAG-M2-beads (Sigma) previously washed in lysis buffer.

Extracts were incubated with FLAG-M2-beads on a rotating wheel at 4°C for 1 h, subsequently, beads were washed 5 times with lysis buffer and transferred to a fresh eppendorf tube in order to remove a-specifically bound proteins. Finally, the beads were dried by aspiration (needle Ø 0.4mm) and bound protein complexes were eluted by with 2 subsequent incubations with 3xFLAG peptide 0.5 mg/ml (sigma) at 4°C. The two eluates were pooled and proteins were precipitated with 15 µl of 55% TCA on ice. Precipitated proteins were then resuspended in 20 µl of HU and denatured by heating at 65°C for 10 min, the obtained proteins were subsequently identified by western blot analysis.

SDS-polyacrylamide gel electrophoresis (SDS-PAGE)

For separation of proteins, SDS-PAGE was performed using self-poured or pre-cast 4-12% gradient NuPAGE Bis-Tris polyacrylamide gels (Invitrogen) which allow resolution of proteins over a large range of different molecular weight (from 10 to 200 kDa) and do not require stacking gels. Electrophoresis was carried out at a constant voltage of 200 V using MOPS running buffer and pre-cast gels or at 150 V using SDS-PAGE running buffer and self-poured gels. The Novex Sharp pre-stained protein standard (Invitrogen) was used as a molecular weight marker. The gels were subsequently subjected to immunoblotting.

Western blot analysis

For western blot analysis, proteins separated by PAGE were transferred to polyvinylidene fluoride (PVDF) membranes (Immonilion-P, 0.45 µm pore size; Millipore)

using a wet tank blotter (Hoefer). The blotting was carried in transfer buffer at a constant voltage of 90 V at 4ºC for 90min.

Subsequently, membranes were incubated over night with primary antibody in TBS-T + 5% milk at 4ºC. After 1 wash with TBS-T (5min), blots were incubated with horse radish peroxidase (HRP)-coupled secondary antibody (1:5000 dilution, Dianova) for 1-3 h in TBS-T + 5% milk at room temperature. After 5 further washes with TBS-T (5min each) signals were obtained by chemiluminescence reactions using ECL kit, (Amersham/GE Healthcare) following the manufacturer's instructions. Signal detection was performed taking qualitative exposures with a film.

Preparation of denaturing protein extracts for immunoprecipitation (IP)

In order to detect the phosphorylation of the residues T474 and S462 on Rad9, denaturing extracts were prepared and were subjected either to TCA precipitation of proteins from the whole cell exctract (as previously described) or used as inputs for enrichment of Rad9 protein (Immunoprecipitation of $Rad9^{3FLAG}$). For the latter technique a lysis buffer containing high salt concentration was used (IP lysis buffer).

Typically 200 OD of log-phase of yeast culture (previously treated with phleomycin to induce DNA-damage dependent phosphorylation of Rad9) was pelleted by centrifugation, washed, resuspended in IP lysis buffer and grinded in a Sphex Sample Prep cryo mill as previously described. After clearing of the lysates by centrifugation (20000 g, 4°C ,5 min) the obtained supernatant served as input for immunoprecipitations using 30 µl (bed volume) of FLAG-M2-beads (Sigma) previously washed in lysis buffer.

Extracts were incubated with FLAG-M2-beads on a rotating wheel at 4°C for 1.5 h, subsequently, beads were washed 5 times with lysis buffer and transferred to a fresh eppendorf tube in order to remove a-specifically bound proteins. Finally, the beads were dried by aspiration (needle Ø 0.4mm) and bound protein complexes were eluted by with 2 subsequent incubations with 3xFlag peptide 0.5 mg/ml (sigma) at 4°C as previously described and subjected to TCA precipitation or directly eluted and denatured in 30 μl of HU buffer at 65°C for 10 min .

6.2.5 Chromatin techniques

DSB-induction at MAT by HO endonuclease

All strains isogenic to JKM179, JKM139 or JKM161 (285; 322) contain the HO gene under the control of a GAL promoter. For efficient galactose induction and to avoid glucose repression, cultures were pre-grown in YP-Raffinose and when log-phase growth was reached, after arrest at the designated cell cycle phase, HO expression was induced by the addition of galactose to a final concentration of 2%. DSB-induction at MAT could be monitored by real time (RT)-PCR with primers flanking the DSB site

Chromatin immunuprecipitation (ChIP)

Time-course experiments and ChIP assays were essentially done as described (322, 323). For each time point, 100 ml culture were aliquoted into 500 mL shake flasks, which had been pre-equilibrated at 30ºC. At the prefixed time points post DSB induction, the OD600 was measured, a 1 OD sample harvested and the remaining 200 ml culture aliquot was fixed by the addition 37% formaldehyde solution to final concentration of 1%. After incubation of exactly 16 min with moderate shaking at 23°C addition of 2.5 M Glycine was used to quench the reaction for 20' (minimum incubation time) at 23°C. A volume worth 100 OD of cells was then pelleted by centrifugation (5000g, 5min, 4°C), washed once in PBS and transferred to a 2ml Eppendorf tube. Cell pellets were frozen in liquid N_2 until further use.

Although proteases were likely inactivated during cross-linking, subsequent cell lysis was performed at 4°C and the FA lysis buffer freshly supplemented with protease inhibitors (1x EDTA-free complete cocktail and 1 mg/ml Pefabloc SC, Roche). Pellets were then resuspended in 800 µl of FA lysis buffer, an equal volume of zirconia/silica beads (BioSpec Inc.) was added and lysis performed on a multi-tube beadbeater (MM301, Retsch GmbH) in 6 intervals of 3 min shaking (frequency 30/s) and 3 min pausing for cool-down (bead-beater was used in a 4°C room).

Lysed samples were collected in a fresh tube by piggyback elution and the chromatin fraction was enriched by centrifugation (20000 g, 15 min, 4°C), followed by resuspension of the pellet in 1 ml of cold FA lysis buffer and transferred to hard plastic 15 ml TPX tubes (Diagenode).

The chromatin fraction was subjected to 50 cycles of sonication (output 200 W; each cycle 30 s sonication and 30 s break) using the Bioruptor UCD-200 sonication system (Diagenode), in order to shear the DNA to an average length of 250-500 bp (occasionally controlled by phenol-chloroform purification and subsequent agarose gel electrophoresis of input DNA). Throughout the sonication process low temperatures were maintained (4°C).

An additional ml of FA lysis buffer was then added to the sheared chromatin and cell debris removed by centrifugation (6150 g, 30 min, 4°C). 20 µl of chromatin lysate were taken aside as input reference and 800 µl used for immunoprecipitation and incubated with either anti-FLAG-M2 magnetic beads (Sigma) for 2 hours ($Rad9^{3FLAG}$ ChIPs) or with anti-RPA antibody (AS07-214, Agrisera) followed by 30 min with Dynabeads Protein A (Invitrogen, for RPA ChIPs). The beads were washed 3x in lysis buffer, 2x in lysis buffer with 500 mM NaCl, 2x in wash buffer (10 mM Tris-Cl pH 8.0, 0.25 M LiCl, 1 mM EDTA, 0.5% NP-40, 0.5% Na-deoxycholate) and 2x in TE pH 8.0. DNA-protein complexes were eluted in 1% SDS, proteins were removed via Proteinase K digestion (3 h, 42°C) and crosslinks were reversed (8 h or overnight, 65°C). The DNA was subsequently purified using phenol-chloroform extraction and ethanol precipitation and quantified by quantitative PCR (Roche LightCycler 480 System, KAPA SYBR FAST 2x qPCR Master Mix, KAPA Biosystems) at indicated positions with respect to the DNA double-strand break. As a control, 2-3 control regions on other chromosomes were quantified.

Real time PCR quantification

Quantitative, real time (RT)-PCR was performed on a LightCycler 480 System, using the LightCycler 480 SYBR Green I Master hot-start reaction mix (Roche Diagnostics GmbH, Mannheim, Germany). 18 μl mastermix containing primers, SYBR Green I Master and H2O was aliquoted into 384-well LightCycler plates and either 2µl ChIP sample (undiluted) or 2µl input sample (in a 1:10 dilution) was added. Reactions were done in triplicates.

Template DNA concentrations were quantified from the second derivative maximum of the LightCycler PCR amplification curves, using for each primer pair an input sample dilution series as standard (1:5, 1:50, 1:500, 1:5000). Amplification was followed by a melting curve analysis, which served as quality control that primers were specific and only a single PCR product was amplified per reaction. Primers were aliquoted upon receipt and not refrozen after use.

Normalization of ChIP data

For all RT-PCR experiments on ChIP samples, signals at MAT were normalized to the average signal of 3 separate unaffected control loci using the formula: Fold-enrichment = [IP(test)/input(test)] / [IP(control)/input(control)]. The efficiency of DSB induction was measured by quantitative PCR with primers spanning the break. All signals were finally normalized to 1 for the signal before induction to visualize protein factor recruitment after break induction.

6.2.6 Mass Spectrometry techniques

SILAC-based mass spectrometry

For the detection of chromatin-assembled checkpoint complexes responding to DNA damage stable isotope labeling with amino acids in cell culture (SILAC) and *in-vivo* formaldehyde crosslinking was used. As DNA damaging agent mainly MMS was used, at the final concentration of 0.3%. In order to detect and discriminate between checkpoint protein complexes located at sites of ongoing DSBs repair or at sites of intact chromatin FLAG-tagged RFA or HTA1 were used respectively as bait proteins.

For detection of RPA or HTA1 specific interactors yeast cells deficient in biosynthesis of lysine and arginine (lys1Δ arg4 Δ) expressing either $RPA1^{3FLAG}$ or $Hta1^{3FLAG}$ were grown in SC media supplemented either with unlabeled (Lyso, Argo; Light) or heavy isotope labeled amino acids (Lys8, Arg10; Heavy) from Cambridge Isotope Laboratories. In order to ensure incorporation of the Heavy isotopes the cells were grown overnight to stationary phase and subsequently re-inoculated in fresh media for a second and then a third overnight culture. From the third overnight culture cells were inoculated in fresh media and grown to an OD600=0.8, exponentially growing cells in Light media were treated with 0,3% MMS and incubated for one hour. The protein-protein and protein-DNA crosslinking was achieved by

adding 1% Formaldehyde from Sigma (37 wt. % in H_2O plus 10-15% Methanol as stabilizer) and incubating for 16 minutes at room temperature.

After incubation of exactly 16 min with moderate shaking at 23ºC addition of 2.5 M Glycine was used to quench the reaction for 20' (minimum incubation time) at 23ºC. Cells were then pelleted by centrifugation (5000 g, 5 min, 4°C), and treated cells from light medium were combined with equal amount of untreated cells grown in heavy medium, washed once in Sorbitol buffer and transferred to 2 ml Eppendorf tubes. Cell pellets were frozen in liquid N_2 until further use.

Subsequent cell lysis was performed at 4°C and the Lysis buffer freshly supplemented with protease inhibitors (1x EDTA-free complete cocktail and 1 mg/ml Pefabloc SC, Roche). Pellets were then resuspended in 800 µl of Lysis buffer, an equal volume of zirconia/silica beads (BioSpec Inc.) was added and lysis performed on a multi-tube beadbeater (MM301, Retsch GmbH) in 6 intervals of 3 min shaking (frequency 30/s) and 3 min pausing for cool-down (bead-beater was used in a 4°C room). Lysed samples were collected in a fresh tube by piggyback elution and the chromatin fraction was enriched by centrifugation (20000 g, 15 min, 4°C), followed by resuspension of the pellet in 1 ml of cold FA lysis buffer and transferred to hard plastic 15 ml TPX tubes (Diagenode).

The chromatin fraction was subjected to 50 cycles of sonication (output 200 W; each cycle 30 s sonication and 30 s break) using the Bioruptor UCD-200 sonication system (Diagenode), in order to shear the DNA to an average length of 250-500 bp (occasionally controlled by phenol-chloroform purification and subsequent agarose gel electrophoresis of input DNA). Throughout the sonication process low temperatures were maintained (4°C).
Cell debris were removed by centrifugation (6150 g, 30 min, 4°C) and 800 µl were used for immunoprecipitation and incubated with anti-FLAG-M2 beads (Sigma ANTI-FLAG® M2 Affinity Gel) for 2 hours at 23ºC. Beads were then washed in Lysis Buffer, and crosslink reversal and protein elution were achieved by boiling samples in 20 μl of Laemmli buffer for 10 minutes at 95ºC.
The samples were then run on 4-12% Bis-Tris gel and handed to the Core Facility of Max Planck Institute of Biochemistry were in-gel digestion of proteins was carried out using trypsin. Proteins were then analyzed by LC-MS/MS using LTQ-Orbitrap mass spectrometer (324) and proteins of interest identified using MaxQuant Software (325). SILAC ratios for quantified proteins were plotted against the sum of the relevant pepetide intensities using the GraphPad Prism version 5.0 for MAC OS X and proteins were colored according to values of MaxQuant Significance(B).

The same protocol was followed in SILAC experiments performed to detect specific interactors of RPA1 under DNA damage condition, in this case $RPA1^{3FLAG}$ cells were grown as described in heavy and light media, and exponentially growing cells in heavy media were treated with 0.3% MMS.

References

1. Lindahl T, Barnes DE (2000) Repair of endogenous DNA damage. Cold Spring Harb Symp Quant Biol 65:127-33.
2. Hoeijmakers JH (2009) DNA damage, aging, and cancer. N Engl J Med. 8;361(15):1475-85.
3. Caldecott KW (2008) Single-strand break repair and genetic disease. Nat Rev Genet. Aug;9(8):619-31.
4. West SC (2003) Molecular views of recombination proteins and their control. Nat Rev Mol Cell Biol.;4(6):435-45.
5. Hanahan D, Weinberg RA (2011) Hallmarks of cancer: the next generation. Cell ;144(5):646-74.
6. Jackson SP, Bartek J (2009) The DNA-damage response in human biology and disease. Nature. 22;461(7267):1071-8.
7. Keeney S (2008) Spo11 and the Formation of DNA Double-Strand Breaks in Meiosis. Genome Dyn Stab. 1; 2:81-123
8. Neale MJ1, Keeney S (2006) Clarifying the mechanics of DNA strand exchange in meiotic recombination. Nature. 13;442(7099):153-8.
9. Dudley DD, Chaudhuri J, Bassing CH, Alt FW (2005) Mechanism and control of V(D)J recombination versus class switch recombination: similarities and differences. Adv Immunol. 86:43-112.
10. Gostissa M, Alt FW, Chiarle R (2011) Mechanisms that promote and suppress chromosomal translocations in lymphocytes. Annual review of immunology. 29:319–350.
11. Hartlerode AJ1, Scully R. (2009) Mechanisms of double-strand break repair in somatic mammalian cells. Biochem J. 25;423(2):157-68.
12. Lieber MR. (2008) The mechanism of human nonhomologous DNA end joining. J. Biol. Chem. 283:1–5.
13. Lieber MR (2010) The mechanism of double-strand DNA break repair by the nonhomologous DNA end-joining pathway. Annu Rev Biochem. 79:181-211.
14. San Filippo J, Sung P, Klein H. (2008) Mechanism of eukaryotic homologous recombination. Annu Rev Biochem. 77:229-57.
15. Lowndes NF, Murguia JR (2000) Sensing and responding to DNA damage. Curr Opin Genet Dev 10(1):17–25
16. Zhou BB, Elledge SJ (2000) The DNA damage response: putting checkpoints in perspective. Nature 408(6811):433–439
17. Bartek J, Lukas J (2007) DNA damage checkpoints: from initiation to recovery or adaptation. Curr Opin Cell Biol 19(2): 238–245
18. Clemenson C, Marsolier-Kergoat MC (2009) DNA damage checkpoint inactivation: adaptation and recovery. DNA Repair (Amst) 8(9):1101–1109
19. Futcher B (1996) Cyclins and the wiring of the yeast cell cycle. Yeast 12(16):1635–1646
20. Bahler J (2005) Cell-cycle control of gene expression in budding and fission yeast. Annu Rev Genet 39:69–94
21. Morgan DO (2007) The cell cycle: principles of control. Primers in biology. New Science, London

22. Forsburg SL, Nurse P (1991) Cell cycle regulation in the yeasts Saccharomyces cerevisiae and Schizosaccharomyces pombe. Annu Rev Cell Biol 7:227–256.
23. Lim HH, Goh PY, Surana U (1996) Spindle pole body separation in Saccharomyces cerevisiae requires dephosphorylation of the tyrosine 19 residue of Cdc28. Mol Cell Biol 16(11): 6385–6397
24. Yamamoto A, Guacci V, Koshland D (1996) Pds1p, an inhibitor of anaphase in budding yeast, plays a critical role in the APC and checkpoint pathway(s). J Cell Biol 133(1):99–110
25. Fitz Gerald JN, Benjamin JM, Kron SJ (2002) Robust G1 checkpoint arrest in budding yeast: dependence on DNA damage signaling and repair. J Cell Sci 115(Pt 8):1749–1757
26. Siede W, Friedberg AS, Dianova I, Friedberg EC (1994) Characterization of G1 checkpoint control in the yeast Saccharomyces cerevisiae following exposure to DNA-damaging agents. Genetics 138(2):271–281
27. Siede W, Friedberg AS, Friedberg EC (1993) RAD9-dependent G1 arrest defines a second checkpoint for damaged DNA in the cell cycle of Saccharomyces cerevisiae. Proc Natl Acad Sci USA 90(17):7985–7989
28. Siede W, Allen JB, Elledge SJ, Friedberg EC (1996) The Saccharomyces cerevisiae MEC1 gene, which encodes a homolog of the human ATM gene product, is required for G1 arrest following radiation treatment. J Bacteriol 178(19):5841–5843
29. Longhese MP, Clerici M, Lucchini G (2003) The S-phase checkpoint and its regulation in Saccharomyces cerevisiae. Mutat Res 532(1–2):41–58
30. Paulovich AG, Hartwell LH (1995) A checkpoint regulates the rate of progression through S phase in S. cerevisiae in response to DNA damage. Cell 82(5):841–847
31. Lindahl T (2000) Suppression of spontaneous mutagenesis in human cells by DNA base excision-repair. Mutat Res 462(2- 3):129–135
32. Harrison JC, Haber JE (2006) Surviving the breakup: the DNA damage checkpoint. Annu Rev Genet 40:209–235
33. Finn K, Lowndes NF, Grenon M (2012) Eukaryotic DNA damage checkpoint activation in response to double-strand breaks Cell Mol Life Sci 69(9):1447-73
34. Lovejoy CA, Cortez D (2009) Common mechanisms of PIKK regulation. DNA Repair (Amst) 8(9):1004–1008
35. Paciotti V, Clerici M, Scotti M, Lucchini G and Longhese MP (2001) characterization of *mec1* kinase-deficient mutants and of new hypomorphic *mec1* alleles impairing subsets of the dna damage response pathway Mol Cell Biol. 21(12):3913-25.
36. Suzuki K, Kodama S, Watanabe M (1999) Recruitment of ATM protein to double strand DNA irradiated with ionizing radiation. J Biol Chem 274(36):25571–25575
37. Zou L, Elledge SJ (2003) Sensing DNA damage through ATRIP recognition of RPA-ssDNA complexes. Science 300(5625): 1542–1548
38. Dart DA, Adams KE, Akerman I, Lakin ND (2004) Recruitment of the cell cycle checkpoint kinase ATR to chromatin during S-phase. J Biol Chem 279(16):16433–16440.
39. Cuadrado M, Martinez-Pastor B, Murga M, Toledo LI, Gutierrez-Martinez P, Lopez E, Fernandez-Capetillo O (2006) ATM regulates ATR chromatin loading in response to DNA doublestrand breaks. J Exp Med 203(2):297–303.
40. Jazayeri A, Falck J, Lukas C, Bartek J, Smith GC *et. al* (2006) ATM- and cell cycle-dependent regulation of ATR in response to DNA double-strand breaks. Nat Cell Biol 8(1):37–45

41. Adams KE, Medhurst AL, Dart D, Lakin ND (2006) Recruitment of ATR to sites of ionising radiation-induced DNA damage requires ATM and components of the MRN protein complex. Oncogene 25(28):3894–3904.
42. Stracker TH, Usui T, Petrini JH (2009) Taking the time to make important decisions: the checkpoint effector kinases Chk1 and Chk2 and the DNA damage response. DNA Repair (Amst) 8(9):1047–1054
43. Branzei D, Foiani M (2008) Regulation of DNA repair throughout the cell cycle. Nat Rev Mol Cell Biol 9(4):297–308
44. Harper JW, Elledge SJ (2007) The DNA damage response: ten years after. Mol Cell 28(5):739–745
45. Weinert TA and Hartwell LH (1988) The RAD9 gene controls the cell cycle response to DNA damage in Saccharomyces cerevisiae. Science 241(4863):317-22
46. Sidorova JM, Breeden LL (1997) Rad53-dependent phosphorylation of Swi6 and down-regulation of CLN1 and CLN2 transcription occur in response to DNA damage in Saccharomyces cerevisiae. Genes Dev 11(22):3032–3045
47. Sidorova JM, Breeden LL (2003) Rad53 checkpoint kinase phosphorylation site preference identified in the Swi6 protein of Saccharomyces cerevisiae. Mol Cell Biol 23(10):3405–3416
48. Ghavidel A, Kislinger T, Pogoutse O, Sopko R, Jurisica I, *et. al* (2007) Impaired tRNA nuclear export links DNA damage and cell-cycle checkpoint. Cell 131(5):915–926
49. Schwob E, Bohm T, Mendenhall MD, Nasmyth K (1994) The B-type cyclin kinase inhibitor p40SIC1 controls the G1 to S transition in S. cerevisiae. Cell 79(2):233–244
50. Verma R, Annan RS, Huddleston MJ, Carr SA, Reynard G *et. al* (1997) Phosphorylation of Sic1p by G1 Cdk required for its degradation and entry into S phase. Science 278(5337):455–460
51. Grenon M, Gilbert C, Lowndes NF (2001) Checkpoint activation in response to double-strand breaks requires the Mre11/ Rad50/Xrs2 complex. Nat Cell Biol 3(9):844–847
52. Nyberg KA, Michelson RJ, Putnam CW, Weinert TA (2002) Toward maintaining the genome: DNA damage and replication checkpoints. Annu Rev Genet 36:617–656
53. Blasina A, de Weyer IV, Laus MC, Luyten WH, Parker AE *et. al* (1999) A human homologue of the checkpoint kinase Cds1 directly inhibits Cdc25 phosphatase. Curr Biol 9(1):1–10
54. Mailand N, Falck J, Lukas C, Syljuasen RG, Welcker M *et. al* (2000) Rapid destruction of human Cdc25A in response to DNA damage. Science 288(5470):1425–1429
55. Falck J, Mailand N, Syljuasen RG, Bartek J, Lukas J (2001) The ATM-Chk2-Cdc25A checkpoint pathway guards against radioresistant DNA synthesis. Nature 410(6830):842–847.
56. Hoffmann I, Draetta G, Karsenti E (1994) Activation of the phosphatase activity of human cdc25A by a cdk2-cyclin E dependent phosphorylation at the G1/S transition. EMBO J 13(18):4302–4310
57. Canman CE, Lim DS, Cimprich KA, Taya Y, Tamai K *et. al* (1998) Activation of the ATM kinase by ionizing radiation and phosphorylation of p53. Science 281(5383):1677–1679
58. Dumaz N, Meek DW (1999) Serine15 phosphorylation stimulates p53 transactivation but does not directly influence interaction with HDM2. EMBO J 18(24):7002–7010

59. Chehab NH, Malikzay A, Appel M, Halazonetis TD (2000) Chk2/hCds1 functions as a DNA damage checkpoint in G(1) by stabilizing p53. Genes Dev 14(3):278–288
60. Shieh SY, Ahn J, Tamai K, Taya Y, Prives C (2000) The human homologs of checkpoint kinases Chk1 and Cds1 (Chk2) phosphorylate p53 at multiple DNA damage-inducible sites. Genes Dev 14(3):289–300
61. Zhang Y, Xiong Y (2001) A p53 amino-terminal nuclear export signal inhibited by DNA damage-induced phosphorylation. Science 292(5523):1910–1915.
62. Sherr CJ, Roberts JM (1999) CDK inhibitors: positive and negative regulators of G1-phase progression. Genes Dev 13(12):1501–1512 294.
63. Ekholm SV, Reed SI (2000) Regulation of G(1) cyclin-dependent kinases in the mammalian cell cycle. Curr Opin Cell Biol 12(6):676–684
64. Brush GS, Kelly TJ (2000) Phosphorylation of the replication protein A large subunit in the Saccharomyces cerevisiae checkpoint response. Nucleic Acids Res 28(19):3725–3732
65. Longhese MP, Neecke H, Paciotti V, Lucchini G, Plevani P (1996) The 70 kDa subunit of replication protein A is required for the G1/S and intra-S DNA damage checkpoints in budding yeast. Nucleic Acids Res 24(18):3533–3537
66. Brush GS, Morrow DM, Hieter P, Kelly TJ (1996) The ATM homologue MEC1 is required for phosphorylation of replication protein A in yeast. Proc Natl Acad Sci USA 93(26):15075–15080
67. Marini F, Pellicioli A, Paciotti V, Lucchini G, Plevani P, Stern DF, Foiani M (1997) A role for DNA primase in coupling DNA replication to DNA damage response. EMBO J 16(3):639–650
68. Longhese MP, Fraschini R, Plevani P, Lucchini G (1996) Yeast pip3/mec3 mutants fail to delay entry into S phase and to slow DNA replication in response to DNA damage, and they define a functional link between Mec3 and DNA primase. Mol Cell Biol 16(7):3235–3244
69. Labib K (2010) How do Cdc7 and cyclin-dependent kinases trigger the initiation of chromosome replication in eukaryotic cells? Genes Dev 24(12):1208–1219.
70. Lopez-Mosqueda J, Maas NL, Jonsson ZO, Defazio-Eli LG, Wohlschlegel J *et. al* (2010) Damage-induced phosphorylation of Sld3 is important to block late origin firing. Nature 467(7314):479–483.
71. Zegerman P, Diffley JF (2010) Checkpoint-dependent inhibition of DNA replication initiation by Sld3 and Dbf4 phosphorylation. Nature 467(7314):474–478.
72. Segurado M, Diffley JF (2008) Separate roles for the DNA damage checkpoint protein kinases in stabilizing DNA replication forks. Genes Dev 22(13):1816–1827.
73. Morin I, Ngo HP, Greenall A, Zubko MK, Morrice N *et. al* (2008) Checkpoint-dependent phosphorylation of Exo1 modulates the DNA damage response. EMBO J 27(18):2400–2410.
74. Cotta-Ramusino C, Fachinetti D, Lucca C, Doksani Y, Lopes M *et. al* (2005) Exo1 processes stalled replication forks and counteracts fork reversal in checkpoint-defective cells. Mol Cell 17(1):153–159.
75. Smolka MB, Albuquerque CP, Chen SH, Zhou H (2007) Proteome- wide identification of in vivo targets of DNA damage checkpoint kinases. Proc Natl Acad Sci USA 104(25):10364–10369.
76. Cimprich KA, Cortez D (2008) ATR: an essential regulator of genome integrity. Nat Rev Mol Cell Biol 9(8):616–627.

77. Zachos G, Rainey MD, Gillespie DA (2005) Chk1-dependent S-M checkpoint delay in vertebrate cells is linked to maintenance of viable replication structures. Mol Cell Biol 25(2):563–574.
78. Zachos G, Rainey MD, Gillespie DA (2003) Chk1-deficient tumour cells are viable but exhibit multiple checkpoint and survival defects. EMBO J 22(3):713–723.
79. Trenz K, Smith E, Smith S, Costanzo V (2006) ATM and ATR promote Mre11 dependent restart of collapsed replication forks and prevent accumulation of DNA breaks. EMBO J 25(8):1764–1774.
80. Grallert B, Boye E (2008) The multiple facets of the intra-S checkpoint. Cell Cycle 7(15):2315–2320.
81. Falck J, Petrini JH, Williams BR, Lukas J, Bartek J (2002) The DNA damage-dependent intra-S phase checkpoint is regulated by parallel pathways. Nat Genet 30(3):290–294.
82. Sorensen CS, Syljuasen RG, FalckSchroeder J, Ronnstrand L, Khanna KK *et. al* (2003) Chk1 regulates the S phase checkpoint by coupling the physiological turnover, ionizing radiation-induced accelerated proteolysis of Cdc25A. Cancer Cell 3(3):247–258.
83. Kim ST, Xu B, Kastan MB (2002) Involvement of the cohesin protein, Smc1, in Atm-dependent and independent responses to DNA damage. Genes Dev 16(5):560–570.
84. Yazdi PT, Wang Y, Zhao S, Patel N, Lee EY *et. al* (2002) SMC1 is a downstream effector in the ATM/NBS1 branch of the human S-phase checkpoint. Genes Dev 16(5):571–582. doi:
85. Kitagawa R, Bakkenist CJ, McKinnon PJ, Kastan MB (2004) Phosphorylation of SMC1 is a critical downstream event in the ATM-NBS1-BRCA1 pathway. Genes Dev 18(12):1423–1438.
86. Luo H, Li Y, Mu JJ, Zhang J, Tonaka T *et. al* (2008) Regulation of intra-S phase checkpoint by ionizing radiation (IR)-dependent and IR-independent phosphorylation of SMC3. J Biol Chem 283(28):19176–19183.
87. Sancar A, Lindsey-Boltz LA, Unsal-Kacmaz K, Linn S (2004) Molecular mechanisms of mammalian DNA repair and the DNA damage checkpoints. Annu Rev Biochem 73:39–85.
88. Amon A, Surana U, Muroff I, Nasmyth K (1992) Regulation of p34CDC28 tyrosine phosphorylation is not required for entry into mitosis in S. cerevisiae. Nature 355(6358):368–371.
89. Sorger PK, Murray AW (1992) S-phase feedback control in budding yeast independent of tyrosine phosphorylation of p34cdc28. Nature 355(6358):365–368.
90. Cohen-Fix O, Koshland D (1997) The metaphase-to-anaphase transition: avoiding a mid-life crisis. Curr Opin Cell Biol 9(6):800–806.
91. Sanchez Y, Bachant J, Wang H, Hu F, Liu D *et. al* (1999) Control of the DNA damage checkpoint by chk1 and rad53 protein kinases through distinct mechanisms. Science 286(5442):1166–1171.
92. Wang H, Liu D, Wang Y, Qin J, Elledge SJ (2001) Pds1 phosphorylation in response to DNA damage is essential for its DNA damage checkpoint function. Genes Dev 15(11):1361–1372.
93. Agarwal R, Tang Z, Yu H, Cohen-Fix O (2003) Two distinct pathways for inhibiting Pds1 ubiquitination in response to DNA damage. J Biol Chem 278(45):45027–45033.
94. Cheng L, Hunke L, Hardy CF (1998) Cell cycle regulation of the Saccharomyces cerevisiae polo-like kinase Cdc5p. Mol Cell Biol 18(12):7360–7370.

95. Liang F, Wang Y (2007) DNA damage checkpoints inhibit mitotic exit by two different mechanisms. Mol Cell Biol 27(14):5067–5078
96. Ciccia A, Elledge S.J (2010), The DNA damage response: making it safe to play with knives, Molecular Cell 40:179–204.
97. Savitsk K, Sfez S, Tagle DA, Ziv Y, Sartiel A *et. al* (1995) The complete sequence of the coding region of the ATM gene reveals similarity to cell cycle regulators in different species, Human Molecular Genetics 4:2025–2032.
98. O'Driscoll M., Ruiz-Perez VL, Woods CG, Jeggo PA, GoodshipJA (2003) A splicing mutation affecting expression of ataxia-telangiectasia and Rad3-related protein (ATR) results in Seckel syndrome Nat Genet. 33(4):497-501
99. Lempiäinen H., Halazonetis T.D, (2009) Emerging common themes in regulation of PIKKs and PI3Ks, EMBO Journal 28:3067–3073
100. Bosotti R, Isacchi A, Sonnhammer EL,(2000) FAT: a novel domain in PIK-related kinases Trends in Biochemical Sciences 25:225–227.
101. Bakkenist CJ, Kastan MB. DNA damage activates ATM through intermolecular autophosphorylation and dimer dissociation. Nature. 2003;421:499–506.
102. Lee J-H, Paull TT (2005) ATM activation by DNA double-strand breaks through the Mre11-Rad50-Nbs1 complex. Science. 308:551–554.
103. Lustig AJ, Petes TD (1986) Identification of yeast mutants with altered telomere structure. Proc Natl Acad Sci USA. 83(5):1398–1402.
104. Greenwell PW, Kronmal SL, Porter SE, Gassenhuber J, Obermaier B *et. al* (1995) TEL1, a gene involved in controlling telomere length in S. cerevisiae, is homologous to the human ataxia telangiectasia gene. Cell. 82(5):823–829.
105. Morrow DM, Tagle DA, Shiloh Y, Collins FS, Hieter P (1995) TEL1, an S. cerevisiae homolog of the human gene mutated in ataxia telangiectasia, is functionally related to the yeast checkpoint gene MEC1. . Cell. 82(5):831–840.
106. Wellinger RJ, Zakian VA. (2012) Everything you ever wanted to know about Saccharomyces cerevisiae telomeres: beginning to end. Genetics 191(4):1073–1105.
107. Wu Y, Xiao S, and Zhu X.-D, (2007) MRE11-RAD50-NBS1 and ATM function as co-mediators of TRF1 in telomere length control, Nature Structural & Molecular Biology, 14(9):832–840.
108. Smileno LB, Dhar S, and Pandita TK, (1999) Altered telomere nuclear matrix interactions and nucleosomal periodicity in ataxia telangiectasia cells before and after ionizing radiation treatment, Molecular and Cellular Biology, 19(10):6963–6971.
109. Qi L, Strong MA, Karim BO, Armanios M, Huso DL, and Greider CW (2003) Short telomeres and ataxia-telangiectasia mutated deficiency cooperatively increase telomere dysfunction and suppress tumorigenesis. Cancer Research, 63(23):. 8188–8196.
110. Lisby M, Barlow JH, Burgess RC, Rothstein R (2004) Choreography of the DNA damage response: spatiotemporal relationships among checkpoint and repair proteins, Cell 118: 699–713.
111. Ivanov EL, Sugawara N, White CI, Fabre F, Haber JE (1994) Mutations in XRS2 and RAD50 delay but do not prevent mating-type switching in Saccharomyces cerevisiae, Molecular and Cellular Biology 14:3414–3425.
112. Clerici M, Mantiero D, Lucchini G, Longhese MP (2005) The Saccharomyces cerevisiae Sae2 protein promotes resection and bridging of double strand break ends, Journal of Biological Chemistry 280:38631–38638.
113. Mimitou EP, Symington LS (2008) Sae2, Exo1, Sgs1 collaborate in DNA doublestrand

break processing, Nature 455:770–774.
114. Zhu Z, Chung WH, Shim EY, Lee SE, Ira G (2008) Sgs1 helicase and two nucleases Dna2 and Exo1 resect DNA double-strand break ends, Cell 134:981–994.
115. Symington LS (2014) End resection at double-strand breaks: mechanism and regulation. Cold Spring Harb Perspect Biol. 6(8).
116. Longhese MP, Bonetti D, Manfrini N, Clerici M. (2010) Mechanisms and regulation of DNA end resection. EMBO J. 29(17):2864–2874.
117. Stracker TH, Petrini JH. The (2011) MRE11 complex: starting from the ends. Nat Rev Mol Cell Biol. 12(2):90–103.
118. Nakada D, Matsumoto K, Sugimoto K (2003) ATM-related Tel1 associates with double-strand breaks through an Xrs2-dependent mechanism, Genes and Development 17:1957–1962.
119. Falck J, Coates J, Jackson SP (2005) Conserved modes of recruitment of ATM, ATR and DNA-PKcs to sites of DNA damage. Nature 434:605–611.
120. You Z, Chahwan C, Bailis J, Hunter T, Russell P (2005) ATM activation and its recruitment to damaged DNA require binding to the C terminus of Nbs1, Molecular and Cellular Biology 25:5363–5379.
121. Fukunaga K, Kwon Y, Sung P, Sugimoto K (2011) Activation of protein kinase Tel1 through recognition of protein-bound DNA ends Mol Cell Biol. 31(10): 1959–1971.
122. Usui T, Ogawa H, Petrini JH (2001) A DNA damage response pathway controlled by Tel1 and the Mre11 complex. Mol Cell 7(6):1255–1266
123. D'Amours D, Jackson SP (2001)The yeast Xrs2 complex functions in S phase checkpoint regulation. Genes Dev 15(17):2238–2249
124. Baroni E, Viscardi V, Cartagena-Lirola H, Lucchini G, Longhese MP (2004) The functions of budding yeast Sae2 in the DNA damage response require Mec1- and Tel1-dependent phosphorylation. Mol Cell Biol 24(10):4151–4165.
125. Mantiero D, Clerici M, Lucchini G, Longhese MP (2007) Dual role for Saccharomyces cerevisiae Tel1 in the checkpoint response to double-strand breaks. EMBO Rep 8(4):380–387.
126. Sanchez Y, Desany BA, Jones WJ, Liu Q, Wang B, Elledge SJ (1996) Regulation of RAD53 by the ATM-like kinases MEC1 and TEL1 in yeast cell cycle checkpoint pathways. Science 271(5247):357–360.
127. Shiotani B, Zou L. (2009) Single-stranded DNA orchestrates an ATM-to-ATR switch at DNA breaks. Mol Cell 33(5):547–558.
128. Paciotti V, Clerici M, Lucchini G, Longhese MP. (2000) The checkpoint protein Ddc2, functionally related to S. pombe Rad26, interacts with Mec1 and is regulated by Mec1-dependent phosphorylation in budding yeast. Genes Dev. 14:2046–2059.
129. Majka J, Niedziela-Majka A, Burgers PMJ. (2006) The checkpoint clamp activates Mec1 kinase during initiation of the DNA damage checkpoint. Mol Cell. 24:891–901.
130. Ball HL, Cortez D. (2005) ATRIP oligomerization is required for ATR-dependent checkpoint signaling. J Biol Chem. 280:31390–31396.
131. Araki H, Leem SH, Pongdara A, Sungino A. (1995) Dpb11, which interacts with DNA polymerase II(epsilon) in Saccharomyces cerevisiae, has a dual role in S-phase progression and at a cell cycle checkpoint. Proc Natl Acad Sci U S A 92(25):11791-5.
132. Aparicio OM, Stout AM, Bell SP (1999) Differential assembly of Cdc45p and DNA polymerases at early and late origins of DNA replication Proc Natl Acad Sci U S A, 96:9130–9135.

133. Paulsen RD, Cimprich KA (2007) The ATR pathway: fine-tuning the fork DNA Repair (Amst), 6:953–966.
134. Paciotti V, Clerici M, Lucchini G, Longhese MP (2000) The checkpoint protein Ddc2, functionally related to S. pombe Rad26, interacts with Mec1 and is regulated by Mec1-dependent phosphorylation in budding yeast. Genes and Development 14 2046–2059.
135. Cortez D, Guntuku S, Qin J, Elledge SJ (2001) ATR and ATRIP: partners in checkpoint signaling, Science 294:1713–1716.
136. Navadgi-Patil VM, Burgers PM (2009) The unstructured C-terminal tail of the 9-1-1 clamp subunit Ddc1 activates Mec1/ATR via two distinct mechanisms. Mol. Cell 36:743–753.
137. Bonilla CY, Melo JA, Toczyski DP (2008) Colocalization of sensors is sufficient to activate the DNA damage checkpoint in the absence of damage. Mol. Cell 30:267–276.
138. S. Delacroix JM, Wagner M, Kobayashi K, Yamamoto LM, Karnitz (2007) The Rad9-Hus1-Rad1 (9-1-1) clamp activates checkpoint signaling via TopBP1 Genes Dev, 21 pp. 1472–1477.
139. Lee J, Kumagai A, Dunphy WG (2007) The Rad9-Hus1-Rad1 checkpoint clamp regulates interaction of TopBP1 with ATR J Biol Chem. 282 pp. 28036–28044
140. Furuya K, Poitelea M, Guo L, Caspari T, Carr AM. Chk1 activation requires Rad9 S/TQ-site phosphorylation to promote association with C-terminal BRCT domains of Rad4TOPBP1. Genes Dev. 2004;18:1154–1164.
141. Navadgi-Patil VM, Burgers PM Yeast DNA replication protein Dpb11 activates the Mec1/ATR checkpoint kinase J Biol Chem, 283 pp. 35853–35859
142. Mordes DA, Nam EA, Cortez D (2008) Dpb11 activates the Mec1-Ddc2 complex Proc Natl Acad Sci U S A, 105 pp. 18730–18734
143. Pfander B, Diffley J (2011) Dpb11 coordinates Mec1 kinase activation with cell cycle-regulated Rad9 recruitment. EMBO J. 30(24):4897-907.
144. Navadgi-Patil VM, Kumar S, Burger P (2011) The Unstructured C-terminal Tail of Yeast Dpb11 (Human TopBP1) Protein Is Dispensable for DNA Replication and the S Phase Checkpoint but Required for the G2/M Checkpoint J Biol Chem 286(47): 40999–41007.
145. Budd ME, Campbell JL. (1995) A yeast gene required for DNA replication encodes a protein with homology to DNA helicases. Proc Natl Acad Sci USa. 92:7642–7646.
146. Kuo C, Nuang H, Campbell JL (1983) Isolation of yeast DNA replication mutants in permeabilized cells. Proc Natl Acad Sci USa. 80:6465–6469.
147. Cejka P, Cannavo E, Polaczek P, Masuda-Sasa T, Pokharel S, *et al.* DNA end resection by Dna2-Sgs1-RPA and its stimulation by Top3-Rmi1 and Mre11-Rad50-Xrs2. Nature. 2010;467:112–116
148. Niu H, Chung W-H, Zhu Z, Kwon Y, Zhao W, *et al.* (2010) Mechanism of the ATP-dependent DNA end-resection machinery from Saccharomyces cerevisiae. Nature. 467:108–111
149. Nimonkar AV, Genschel J, Kinoshita E, Polaczek P, Campbell JL, Wyman C, et al. (2011) BLM-DNA2-RPA-MRN and EXO1-BLM-RPA-MRN constitute two DNA end resection machineries for human DNA break repair. Genes Dev. 25:350–362
150. Kumar S, Burgers PM. (2013) Lagging strand maturation factor Dna2 is a component of the replication checkpoint initiation machinery. Genes Dev. 27:313–321.
151. Mallory JC, Petes TD (2000) Protein kinase activity of Tel1p and Mec1p, two Saccharomyces cerevisiae proteins related to the human ATM protein kinase Prot Natl

Acad Sci Usa 97:13749-13754.10.1073/pnas.250475697
152. Myers JS, Cortez D (2006) Rapid activation of ATR by ionizing radiation requires ATM and Mre11, Journal of Biological Chemistry 281 9346–9350. H.
153. Cartagena-Lirola, Guerini I, Viscardi V, Lucchini G, Longhese MP (2006) Budding yeast Sae2 is an in vivo target of the Mec1 and Tel1 checkpoint kinases during meiosis, Cell Cycle 5 1549–1559.
154. Eapen VV, Sugawara N, Tsabar M, Wu WH, J.E. Haber (2012) The Saccharomyces cerevisiae chromatin remodeler Fun30 regulates DNA end resection and checkpoint deactivation, Molecular and Cellular Biology 32 4727–4740.
155. Giannattasio M, Lazzaro F, Longhese MP, Plevani P, Muzi-Falconi M (2004) Physical and functional interactions between nucleotide excision repair and DNA damage checkpoint, EMBO J. 23 429–438.
156. F. Marini F, T. Nardo T, M. Giannattasio M, M. Minuzzo M, M. Stefanini M, *et al.* (2006) DNA nucleotide excision repair-dependent signaling to checkpoint activation, Proc. Natl. Acad. Sci. USA 103 17325–17330.
157. Lydall D, Weinert T (1995) Yeast checkpoint genes in DNA damage processing: implications for repair and arrest. Science 270:1488–1491
158. Sohn SY, Cho Y (2009) Crystal structure of the human Rad9–Hus1–Rad1 clamp. J. Mol. Biol.390:490–502.
159. Majka J, Burgers PM (2003) Yeast Rad17/Mec3/Ddc1: a sliding clamp for the DNA damage checkpoint. Proc. Natl. Acad. Sci. U.S.A. 100:2249–2254.
160. Majka J, Chung BY, Burgers PM (2004) Requirement for ATP by the DNA damage checkpoint clamp loader, J. Biol. Chem. 279 20921–20926.
161. Naiki T, Shimomura T, Kondo T, Matsumoto K, Sugimoto K (2000) Rfc5, in cooperation with Rad24, controls DNA damage checkpoints throughout the cell cycle in Saccharomyces cerevisiae, Mol. Cell. Biol. 20 5888–5896.
162. Majka J, Binz SK, Wold MS, Burgers PM (2006) Replication protein A directs loading of the DNA damage checkpoint clamp to 5'-DNA junctions. J. Biol. Chem. **281**:27855–27861.
163. Burtelow MA, Roos-Mattjus PM, Rauen M, Babendure JR, Karnitz LM (2001) Reconstitution and molecular analysis of the hRad9-hHus1-hRad1 (9-1-1) DNA damage responsive checkpoint complex, J. Biol. Chem. 276:25903–25909.
164. Mordes D, Nam EA, Cortez D (2008) Dpb11 activates the Mec1-Ddc2 complex Proc Natl Acad Sci U S A. 2008 Dec 2;105(48):18730-4.
165. Marchetti MA, Kumar S, Hartsuiker E, Maftahi M, Carr AM *et al.* (2002) A single unbranched S-phase DNA damage and replication fork blockage checkpoint pathway, in: Proceedings of the National Academy of Sciences of the United States of America, 99 pp. 7472–7477.
166. Zegerman P, Diffley JF (2007) Phosphorylation of Sld2 and Sld3 by cyclin-dependent kinases promotes DNA replication in budding yeast, Nature 445 281–285.
167. Tanaka S, Umemori T, Hirai K, Muramatsu S, Kamimura Y *et al.* (2007) CDKdependent phosphorylation of Sld2 and Sld3 initiates DNA replication in budding yeast, Nature 445 328–332.
168. Masumoto H, Sugino A, Araki H (2000) Dpb11 controls the association between DNA polymerases alpha and epsilon and the autonomously replicating sequence region of budding yeast, Mol. Cell. Biol. 20 2809–2817.
169. Gambus A, Jones RC, Sanchez-Diaz A, Kanemaki M, van Deursen F *et al.* (2006) GINS

maintains association of Cdc45 with MCM in replisome progression complexes at eukaryoticDNA replication forks,Nat. Cell. Biol. 8:358–366.
170. Hodgson B, Calzada A, Labib K Mrc1 (2007) Tof1, regulate DNA replication forks in different ways during normal S phase, Mol. Biol. Cell. 18:3894–3902.
171. Makiniemi M, Hillukkala T, Tuusa J, Reini K, Vaara M (2001) BRCT domain-containing protein TopBP1 functions in DNA replication and damage response, J. Biol. Chem. 276:30399–30406.
172. Kumagai A, Lee J, Yoo HY, Dunphy WG (2006) TopBP1 activates the ATR–ATRIP complex. Cell 124:943–955.
173. Choi JH, Lindsey-Boltz LA, Sancar A (2007) Reconstitution of a human ATR-mediated checkpoint response to damaged DNA. Proc. Natl. Acad. Sci. U.S.A. 104:13301–13306.
174. Pellicioli A, Lucca C, Liberi G, Marini F, Lopes M *et al.* (1999) Activation of Rad53 kinase in response to DNA damage and its effect in modulating phosphorylation of the lagging strand DNA polymerase. EMBO J. **18**:6561–6572.
175. Granata M lazzaro F, Novarina D, Panigada D, Puddu F *et al.* (2010) Dynamics of Rad9 Chromatin Binding and Checkpoint Function Are Mediated by Its Dimerization and Are Cell Cycle–Regulated by CDK1 Activity. PLoS Genet. 43 6, e1001047.
176. Gritenaite D, Princz LN, Szakal B, Bantele SCS, Wendeler L *et al.* (2014) A cell cycle-regulated slx4 dpb11 complex promotes the resolution of DNA repair intermediates linked to stalled replication. Genes Dev; 28:1604-19.
177. Ohouo PY, de Oliveira FMB, Almeida BS, Smolka MB. (2010) DNA Damage signaling recruits the Rtt107-Slx4 scaffolds via dpb11 to mediate replication stress response. Mol Cell 39:3006
178. Wardlaw CP, Carr AM, Oliver AW (2014) TopBP1: A BRCT-scaffold protein functioning in multiple cellular pathways. DNA Repair (Amst.); 22:165-174; PMID:25087188;
179. Bantele CSC, Ferreira P, Gritenaite D, Boos D, Pfander B (2017) Targeting of the Fun30 nucleosome remodeller by the Dpb11 scaffold facilitates cell cycle-regulated DNA end resection eLife 6: e21687.
180. Weinert TA, Hartwell LH (1990) Characterization of RAD9 of Saccharomyces cerevisiae and evidence that its function acts posttranslationally in cell cycle arrest after DNA damage. Mol Cell Biol 10: 6554–6564.
181. Wysocki, R Javaheri A, Allard S, Sha F, Côté J *et al.* (2005) Role of Dot1-dependent histone H3 methylation in G1 and S phase DNA damage checkpoint functions of Rad9. Mol. Cell. Biol. 25, 8430–8443
182. Javaheri A, Wysocki R, Jobin-Robitaille O, Altaf M, Côté J *et al.* (2006) Yeast G1 DNA damage checkpoint regulation by H2A phosphorylation is independent of chromatin remodeling. Proceedings of the National Academy of Sciences 48 103, 13771–13776
183. Hammet A, Magill C, Heierhorst J, Jackson SP (2007) Rad9 BRCT domain interaction with phosphorylated H2AX regulates the G1 checkpoint in budding yeast. EMBO Rep. 8, 851–51 857
184. Grenon M, Costelloe T, Jimeno S, O'Shaughnessy A, Fitzgerald J *et al.* (2007) Docking onto chromatin via the Saccharomyces cerevisiae Rad9 Tudor domain. Yeast 24, 105–119
185. Sweeney FD, Yang F, Chi A, Shabanowitz J, Hunt DF *et al.* (2005) Saccharomyces cerevisiae Rad9 acts as a Mec1 adaptor to allow Rad53 activation. Current Biology 15,

1364–1375
186. Vialard JE, Gilbert CS, Green CM, Lowndes NF (1998) The budding yeast Rad9 checkpoint protein is subjected to Mec1/Tel1-dependent hyperphosphorylation and interacts with Rad53 after DNA damage. EMBO J. 17, 5679–5688
187. Durocher D, Henckel J, Fersht AR, Jackson SP (1999) The FHA domain is a modular phosphopeptide recognition motif. Mol. Cell 4, 387–394
188. Sun Z, Hsiao J, Fay DS, Stern DF (1998) Rad53 FHA domain associated with phosphorylated Rad9 in the DNA damage checkpoint. Science 281, 272–274
189. Emili A (1998) MEC1-dependent phosphorylation of Rad9p in response to DNA damage. Mol. Cell 2, 183 189
190. Schwartz MF, Duong JK, Sun Z, Morrow JS, Pradhan D *et al.* (2002) Rad9 phosphorylation sites couple Rad53 to the Saccharomyces cerevisiae DNA damage checkpoint. Mol. Cell 9, 1055–1065
191. Gilbert CS, Van den Bosch M, Green CM, Vialard JE, Grenon M, *ET AL.* (2003) The budding yeast Rad9 checkpoint complex: chaperone proteins are required for its function. EMBO Rep 4(10):953–958.
192. Gilbert CS, Green CM, Lowndes NF (2001) Budding yeast Rad9is an ATP-dependent Rad53 activating machine. Mol Cell 8(1):129–136.
193. Schwartz MF, Lee S, Duong JK, Eminaga S, Stern DF (2003) FHA domain-mediated DNA checkpoint regulation of Rad53. Cell Cycle 2(4):384–396.
194. Lazzaro F, Sapountzi V, Granata M, Pellicioli A, Vaze M *et al.* (2008) Histone methyltransferase Dot1 and Rad9 inhibit single-stranded DNA accumulation at DSBs and uncapped telomeres. EMBO J. 27, 1502–1512
195. Trovesi C, Falcettoni M, Lucchini G, Clerici M, Longhese MP (2011) Distinct Cdk1 requirements during single-strand annealing, noncrossover, and crossover recombination. PLoS Genet. 7, e1002263
196. Ferrari M, Dibitetto D, De Gregorio G, Eapen V, Rawal C *et al.* (2015) Functional Interplay between the 53BP1-Ortholog Rad9 and the Mre11 Complex Regulates Resection, End-Tethering and Repair of a Double-Strand Break. PLoS Genet. 11, e1004928
197. Bonetti D, Villa M, Gobbini E, Cassani C, Tedeschi G *et al.* (2015) Escape of Sgs1 from Rad9 inhibition reduces the requirement for Sae2 and functional MRX in DNA end resection. EMBO Rep 16:351–361.
198. Chen X, Cui D, Papusha A, Zhang X, Chu CD *et al.* The Fun30 nucleosome remodeller promotes resection of DNA double30 strand break ends. Nature 489, 576–580 (2012).
199. Costelloe T, Louge R, Tomimatsu N et al (2012) The yeast Fun30 and human SMARCAD1 chromatin remodellers promote DNA end resection. Nature 489:581–584.
200. Giannattasio M, Lazzaro F, Plevani P, Muzi-Falconi M (2005) The DNA damage checkpoint response requires histone H2B ubiquitination by Rad6-Bre1 and H3 methylation by Dot1. J. Biol. Chem. 280, 9879–9886
201. Toh GW, O'Shaughnessy AM, Jimeno S, Dobbie IM, Grenon M, et al(2006) Histone H2A phosphorylation and H3 methylation are required for a novel Rad9 DSB repair function following checkpoint activation. DNA Repair (Amst.) 5(10):693–703
202. Downs JA, Lowndes NF, Jackson SP (2000) A role for Saccharomyces cerevisiae histone H2A in DNA repair. Nature 408, 1001–1004
203. Clerici M, Trovesi C, Galbiati A *et al.* (2014) Mec1/ATR regulates the generation of single-stranded DNA that attenuates Tel1/ATM signaling at DNA ends. EMBO J 33:198–

216.
204. Fradet-Turcotte A, Canny MD, Escribano-Díaz C, Orthwein A, Leung CC *et al.* (2013) 53BP1 is a reader of the DNA-damage-induced H2A Lys 15 ubiquitin mark. Nature 499, 50–54
205. Wilson MD, Benlekbir S, Fradet-Turcotte A, Sherker A, Julien JP *et al.* (2016) The structural basis of modified nucleosome recognition by 53BP1. Nature 536, 100–103
206. Du LL, Nakamura TM, Russell P (2006) Histone modification-dependent and -independent pathways for recruitment of checkpoint protein Crb2 to double-strand breaks. Genes Dev. 20, 1583–1596
207. Sanders SL, Portoso M, Mata J, Bähler J, Allshire RC *et al.* (2004) Methylation of histone H4 lysine 20 controls recruitment of Crb2 to sites of DNA damage. Cell 119, 603–614
208. Botuyan MV, Lee J, Ward IM, Kim JE *et al.* (2006) Structural Basis for the Methylation State-Specific Recognition of Histone H4-K20 by 53BP1 and Crb2 in DNA Repair. Cell 127, 1361–1373
209. Pellegrino S, Michelena J, Teloni F, Imhof R, Altmeyer, M. (2017) Replication-Coupled Dilution of H4K20me2 Guides 53BP1 to Pre-replicative Chromatin. *CellReports* **19**, 1819–1831
210. Puddu, F. Granata M, Di Nola L, Balestrini A, Piergiovanni G *et al.* (2008) Phosphorylation of the Budding Yeast 9-1-1 Complex Is Required for Dpb11 Function in the Full Activation of the UV-Induced DNA Damage Checkpoint. Mol. Cell. Biol. 28, 4782–4793
211. Greeson NT, Sengupta R, Arida AR, Jenuwein T, Sanders SL (2008) Di-methyl H4 lysine 20 targets the checkpoint protein Crb2 to sites of DNA damage. J Biol Chem 283(48):33168–33174.
212. Kilkenny ML, Dore AS, Roe SM, Nestoras K, Ho JC, Watts FZ, Pearl LH (2008) Structural and functional analysis of the Crb2- BRCT2 domain reveals distinct roles in checkpoint signaling and DNA damage repair. Genes Dev 22(15):2034–2047.
213. Nakamura TM, Du LL, Redon C, Russell P (2004) Histone H2A phosphorylation controls Crb2 recruitment at DNA breaks, maintains checkpoint arrest, and influences DNA repair in fission yeast. Mol Cell Biol 24(14):6215–6230.
214. Fernandez-Capetillo O, Chen HT, Celeste A, Ward I, Romanienko PJ *et al.* (2002) DNA damage-induced G2-M checkpoint activation by histone H2AX and 53BP1. Nat Cell Biol 4(12):993–997.
215. Ward IM, Minn K, van Deursen J, Chen J (2003) p53 Binding protein 53BP1 is required for DNA damage responses and tumor suppression in mice. Mol Cell Biol 23(7):2556–2563
216. Wang B, Matsuoka S, Carpenter PB, Elledge SJ (2002) 53BP1, a mediator of the DNA damage checkpoint. Science 298(5597): 1435–1438
217. DiTullio RA Jr, Mochan TA, Venere M, Bartkova J, Sehested M, Bartek J, Halazonetis TD (2002) 53BP1 functions in an ATM-dependent checkpoint pathway that is constitutively activated in human cancer. Nat Cell Biol 4(12):998–1002
218. Wilson KA, Stern DF (2008) NFBD1/MDC1, 53BP1 and BRCA1 have both redundant and unique roles in the ATM pathway. Cell Cycle 7(22):3584–3594
219. Lee JH, Goodarzi AA, Jeggo PA, Paull TT (2010) 53BP1 promotes ATM activity through direct interactions with the MRN complex. EMBO J 29(3):574–585.
220. Huyen Y, Zgheib O, Ditullio RA Jr, Gorgoulis VG, Zacharatos P *et al.* (2004)

Methylated lysine 79 of histone H3 targets 53BP1 to DNA double-strand breaks. Nature 432(7015):406–411.
221. Pei H, Zhang L, Luo K, Qin Y, Chesi M *et al.* (2011) MMSET regulates histone H4K20 methylation and 53BP1 accumulation at DNA damage sites. Nature 470(7332):124–128.
222. Mailand N, Bekker-Jensen S, Faustrup H, Melander F, Bartek J *et al.* (2007) RNF8 ubiquitylates histones at DNA double-strand breaks and promotes assembly of repair proteins. Cell 131(5):887–900
223. Huen MS, Grant R, Manke I, Minn K, Yu X *et al.* (2007) RNF8 transduces the DNA-damage signal via histone ubiquitylation and checkpoint protein assembly. Cell 131(5):901–914
224. Kolas NK, Chapman JR, Nakada S, Ylanko J, Chahwan R *et al.* (2007) Orchestration of the DNA-damage response by the RNF8 ubiquitin ligase. Science 318(5856):1637–1640
225. Stewart GS, Panier S, Townsend K, Al-Hakim AK, Kolas NK *et al.* (2009) The RIDDLE syndrome protein mediates a ubiquitindependent signaling cascade at sites of DNA damage. Cell 136(3):420–434
226. Doil C, Mailand N, Bekker-Jensen S, Menard P, Larsen DH *et al.* (2009) RNF168 binds and amplifies ubiquitin conjugates on damaged chromosomes to allow accumulation of repair proteins. Cell 136(3):435–446.
227. Celeste A, Fernandez-Capetillo O, Kruhlak MJ, Pilch DR, Staudt DW *et al.* (2003) Histone H2AX phosphorylation is dispensable for the initial recognition of DNA breaks. Nat Cell Biol 5(7):675–679.
228. Lou Z, Minter-Dykhouse K, Franco S, Gostissa M, Rivera MA, *et al.* (2006) MDC1 maintains genomic stability by participating in the amplification of ATM-dependent DNA damage signals. Mol Cell 21(2):187–200
229. Stucki M, Clapperton JA, Mohammad D, Yaffe MB, Smerdon SJ *et al.* (2005) MDC1 directly binds phosphorylated histone H2AX to regulate cellular responses to DNA doublestrand breaks. Cell 123(7):1213–1226
230. Yamane K, Wu X, Chen J (2002) A DNA damage-regulated BRCT-containing protein, TopBP1, is required for cell survival. Mol Cell Biol 22(2):555–566
231. Cescutti R, Negrini S, Kohzaki M, Halazonetis TD (2010) TopBP1 functions with 53BP1 in the G1 DNA damage checkpoint. EMBO J 29(21):3723–3732.
232. Dephoure N, Zhou C, Villen J, Beausoleil SA, Bakalarski CE *et al.* (2008) A quantitative atlas of mitotic phosphorylation. Proc Natl Acad Sci USA 105(31):10762–10767.
233. Jowsey P, Morrice NA, Hastie CJ, McLauchlan H, Toth R *et al.* (2007) Characterisation of the sites of DNA damageinduced 53BP1 phosphorylation catalysed by ATM and ATR. DNA Repair (Amst) 6(10):1536–1544
234. Van Hoof D, Munoz J, Braam SR, Pinkse MW, Linding R *et al.* (2009) Phosphorylation dynamics during early differentiation of human embryonic stem cells. Cell Stem Cell 5(2):214–226
235. Olsen JV, Blagoev B, Gnad F, Macek B, Kumar C *et al.* (2006) Global, in vivo, and site-specific phosphorylation dynamics in signaling networks. Cell 127(3):635–648
236. Stokes MP, Rush J, Macneill J, Ren JM, Sprott K *et al.* (2007) Profiling of UV-induced ATM/ATR signaling pathways. Proc Natl Acad Sci USA 104(50):19855–19860
237. Molina H, Horn DM, Tang N, Mathivanan S, Pandey A (2007) Global proteomic profiling of phosphopeptides using electron transfer dissociation tandem mass spectrometry. Proc Natl Acad Sci USA 104(7):2199–2204

238. Tao WA, Wollscheid B, O'Brien R, Eng JK, Li XJ *et al.* (2005) Quantitative phosphoproteome analysis using a dendrimer conjugation chemistry and tandem mass spectrometry. Nat Methods 2(8):591–598
239. Choudhary C, Olsen JV, Brandts C, Cox J, Reddy PN *et al.* (2009) Mislocalized activation of oncogenic RTKs switches downstream signaling outcomes. Mol Cell 36(2):326–339.
240. Zhang W, Durocher D (2008) Dun1 counts on rad53 to be turned on Mol Cell, 31:pp. 1–2
241. Matsuoka S, Ballif BA, Smogorzewska A, McDonald ER 3rd, Hurov KE (2007) *et al.* ATM and ATR substrate analysis reveals extensive protein networks responsive to DNA damage Science, 316 pp. 1160–1166
242. Smith J, Tho LM, Xu N, Gillespie DA (2010) The ATM-Chk2 and ATR-Chk1 pathways in DNA damage signaling and cancer. Adv Cancer Res 108:73–112.
243. Usui T, Foster SS, Petrini JH (2009) Maintenance of the DNA damage checkpoint requires DNA-damage-induced mediator protein oligomerization. Mol Cell 33(2):147–159
244. Osborn AJ, Elledge SJ (2003) Mrc1 is a replication fork component whose phosphorylation in response to DNA replication stress activates Rad53. Genes Dev 17(14):1755–1767
245. Alcasabas AA, Osborn AJ, Bachant J, Hu F, Werler PJ *et al.* (2001) Mrc1 transduces signals of DNA replication stress to activate Rad53. Nat Cell Biol 3(11):958–965.
246. O'Neill T, Giarratani L, Chen P, Iyer L, Lee CH *et al.* (2002) Determination of substrate motifs for human Chk1 and hCds1/Chk2 by the oriented peptide library approach. J. Biol. Chem. 277:16102–15
247. de la Torre Ruiz MA, Lowndes NF (2000) DUN1 defines one branch downstream of RAD53 for transcription and DNA damage repair in Saccharomyces cerevisiae. FEBS Lett 485(2–3):205–206
248. Zhou Z, Elledge SJ (1993) DUN1 encodes a protein kinase that controls the DNA damage response in yeast. Cell 75(6):1119-1127
249. Chen SH, Smolka MB, Zhou H (2007) Mechanism of Dun1 activation by Rad53 phosphorylation in Saccharomyces cerevisiae. J Biol Chem 282(2):986–995.
250. Blankley RT, Lydall D (2004) A domain of Rad9 specifically required for activation of Chk1 in budding yeast. J Cell Sci 117(Pt 4):601–608.
251. Uetz P, Giot L, Cagney G, Mansfield TA, Judson RS (2000) A comprehensive analysis of protein–protein interactions in Saccharomyces cerevisiae. Nature 403(6770):623–627
252. Tapia-Alveal C, Calonge TM, O'Connell MJ (2009) Regulation of chk1. Cell Div 4:8
253. Foss EJ (2001) Tof1p regulates DNA damage responses during S-phase in Saccharomyces cerevisiae. Genetics 157(2):567–577
254. Gardner R, Putnam CW, Weinert T (1999) RAD53, DUN1 and PDS1 define two parallel G2/M checkpoint pathways in budding yeast. EMBO J 18(11):3173–3185
255. Lee J, Kumagai A, Dunphy WG (2003) Claspin, a Chk1-regulatory protein, monitors DNA replication on chromatin independently of RPA, ATR, Rad17. Mol Cell 11(2):329–340
256. Guo Z, Kumagai A, Wang SX, Dunphy WG (2000) Requirement for Atr in phosphorylation of Chk1 and cell cycle regulation in response to DNA replication blocks and UVdamaged DNA in Xenopus egg extracts. Genes Dev 14(21): 2745–2756

257. Kumagai A, Dunphy WG (2000) Claspin, a novel protein required for the activation of Chk1 during a DNA replication checkpoint response in Xenopus egg extracts. Mol Cell 6(4):839–849
258. Chini CC, Chen J (2003) Human claspin is required for replication checkpoint control. J Biol Chem 278(32):30057–30062.
259. Katsuragi Y, Sagata N (2004) Regulation of Chk1 kinase by autoinhibition and ATR-mediated phosphorylation. Mol Biol Cell 15(4):1680–1689.
260. Oe T, Nakajo N, Katsuragi Y, Okazaki K, Sagata N (2001) Cytoplasmic occurrence of the Chk1/Cdc25 pathway and regulation of Chk1 in Xenopus oocytes. Dev Biol 229(1):250–261.
261. Chen P, Luo C, Deng Y, Ryan K, Register J *et al.* (2000) The 1.7 A crystal structure of human cell cycle checkpoint kinase Chk1: implications or Chk1 regulation. Cell 100(6):681–692
262. Walker M, Black EJ, Oehler V, Gillespie DA, Scott MT (2009) Chk1 C-terminal regulatory phosphorylation mediates checkpoint activation by de-repression of Chk1 catalytic activity. Oncogene 28(24):2314–2323.
263. Smits VA, Reaper PM, Jackson SP (2006) Rapid PIKK-dependent release of Chk1 from chromatin promotes the DNAdamage checkpoint response. Curr Biol 16(2):150–159.
264. Shimada M, Niida H, Zineldeen DH, Tagami H, Tanaka M (2008) Chk1 is a histone H3 threonine 11 kinase that regulates DNA damage-induced transcriptional repression. Cell 132(2):221–232.
265. Lee J, Kumagai A, Dunphy WG (2001) Positive regulation of Wee1 by Chk1 and 14–3-3 proteins. Mol Biol Cell 12(3):551–563.
266. SolomonMJ, Varshavsky A (1985) Formaldehyde-mediated DNA-protein crosslinking: a probe for in vivo chromatin structures. Proc Natl Acad Sci U S A. 1985 Oct; 82(19): 6470–6474.
267. Jackson V. (1978) Studies on histone organization in the nucleosome using formaldehyde as a reversible cross-linking agent. Cell 15, 945–954
268. Vasilescu J., Guo X., and Kast J. (2004) Identification of protein-protein interactions using *in vivo*cross-linking and mass spectrometry. Proteomics 4, 3845–3854
269. Klockenbusch C., and Kast J. (2010) Optimization of formaldehyde cross-linking for protein interaction analysis on non-tagged integrin β1. J. Biomed. Biotechnol. 2010, 927585.
270. Guerrero C., Tagwerker C., Kaiser P., and Huang L. (2006) An integrated mass spectrometry-based proteomic approach: quantitative analysis of tandem affinity-purified *in vivo* cross-linked protein complexes (qtax) to decipher the 26s proteasome-interacting network. Mol. Cell. Proteomics 5, 366–378
271. De Piccoli G et al (2012) Replisome Stability at Defective DNA Replication Forks Is Independent of S Phase Checkpoint Kinases. Mol. Cell 45(5):696-704.
272. Hoffman EA, Frey BL, Lloyd MS and Auble DT (2015) Formaldehyde Crosslinking: A Tool for the Study of Chromatin Complexes J Biol Chem. 290(44):26404–26411.
273. Ong SE, Blagoev B, Kratchmarova I, Kristensen DB et al (2002) Stable isotope labeling by aminoacids in cell culture, SILAC, as a simple and accurate approach to expression proteomic Mol Cell Proteomics. 1(5):376-86
274. Mann M (2006) Functional and quantitative proteomics using SILAC. Nat Rev Mol Cell Biol. 7(12):952-8.
275. Takeda D.Y., Dutta A. DNA replication and progression through S phase. Oncogene.

2005;24:2827–2843.
276. Tercero J.A., Diffley J.F. Regulation of DNA replication fork progression through damaged DNA by the Mec1/Rad53 checkpoint. Nature. 2001;412:553–557.
277. Tercero J.A., Longhese M.P., Diffley J.F. A central role for DNA replication forks in checkpoint activation and response. Mol. Cell. 2003;11:1323–1336.
278. Lupardus P.J., Byun T., Yee M.C., Hekmat-Nejad M., Cimprich K.A. A requirement for replication in activation of the ATR-dependent DNA damage checkpoint. Genes Dev. 2002;16:2327–2332.
279. Stokes M.P., Van Hatten R., Lindsay H.D., Michael W.M. DNA replication is required for the checkpoint response to damaged DNA in *Xenopus* egg extracts. J. Cell. Biol. 2002;158:863–872.
280. Callegari A.J., Clark E., Pneuman A., Kelly T.J. Postreplication gaps at UV lesions are signals for checkpoint activation. Proc. Natl. Acad. Sci. USA. 2010;107:8219–8224. doi: 10.1073/pnas.1003449107.
281. van Attikum H, Fritsch O, Hohn B, Gasser S. (2004) Recruitment of the INO80 complex by H2A phosphorylation links ATP-dependent chromatin remodeling with DNA double-strand break repair Cell 119(6):777-88..
282. Chromatin remodelling at a DNA double-strand break site in Saccharomyces cerevisiae. Tsukuda T, Fleming AB, Nickoloff JA, Osley MA Nature. 2005 Nov 17; 438(7066):379-83.
283. Nucleosome dynamics regulates DNA processing. Adkins NL, Niu H, Sung P, Peterson CL Nat Struct Mol Biol. 2013 Jul; 20(7):836-42.
284. Toh, GWL et al. (2006)Histone H2A phosphorylation and H3 methylation are required for a novel Rad9 DSB repair function following checkpoint activation. DNA Repair (Amst.) 5,10 693–703.
285. Lee, S. E. et al. (1998) Saccharomyces Ku70, mre11/rad50 and RPA proteins regulate adaptation to G2/M arrest after DNA damage. Cell 94, 399–409.
286. Liu, Y. et al. (2017) TOPBP1 Dpb11plays a conserved role in homologous recombination DNA repair through the coordinated recruitment of 53BP1 Rad9. J. Cell Biol. 33, jcb.201607031–17
287. BrachmanCB, et al (1998) Designer deletion strains derived from Saccharomyces cerevisiae S288C: a useful set of strains and plasmids for PCR-mediated gene disruption and other applications. Yeast 14(2):115-32
288. Winston F, et al (1995) Construction of a set of convenient Saccharomyces cerevisiae strains that are isogenic to S288C. Yeast 11(1):53-5 PMID:7762301
289. Malumbres M, (2014) Cyclin-dependent kinases. Genom Biol 15(6):122.
290. Yao S, Neiman A, Prelich G (2000) BUR1 and BUR2 Encode a Divergent Cyclin-Dependent Kinase–Cyclin Complex Important for Transcription In Vivo. Mol Cell Biol 20(19):7080-7.
291. Traven A, Heierhorst J (2005) SQ/TQ cluster domains: concentrated ATM/ATR kinase phosphorylation site regions in DNA-damage-response proteins. Bioessays 27(4):397-407
292. Chen RE and Thorner J (2007) Function and Regulation in MAPK Signaling Pathways Lessons Learned from the Yeast *Saccharomyces cerevisiae* Biochim. Biophys. Acta 1773(8):1311-1340.
293. Gustin MC, Albertin J, Alexander M and Davenport K. (1998) MAP Kinase Pathways in the Yeast Saccharomyces cerevisiae. Microbiol Mol Biol Rev. 62(4): 1264–1300.

294. Bartkowiak B, Liu P, Phatnani HP, Fuda NJ, Cooper JJ, Price DH, Adelman K, Lis JT, Greenleaf AL (2010) CDK12 is a transcription elongation-associated CTD kinase, the metazoan ortholog of yeast Ctk1. Genes Dev. 15; 24(20):2303-16.
295. Wood A, Shilatifard A (2006) Bur1/Bur2 and the Ctk complex in yeast: the split personality of mammalian P-TEFb. Cell Cycle. 5(10):1066-8.
296. Kim M, Suh H, Cho EJ, Buratowski S (2009) Phosphorylation of the yeast Rpb1 C-terminal domain at serines 2, 5, and 7. J Biol Chem. 284(39):26421-6.
297. Kuchin S, Yeghiayan P, Carlson M (1995) Cyclin-dependent protein kinase and cyclin homologs SSN3 and SSN8 contribute to transcriptional control in yeast. Proc Natl Acad Sci U S A. 25; 92(9): 4006–4010.
298. Clausing E et al (2010) Enlongation Factor Bur1-Bur2 interacts with Replication Protein A and maintains Genome Stability during Replication Stress. J Biol Chem. 285(53): 41665–41674
299. Röther and Strasser K (2007) The RNA polymerase II CTD kinase Ctk1 functions in translation elongation Genes & Development 21:1409–1421.
300. Akhtar MS, Heidemann M, Tietjen JR, Zhang DW, Chapman RD, Eick D, Ansari AZ (2009) TFIIH kinase places bivalent marks on the carboxy-terminal domain of RNA polymerase II. Mol Cell 34(3):387-93.
301. Wang G, Tong X, Weng S, Zhou H (2012) Multiple phosphorylation of Rad9 by CDK is required for DNA damage checkpoint activation. Cell cycle 11(20):3792-800.
302. Zimmermann M, Lottersberger F, Buonomo SB, Sfeir A and de Lange T (2013) 53BP1 regulates DSB repair using Rif1 to control 5' end resection. Science 339:700–704.
303. Escribano-Diaz C et al. (2013) A cell cycle-dependent regulatory circuit composed of 53BP1-RIF1 and BRCA1-CtIP controls DNA repair pathway choice. Mol. Cell 49:872–883
304. Feng L, Fong KW, Wang J, Wang W and Chen J (2013) RIF1 counteracts BRCA1-mediated end resection during DNA repair. J. Biol. Chem. 288:11135–11143
305. Holt et al (2009) Global analysis of Cdk1 substrate phosphorylation sites provides insights into evolution. Science 325(5948):1682
306. Trovesi C, Manfrini N, Falcettoni M, Longhese MP (2013) Regulation of the DNA damage response by cyclin-dependent kinases J Mol Biol 425(23):4756-66.
307. Fu Q et al (2014) Correction for Fu et al., Phosphorylation-Regulated Transitions in an Oligomeric State Control the Activity of the Sae2 DNA Repair Enzyme. Mol Cell Biol 34(22): 4213.
308. Huertas P, Cortés-Ledesma F, Sartori AA, Aguilera A, Jackson SP (2008) CDK targets Sae2 to control DNA-end resection and homologous recombination. Nature 455(7213):689-92.
309. Symington LS, GautierJ (2011) Double-strand break end resection and repair pathway choice. Annu Rev genet 45:247-71.
310. Ira G et al (2004) DNA end resection, homologous recombination and DNA damage checkpoint activation require CDK1. Nature. 431(7011):1011-7.
311. Olsen JV et al (2010) Quantitative phosphoproteomics reveals widespread full phosphorylation site occupancy during mitosis. Sci Signal. 3(104):ra3

312. Falck J, Forment JV, Coates J, Mistrik M, Lukas J, Bartek J, Jackson SP. 2012 CDK targeting of NBS1 promotes DNA-end resection, replication restart and homologous recombination. EMBO Rep.13(6):561-8.
313. Wohlbold L et al (2012) Chemical genetics reveals a specific requirement for Cdk2 activity in the DNA damage response and identifies Nbs1 as a Cdk2 substrate in human cells. PLoS Genet. 8(8):e1002935
314. Albuquerque CP, Smolka MB, Payne SH, Bafna V, Eng J, Zhou H (2008) A multidimensional chromatography technology for in-depth phosphoproteome analysis. Mol Cell Proteomics. 7(7):1389-96.
315. Simoneau A, Robellet X, Ladouceur AM, D'Amours D. (2014) Cdk1-dependent regulation of the Mre11 complex couples DNA repair pathways to cell cycle progression. Cell Cycle 13(7):1078-90.
316. Beli, P. et al. (2012) Proteomic investigations reveal a role for RNA processing 1 factor THRAP3 in the DNA damage response. Mol. Cell 46:212–225
317. Thomas BJ, Rothstein R. (1989) The genetic control of direct-repeat recombination in Saccharomyces: the effect of rad52 and rad1 on mitotic recombination at GAL10, a transcriptionally regulated gene. Genetics. 123(4):725-38
318. Janke C, Magiera MM, Rathfelder N, Taxis C et al. (2004) A versatile toolbox for PCR-based tagging of yeast genes: new fluorescent proteins, more markers and promoter substitution cassettes. Yeast 21(11):947-62.
319. Knop M1, Siegers K, Pereira G, Zachariae W et al. (1999) Epitope tagging of yeast genes using a PCR-based strategy: more tags and improved practical routines. Yeast 15(10B):963-72.
320. James P, Halladay J, Craig EA. (1996) Genomic libraries and a host strain designed for highly efficient two-hybrid selection in yeast. Genetics 144(4):1425-36.
321. Sambrook, J., and Russell, R.W.(2001). Molecular cloning: A laboratory manual, 3rd ed. Cold spring harbor laboratory press, cold spring harbor, N.Y.
322. Sugawara N, Wang X, Haber JE (2003) In vivo roles of Rad52, Rad54, and Rad55 proteins in Rad51-mediated recombination. Mol Cell 12(1):209-19.
323. Aparicio O1, Geisberg JV, Struhl K (2004) Chromatin immunoprecipitation for determining the association of proteins with specific genomic sequences in vivo. Curr Protoc Cell Biol. Chapter 17:Unit 17.7.
324. Olsen JV, de Godoy LM, Li G, Macek B, Mortensen P et al (2005) Parts per million mass accuracy on an Orbitrap mass spectrometer via lock mass injection into a C-trap. Mol Cell Proteomics. 4(12):2010-21.
325. Cox J, Mann M. (2008) MaxQuant enables high peptide identification rates, individualized p.p.b.-range mass accuracies and proteome-wide protein quantification. Nat Biotechnol. 26(12):1367-72.
326. Nishimura K, Fukagawa T, Takisawa H, Kakimoto T, Kanemaki M. (2009) An auxin-based degron system for the rapid depletion of proteins in nonplant cells. Nat Methods 6(12):917-22.

ABBREVIATIONS

Aa	aminoacid
AAD	ATR activating domai
Alt-NHEJ	alternative-NHEJ
APC	anaphase promoing complex
APS	ammonium persulfate
ATM	ataxia-telangiectasia mutated
ATR	ATM and Rad3-related
bp	base pair
BER	base excision repair
BIR	break induced replication
BRCT	BRCA1 carboxy terminal
CAD	Chk1-activation domain
CDK	cyclin-dependent-kinase
ChIP	Chromatin Immuno Precipitation
CoIP	Co-Immuniprecipitation
CPT	camptothecin
C-terminal	carboxy terminal
C-terminus	carboxi terminus
DDK	Dbf4-dependent kinase
DDR	DNA damage response
DMSO	dimethylsulfoxide
DNA	deoxyribonucleic acid
DNA PKCs	DNA dependent protein kinase catalitic subunits
dNTP	deoxynucleotide triphosphate
Dpb11	DNA Polymerase B (II)
DSBs	double-strand breaks
dsDNA	double-stranded DNA
DTT	dithiothreitol
EDTA	ethylenediaminetetraacidic acid
EF3	enlongation factor 3
FACS	fluorescence-activated cell sorting
γH2A	S129-phosphorylated Histone H2A
g	gram
GAL	galactose
GCRs	gross chromosomal rearrangements
G1-phase	gap phase 1
G2-phase	gap phase 2
G418	geneticin
h	hour(s)
h	human
HEAT domain	Huntingtin, EF3, PP2A, TOR1-domain
HJ	holliday junction
HO	HO endonuclease
Hph	hygromycin
HR	homologous recombination
HRP	horseradish peroxidase
HU	hydroxyurea
H3	histone 3
H3-K79^{me}	K79-methylated histone H3
IP	immunoprecipitation
K	lysine
Kb	kilo base pairs
KDa	kilo dalton
l	liter

LB	Luria-Bertani
log	logarithmic
µ	micro (x 10^{-6})
M	molar
m	milli (x 10^{-3})
M-phase	mitosis
min	minute(s)
MAPK	mitogen-activated-kinase
MEN	mitotic exit networs
MMC	mitomycin C
MMEJ	micro-homology mediated end joining
MMR	mismatch repair
MMS	methyl methanesulfonate
MOPS	3-(N-morpholino) propanesulfonic acid
MRN	Mre11-Rad50-Xrs2
MRX	Mre11-Rad50-Xrs2 complex
MS	mass spectrometry
n	nano (x10^{-9})
N-terminal	amino terminal
N-terminus	amino terminus
NAT	noursethricin
NER	nucleotide excision repair
NHEJ	non homologous end joining
OD	optical density
ON	over night
ORF	open reading frame
P	proline
PAGE	polyacrylamide gel electrophoresis
PCNA	proliferating cell nuclear antigen
PCR	polymerase chain reaction
PEG	polyethylene glycol
PIKKs	phosphatidylinositol 3-kinase-related kinases
PP2A	protein-phosphatase 2A
PVDF	Polyvinylidene difluoride
Rad9	RADiation sensitive 9
Rad9-S462^{P}	Rad9 phosphorylated on Serine 462
Rad9-T474^{P}	Rad9 phosphorylated on Threonine 474
RFC	replication factor C
RNA	ribonucleic acid
RNase	ribonuclease A
RNR	ribonucleotide reductase
RPA	replication protein A
Rpm	rotation per minute
S	serine
s	seconds
S^{P}	phosphorylated serine
S-phase	synthesis phase of the cell cycle
SDS	sodium dodecylsulfate
SC	synthetic complete
S. cerevisiae / pombe	Saccharomyces cerevisiae/pombe
Sc	Saccharomyces cerevisiae
Sp	Saccharomyces pombe
SLIC	sequence-and-ligation-independent-cloning
Smc	structural maintenance of chromosome
SSA	single strand annealing
SSBr	single strand break repair
SSBs	single strand breaks

ssDNA	single-stranded DNA
T	threonine
TBST	tris-bufferes saline with Tween-20
TCA	trichloro acidic acid
TE	Tris-EDTA
TEMED	tetramethylethylenediamine
TLS	translesion synthesis
T^P	phosphorylated threonine
Tris	Tris(hydroxymethyl)aminomethane
UV	ultraviolet light
V	Volt
v/v	volume per volume
WT	wild type
w/v	weight per volume
W	Tryptophan
X	Any aminoacid
Y	Tyrosine
YPD	yeast bactopeptone dextrose

Table 2: List of Kinases tested for Rad9-T474 phosphorylation in G1 after DNA damage. The selected genes were from a library of haploid deletion strains from the Saccharomyces genome deletion project (288, 289).

GENE	FUNCTION (SGD DATABASE)
AKL1	Ser-Thr protein kinase; member (with Ark1p and Prk1p) of the Ark kinase family; involved in endocytosis and actin cytoskeleton organization
ATG1	Protein serine/threonine kinase; required for vesicle formation in autophagy and the cytoplasm-to-vacuole targeting (Cvt) pathway; structurally required for phagophore assembly site formation; during autophagy forms a complex with Atg13p and Atg17p; essential for cell cycle progression from G2/M to G1 under nitrogen starvation
ARK1	Serine/threonine protein kinase; involved in regulation of the cortical actin cytoskeleton; involved in control of endocytosis; ARK1 has a paralog, PRK1, that arose from the whole genome duplication
BCK1	MAPKKK acting in the protein kinase C signaling pathway; the kinase C signaling pathway controls cell integrity; upon activation by Pkc1p phosphorylates downstream kinases Mkk1p and Mkk2p; MAPKKK is an acronym for mitogen-activated protein (MAP) kinase kinase kinase
CLA4	Cdc42p-activated signal transducing kinase; member of the PAK (p21-activated kinase) family, along with Ste20p and Skm1p; involved in septin ring assembly, vacuole inheritance, cytokinesis, sterol uptake regulation; phosphorylates Cdc3p and Cdc10p; CLA4 has a paralog, SKM1, that arose from the whole genome duplication
CMK1	Calmodulin-dependent protein kinase; may play a role in stress response, many Ca++/calmodulin dependent phosphorylation substrates demonstrated in vitro, amino acid sequence similar to mammalian Cam Kinase II; CMK1 has a paralog, CMK2, that arose from the whole genome duplication
CMK2	Calmodulin-dependent protein kinase; may play a role in stress response, many CA++/calmodulan dependent phosphorylation substrates demonstrated in vitro, amino acid sequence similar to mammalian Cam Kinase II; CMK2 has a paralog, CMK1, that arose from the whole genome duplication
DUN1	Cell-cycle checkpoint S/T protein kinase; required for transient G2/M arrest after DNA damage, damage-induced transcription, and nuclear-to-cytoplasmic redistribution of Rnr2p-Rnr4p after genotoxic stress and iron deprivation; phosphorylates repair protein Rad55p, transcriptional repressor Sml1p, superoxide dismutase, and ribonucleotide reductase inhibitors Crt1p and Dif1p; functions in the Mec1p pathway to regulate dNTP pools and telomere length; postreplicative repair role

GENE	FUNCTION (SGD DATABASE)
ELM1	Serine/threonine protein kinase; regulates the orientation checkpoint, the morphogenesis checkpoint and the metabolic switch from fermentative to oxidative metabolism by phosphorylating the activation loop of Kin4p, Hsl1p and Snf4p respectively; cooperates with Hsl7p in recruiting Hsl1p to the septin ring, a prerequisite for subsequent recruitment, phosphorylation, and degradation of Swe1p; forms part of the bud neck ring; regulates cytokinesis
ENV7	Vacuolar membrane protein kinase; negatively regulates membrane fusion; associates with vacuolar membrane through palmitoylation of one or more cysteines in consensus sequence; vacuolar membrane association is essential to its kinase activity; mutant shows defect in CPY processing; ortholog of human serine/threonine kinase 16 (STK16)
FPK1	Ser/Thr protein kinase; phosphorylates several aminophospholipid translocase family members, regulating phospholipid translocation and membrane asymmetry; phosphorylates and inhibits upstream inhibitory kinase, Ypk1p; localizes to the cytoplasm, early endosome/TGN compartments and thplasma membrane; localizes to the shmoo tip where it has a redundant role in the cellular response to mating pheromone; FPK1 has a paralog, KIN82, that arose from the whole genome duplication
FRK1	Protein kinase of unknown cellular role; green fluorescent protein (GFP)-fusion protein localizes to the cytoplasm; interacts with rRNA transcription and ribosome biogenesis factors and the long chain fatty acyl-CoA synthetase Faa3p; FRK1 has a paralog, KIN4, that arose from the whole genome duplication
FUN31	PAS domain-containing serine/threonine protein kinase; coordinately regulates protein synthesis and carbohydrate metabolism and storage in response to a unknown metabolite that reflects nutritional status; PSK1 has a paralog, PSK2, that arose from the whole genome duplication
GIN4	Protein kinase involved in bud growth and assembly of the septin ring; proposed to have kinase-dependent and kinase-independent activities; undergoes autophosphorylation; similar to Hsl1p; GIN4 has a paralog, KCC4, that arose from the whole genome duplication
ISR1	Predicted protein kinase; overexpression causes sensitivity to staurosporine, which is a potent inhibitor of protein kinase C
KCC4	Protein kinase of the bud neck involved in the septin checkpoint; associates with septin proteins, negatively regulates Swe1p by phosphorylation, shows structural homology to bud neck kinases Gin4p and Hsl1p; KCC4 has a paralog, GIN4, that arose from the whole genome duplication
KIN1	Serine/threonine protein kinase involved in regulation of exocytosis; localizes to the cytoplasmic face of the plasma membrane; KIN1 has a paralog, KIN2, that arose from the whole genome duplication

GENE	FUNCTION (SGD DATABASE)
KIN2	Serine/threonine protein kinase involved in regulation of exocytosis; localizes to the cytoplasmic face of the plasma membrane; KIN2 has a paralog, KIN1, that arose from the whole genome duplication
KIN4	Serine/threonine protein kinase; inhibits the mitotic exit network (MEN) when the spindle position checkpoint is activated; localized asymmetrically to mother cell cortex, spindle pole body and bud neck; KIN4 has a paralog, FRK1, that arose from the whole genome duplication
KIN82	Putative serine/threonine protein kinase; implicated in the regulation of phospholipid asymmetry through the activation of phospholipid translocases (flippases); involved in the phosphorylation of upstream inhibitory kinase Ypk1p along with Fpk1p; has a redundant role in the cellular response to mating pheromone; KIN82 has a paralog, FPK1, that arose from the whole genome duplication
MEK1	Meiosis-specific serine/threonine protein kinase; functions in meiotic checkpoint, promotes recombination between homologous chromosomes by suppressing double strand break repair between sister chromatids; stabilizes Hop1-Thr318 phosphorylation to promote interhomolog recombination and checkpoint responses during meiosis
MKK1	MAPKK involved in the protein kinase C signaling pathway; involved in control of cell integrity; upon activation by Bck1p phosphorylates downstream target, Slt2p; functionally redundant with Mkk2p; MKK1 has a paralog, MKK2, that arose from the whole genome duplication
MKK2	MAPKK involved in the protein kinase C signaling pathway; involved in control of cell integrity; upon activation by Bck1p phosphorylates downstream target, Slt2p; functionally redundant with Mkk1p; MKK2 has a paralog, MKK1, that arose from the whole genome duplication
NNK1	Protein kinase; implicated in proteasome function; interacts with TORC1, Ure2 and Gdh2; overexpression leads to hypersensitivity to rapamycin and nuclear accumulation of Gln3; epitope-tagged protein localizes to the cytoplasm
NPR1	Protein kinase; stabilizes several plasma membrane amino acid transporters by antagonizing their ubiquitin-mediated degradation; phosphorylates Aly2p; negatively regulates Ldb19p-mediated endocytosis through phosphorylation of Ldb19p, which prevents its association with the plasma membrane; Npr1p activity is negatively regulated via phosphorylation by the TOR complex; NPR1 has a paralog, PRR2, that arose from the whole genome duplication
PAK1	Upstream serine/threonine kinase for the SNF1 complex; plays a role in pseudohyphal groth; partially redundant with Elm1p and Tos3p; members of this family have functional orthology with LKB1, a mammalian kinase associated with Peutz-Jeghers cancer-susceptibility syndrome; SAK1 has a paralog, TOS3, that arose from the whole genome duplication

GENE	FUNCTION (SGD DATABASE)
PKP1	Mitochondrial protein kinase; involved in negative regulation of pyruvate dehydrogenase complex activity by phosphorylating the ser-133 residue of the Pda1p subunit; acts in concert with kinase Pkp2p and phosphatases Ptc5p and Ptc6p
PKP2	Mitochondrial protein kinase; negatively regulates activity of the pyruvate dehydrogenase complex by phosphorylating the ser-133 residue of the Pda1p subunit; acts in concert with kinase Pkp1p and phosphatases Ptc5p and Ptc6p; relocalizes from mitochondrion to cytoplasm upon DNA replication stress
PRK1	Protein serine/threonine kinase; regulates the organization and function of the actin cytoskeleton and reduces endocytic ability of cell through the phosphorylation of the Pan1p-Sla1p-End3p protein complex; PRK1 has a paralog, ARK1, that arose from the whole genome duplication
PSK2	PAS-domain containing serine/threonine protein kinase; regulates sugar flux and translation in response to an unknown metabolite by phosphorylating Ugp1p and Gsy2p (sugar flux) and Caf20p, Tif11p and Sro9p (translation); PSK2 has a paralog, PSK1, that arose from the whole genome duplication
PTK1	Putative serine/threonine protein kinase; regulates spermine uptake; involved in polyamine transport; possible mitochondrial protein; PTK1 has a paralog, PTK2, that arose from the whole genome duplication
PTK2	Serine/threonine protein kinase; involved in regulation of ion transport across plasma membrane; carboxyl terminus is essential for glucose-dependent Pma1p activation via phosphorylation of Pma1p-Ser899; enhances spermine uptake; PTK2 has a paralog, PTK1, that arose from the whole genome duplication
RCK1	Protein kinase involved in oxidative stress response; promotes pseudohyphal growth via activation of Ubp3p phosphorylation; identified as suppressor of S. pombe cell cycle checkpoint mutations; RCK1 has a paralog, RCK2, that arose from the whole genome duplication
RCK2	Protein kinase involved in response to oxidative and osmotic stress; identified as suppressor of S. pombe cell cycle checkpoint mutations; similar to CaM (calmodulin) kinases; RCK2 has a paralog, RCK1, that arose from the whole genome duplication
RIM15	Protein kinase involved in cell proliferation in response to nutrients; glucose-repressible; involved in signal transduction during cell proliferation in response to nutrients, specifically the establishment of stationary phase; identified as a regulator of IME2; phosphorylates Igo1p and Igo2p; substrate of Pho80p-Pho85p kinase

GENE	FUNCTION (SGD DATABASE)
RTK1	Putative protein kinase, potentially phosphorylated by Cdc28p; interacts with ribosome biogenesis factors, Cka2, Gus1 and Arc1; protein abundance increases in response to DNA replication stress
SAT4	Ser/Thr protein kinase involved in salt tolerance; funtions in regulation of Trk1p-Trk2p potassium transporter; overexpression affects the Fe-S and lipoamide containing proteins in the mitochondrion; required for lipoylation of Lat1p, Kgd2p and Gcv3p; partially redundant with Hal5p; has similarity to Npr1p; localizes to the cytoplasm and mitochondrion
SCH9	AGC family protein kinase; functional ortholog of mammalian S6 kinase; phosphorylated by Tor1p and required for TORC1-mediated regulation of ribosome biogenesis, translation initiation, and entry into G0 phase; involved in transactivation of osmostress-responsive genes; regulates G1 progression, cAPK activity and nitrogen activation of the FGM pathway; integrates nutrient signals and stress signals from sphingolipids to regulate lifespan
SCY1	Putative kinase; suppressor of GTPase mutant; similar to bovine rhodopsin kinase; may have a role in intracellular sterol transport
SHA3	Putative serine/threonine protein kinase; involved in the adaptation to low concentrations of glucose independent of the SNF3 regulated pathway; SKS1 has a paralog, VHS1, that arose from the whole genome duplication
SKY1	SR protein kinase (SRPK); involved in regulating proteins involved in mRNA metabolism and cation homeostasis; similar to human SRPK1.
SKM1	Member of the PAK family of serine/threonine protein kinases; similar to Ste20p; involved in down-regulation of sterol uptake; proposed to be a downstream effector of Cdc42p during polarized growth; SKM1 has a paralog, CLA4, that arose from the whole genome duplication
SNF1	AMP-activated S/T protein kinase; forms a complex with Snf4p and members of the Sip1p/Sip2p/Gal83p family; required for transcription of glucose-repressed genes, thermotolerance, sporulation, and peroxisome biogenesis; regulates nucleocytoplasmic shuttling of Hxk2p; regulates filamentous growth and acts as a non-canonical GEF, activating Arf3p during invasive growth; SUMOylation by Mms21p inhibits its function and targets Snf1p for destruction via the Slx5-Slx8 Ub ligase
SPS1	Putative protein serine/threonine kinase; localizes to the nucleus and cytoplasm; required for efficient spore packaging, prospore membrane development and closure and localization of enzymes involved in spore wall synthesis; interacts with and required for Ssp1p phosphorylation and turnover; member of the GCKIII subfamily of STE20 kinases; multiply phosphorylated on S/T residues; interacts with 14-3-3 proteins, Bmh1p and Bmh2p; expressed at the end of meiosis

GENE	FUNCTION (SGD DATABASE)
SSK2	MAP kinase kinase kinase of HOG1 mitogen-activated signaling pathway; interacts with Ssk1p, leading to autophosphorylation and activation of Ssk2p which phosphorylates Pbs2p; also mediates actin cytoskeleton recovery from osmotic stress; a HOG-independent function of Ssk2p mediates the calcium-sensitive phenotype of the ptp2 msg5 double disruptant; SSK2 has a paralog, SSK22, that arose from the whole genome duplication
SSK22	MAP kinase kinase kinase of HOG1 mitogen-activated signaling pathway; interacts with Ssk1p, leading to autophosphorylation and activation of Ssk2p which phosphorylates Pbs2p; also mediates actin cytoskeleton recovery from osmotic stress; a HOG-independent function of Ssk2p mediates the calcium-sensitive phenotype of the ptp2 msg5 double disruptant; SSK2 has a paralog, SSK22, that arose from the whole genome duplication
SWE1	Protein kinase that regulates the G2/M transition; negative regulator of the Cdc28p kinase; morphogenesis checkpoint kinase; positive regulator of sphingolipid biosynthesis via Orm2p; phosphorylates a tyrosine residue in the N-terminus of Hsp90 in a cell-cycle associated manner, thus modulating the ability of Hsp90 to chaperone a selected clientele; localizes to the nucleus and to the daughter side of the mother-bud neck; homolog of S. pombe Wee1p; potential Cdc28p substrate
TOS3	Protein kinase; related to and functionally redundant with Elm1p and Sak1p for the phosphorylation and activation of Snf1p; functionally orthologous to LKB1, a mammalian kinase associated with Peutz-Jeghers cancer-susceptibility syndrome; TOS3 has a paralog, SAK1, that arose from the whole genome duplication
TPK1	cAMP-dependent protein kinase catalytic subunit; promotes vegetative growth in response to nutrients via the Ras-cAMP signaling pathway; inhibited by regulatory subunit Bcy1p in the absence of cAMP; phosphorylates and inhibits Whi3p to promote G1/S phase passage; partially redundant with Tpk2p and Tpk3p; phosphorylates pre-Tom40p, which impairs its import into mitochondria under non-respiratory conditions; TPK1 has a paralog, TPK3, that arose from the whole genome duplication
YPK2	Protein kinase similar to S/T protein kinase Ypk1p; functionally redundant with YPK1 at the genetic level; participates in a signaling pathway required for optimal cell wall integrity; involved in the TORC-dependent phosphorylation of ribosomal proteins Rps6a/b (S6); human homolog SGK2 can complement a ypk1 ypk2 double mutant
TPK3	cAMP-dependent protein kinase catalytic subunit; promotes vegetative growth in response to nutrients via the Ras-cAMP signaling pathway; partially redundant with Tpk1p and Tpk2p; localizes to P-bodies during stationary phase; TPK3 has a paralog, TPK1, that arose from the whole genome duplication

GENE	FUNCTION (SGD DATABASE)
YAK1	Serine-threonine protein kinase; component of a glucose-sensing system that inhibits growth in response to glucose availability; upon nutrient deprivation Yak1p phosphorylates Pop2p to regulate mRNA deadenylation, the co-repressor Crf1p to inhibit transcription of ribosomal genes, and the stress-responsive transcription factors Hsf1p and Msn2p; nuclear localization negatively regulated by the Ras/PKA signaling pathway in the presence of glucose
YPK1	S/T protein kinase; phosphorylates, downregulates flippase activator Fpk1p; inactivates Orm1p and Orm2p by phosphorylation in response to compromised sphingolipid synthesis; involved in the TORC-dependent phosphorylation of ribosomal proteins Rps6a/b (S6); mutations affect receptor-mediated endocytosis and sphingolipid-mediated and cell integrity signaling pathways; human homolog SGK1 can complement a null mutant; human homolog SGK2 can complement a ypk1 ypk2 double mutant
YPK2	Protein kinase similar to S/T protein kinase Ypk1p; functionally redundant with YPK1 at the genetic level; participates in a signaling pathway required for optimal cell wall integrity; involved in the TORC-dependent phosphorylation of ribosomal proteins Rps6a/b (S6); human homolog SGK2 can complement a ypk1 ypk2 double mutant
YPK3	AGC kinase; phosphorylated by cAMP-dependent protein kinase (PKA) in a TORC1-dependent manner; directly phosphorylated by TORC1; phosphorylates ribosomal protein Rps6a/b (S6), in a TORC-dependent manner; undergoes autophosphorylation
YPL150W	Protein kinase of unknown cellular role; binds phosphatidylinositols and cardiolipin in a large-scale study

Acknowledgements

First of all I would like to thank my supervisor Boris Pfander for the opportunity to work in his lab and for his constant support and supervision during the years of my PhD.
I would also like to kindly acknowledge all the members of my doctoral thesis committee for taking the time to read my work and taking part in my oral dissertation.

I would of course like to thank all my colleagues for the nice working atmosphere, constant sweets supply and the daily, fruitful scientific discussions. My gratitude goes also to Uschi Schkölziger for technical support.
A special thanks goes of course to my best desk- and bench-mate Lissa, for her kindness and help not only in the past 6 years of PhD but also and especially in the weeks pre-submission. Thank you for the help in the lab but also for always listening.

These years at the Max-Planck would not have been the same without a group of special people and in particular Vavvi, Alessandro, Verena, Francesca Pietro, Matteo, Thanks for making me feel like I am always at home, in my high-school years.
Thanks to the friends I made in Munich and that now left: Mirela, Anastasia, Zocco, Paola, I miss you guys.

My far away friends that are with me since always or „only“ since a decade: Focca, Laura, Giudy, Agnese, Marta. I miss you every day, maybe one day we will finally live in the same State. Focca: thanks for understanding and sharing all my thoughts and my moods; Laura you are my best crazy, strong friend; Agnese: your determination always inspired me; Marta: we grew up together and we keep on doing it, despite the distance and despite not talking so often; Giudy: you need to travel with me.

Hannes, you were the first beautiful thing I found in this city when it was new, and still are the best bit of these past 5 years, thanks for what you do for me every day.

Finally, I am thankful for my parents, and my two big brothers. Thank you for loving me and encouraging me in pushing myself, exploring the world and be ambitious. I love you